
**ADDIS ABABA UNIVERSITY**
**ADDIS ABABA INSTITUTE OF TECHNOLOGY**
**SCHOOL OF MECHANICAL AND INDUSTRIAL ENGINEERING**

# Static Analysis of Kevlar/E-glass Hybrid Composite Lower Control Arm for Light Weight Vehicle

By: **Tsegaye Abay**
I.D No.: **GSR/0916/09**

A Thesis Submitted to the Graduate School of Addis Ababa University partial fulfillment of degree of masters of Science in mechanical engineering (Specialization Mechanical Design).

Advisor: Dr. Daniel T.
Co Advisor: Mr. Nathnael A. (PhD candidate)

Addis Ababa, Ethiopia
Oct 2018

**Addis Ababa University**
**Addis Ababa Institute of Technology (AAiT)**
**School of Mechanical and Industrial Engineering**

# Static Analysis of Kevlar/E-glass Hybrid Composite Lower Control Arm for Light Weight Vehicle

**By**

Tsegaye Abay

**Approved by Board of Examiners**

| | | |
|---|---|---|
| Dr. Yilma T. | | 16/11/2018 |
| Chairman of school | Signature | Date |
| Dr. Daniel Tilahun | | 14/11/2018 |
| Advisor | Signature | Date |
| Mr. Nathnael A. | | 14/11/2018 |
| Co-Advisor | Signature | Date |
| Dr. Tamrat T. | | 14/11/2018 |
| Internal Examiner | Signature | Date |
| Dr. Samuel | | 14/11/2018 |
| External Examiner | Signature | Date |

## DECLARATION

**Addis Ababa University**

**Institute of Technology**

This is to certify that the thesis prepared by Tsegaye Abay, entitled: Static Analysis of Kevlar/E-glass Hybrid Composite Lower Control Arm for Light Weight Vehicle, do hereby declare this thesis is my original work and that it has not been submitted in full for a degree in any university/institution, which compiles with the regulations of the university and meets the accepted standards with respect to originality and quality.

Tsegaye Abay

Signature _____

Date 14/11/2018

**Place: Addis Ababa, Ethiopia**

This thesis has been submitted for examination with my approval as a university advisor and Co Advisor:

**Advisor:**

Dr. Daniel Tilahun _____ Sign _____ 14/11/2018 Date

**Co Advisor:**

Mr. Nathnael A. _____ Sign _____ 14/11/2018 Date

(PHD candidate)

# Acknowledgment

First of all I want to express my enormous thanks to the Almighty GOD for his continuous and priceless help and permission to finish my graduate study successfully.

Next I would like to express my deep sense of gratitude towards my advisor Dr. Daniel Tilahun and Co Advisor Mr. Nathnael A. for their invaluable guidance, encouragements and inspiration during the path of this work. Their continued interest was a constant source of motivation for me throughout the work.

I would like to extend my special thanks to all my families and friends for their kind help and cooperation in various ways during this thesis work.

# Abstract

The suspension system is one of the key components of the automobile. This system is the mechanism that physically separates the vehicle body from the wheels. Automobile industry is regularly trying to reduce the weight of the vehicle for better acceleration, maneuverability, better responses and shorter braking distance. In this study, Static Analysis of Kevlar/E-glass hybrid composite lower control arm was done by comparing the conventional steel lower control arm which is used by LIFAN 530 VIP a four-wheel light vehicle. The main idea behind this work is to replace the existing steel lower control arm material with a laminated Kevlar/E-glass hybrid composite lower control arm with the same width, thickness and load carrying capacity (removed holes and irregular shape). In this study, the main investigation of the study is to reduce the weight of product while upholding its strength. For this study 50-60% volume fraction of fiber and 40-50% volume fraction of the matrix was selected and done by to reduce the cost of the fiber, increase strength of lower control arm, minimize the brittle of the lower control arm suspension system, and minimize the overall weight of the lower control arm suspension system. The static vertical force acting on lower control arm calculation was done. In this paper, Kevlar/E-glass hybrid composite material was manufactured using Hand Lay-up process for different composition ratio of 60%/40%, 55%/45% and 50%/50% of fiber/epoxy and its mechanical performance such as the tension, compression and flexural properties was determined using laboratory experiments. The work also gives focus on the application of FEA concepts to compare LIFAN 530 VIP conventional steel and laminated Kevlar/E-glass hybrid composite lower control arm. In the present work modeling of lower arm was done with SOLIDWORK and total deflection and equivalent (Von misses) stresses induced in the two lower arms are done on ANSY18.2 workbenches were compared. Finally, new design has been developed to reduce stresses and weight existing in the current design with structural steel lower control arm. The newly designed Kevlar/E-glass hybrid composite suspension arms achieve an average weight saving of 44.5% with respect to the baseline steel arms.

**Key words:** lower arm suspension system, laminated Kevlar/E-glass hybrid composite, solid work software, FEA, design and development

# Table of Contents

# List of Figure

# List of Table

# List of Abbreviations and Acronyms

ANN= Artificial neural network

CAD = computer aided drawing

CCD= Central composite design

CFRP = Carbon fiber reinforced plastic

DOE= Design of experiment

FEA= finite element method

FEM = Finite element modeling

FRP = Fiber reinforced plastic

GPa = Giga Pascal

$\frac{g}{cm^3}$ = Gram per centimeter cubed

HS = high strength

Kg = kilo gram

RBFNN=radial basis function neural network

M = Mass

MMCs = Metal matrix composite

mm = millimeter

MPa = Mega Pascal

N = Newton

PAN = poly acryl nitrile

PMCs = Polymer matrix composite

ROM = rule of mixture

UV = ultra violet

W = weight

RSM=Response surface methodology

VIP= very important person

℃=Degree centigrade

# CHAPTER ONE

# Introduction

## 1.1 Back ground

The suspension system is one of the key components of the automobile. The primary function of the suspension system should have fulfilled for pretentious requirements about stability, safety and maneuverability [1]. The suspension system of the vehicle performs multiple tasks such as maintaining the contact between tires and road surface, providing the vehicle stability, protecting the vehicle chassis of the shocks excited from the uneven road surfaces, etc. This system is the mechanism that physically separates the vehicle body from the wheels and carries the vehicle body transmits all forces between the body and the wheels [1, 2]. Suspension is the system which consists of shock absorber, springs and control arms. Suspension control arm is one of the main components in the suspension systems [3]. The general function of control arm is to keep the wheels of a motor vehicle from uncontrollably swerving when the road conditions are not smooth. The control arm suspension normally consists of upper and lower arms. The upper and lower control arms have different structures based on the model and purpose of the vehicle [2, 3].

The lower control arm is the most vital component in a suspension system. Lower control arm allows the wheels to have up and down motions. It is usually a steel bracket; one end is mounted on the chassis using the rubber bushings and the other end supports the lower ball joint [2, 4, 5]. Significant amount of load is transmitted through the control arm then maintain the contact between the wheel and the road and provides better control of the vehicle. The lower control arm is the better shock absorber than the upper arm because of its position and load bearing capacities. During the actual working condition, the maximum load is transferred from upper wishbone arm to the lower arm, which is the possibility of failure & bending of lower wishbone arm at the ball joint location as well as control arm.

The energy crisis continues to expand globally, fossil fuels are declining, global temperatures are rising, air quality is getting worse, so energy saving and emission reduction is the subject of today's era. Data shows that every 10% reduction in car weight can reduce fuel consumption by 5%-20% [14]. Therefore, the development of lightweight cars has become the mainstream in the car manufacturers: Not only for fuel vehicles, but also for new energy vehicles. Now the method of vehicle lightweight is mainly from three aspects, one is to optimize the design of the body structure

and optimize the size of the various parts of the car to achieve the purpose of lightweight; the second is to use of lightweight materials, such as alloy, plastic, fiber reinforced composite materials, etc. [45]. The characteristic of such materials is light and of high strength; starting from material replacement has become the mainstream method of lightweight car; the third method is to optimize the manufacturing process; through the manufacturing process, the purpose of lightweight can be achieved [48]. As the structure has been difficult to further improve the weight of parts and manufacturing process optimization also requires long-term practice to explore, the lightweight design from the material has become the mainstream direction.

Among the many lightweight materials, hybrid composite materials are balanced strength and stiffness, balanced bending and membrane mechanical properties, balanced thermal distortion stability, reduced weight and/or cost, improved fatigue resistance, reduced notch sensitivity, improved fracture toughness and/or crack resisting properties, and improved impact resistance.

## 1.2 Problem Statement

Automobile industry is regularly trying to reduce the weight of the vehicle component by replacement of steel with composite due to its high strength to weight ratio. Low weight of vehicle leads to better acceleration, maneuverability, better response and shorter braking distance.

The main issue of this paper has to satisfy the interest an automobile industry and better to introduce a new lower control arm suspension system made up of Kevlar/E-glass hybrid composite material to reduce the overall weight of lower control arm suspension system and improve load carrying capacity of the lower control arm. Finally, the new lower control arm suspension system composed of Kevlar/E-glass hybrid composite material will be high strength to weight ratio property, less cost and weight, safe in every design aspect and a better choice to keep the quality of the vehicle for comfortable on road condition.

## 1.3 Objective

### 1.3.1 General Objective

The aim of this thesis paper is a Static Analysis of Kevlar/E-glass Hybrid Composite Lower Control Arm suspension system for commercial Light Weight Vehicle.

### 1.3.2 Specific Objective

In order to meet the main objective of the study, the following specific objectives are adopted:

- Determine volume ratio fiber to matrix of lower control arm suspension system.
- Determine maximum vertical force acting on lower control arm suspension system.
- Manufacturing of hybrid composite plate and specimen preparation.
- Experimental test of tensile, flexural, compressive taste and determine their mechanical property.
- Modeling of the shape and dimension of both steel and composite lower control arm suspension system using SOLID WORKS.
- Conduct appropriate deflection and stress analysis of lower control arm by FEA using ANSYS.
- Comparing weight, load deflection and stress of current structural steel with hybrid composite lower control arm.

## 1.4 Scope and Limitation

### 1.4.1 Scope

In this thesis conducted on analytical solution, force calculation, modeling, finite element analysis, manufacturing composite plate and experimental testing using different machine of lower control arm suspension system made of Kevlar/E-glass with epoxy composite material.

### 1.4.2 Limitation

The study of Kevlar/E-glass with epoxy composite material was not a simple work. The study needs the high accuracy of sample preparation and well-calibrated testing machines. The limitation that challenges the study was:

- Absence of precise tools which are used to prepare the sample accurately according to the ASTM standards.
- The absence of exact calibrated Universal Test Machine (UTM).
- The absence of a machine for leveling the end surface of samples for compressive test.

## 1.5 Methodology

In order to completed this paper for the static analysis of lower control arm suspension system for a commercial light weight vehicle made up of composite material the following general methodologies are used.

1) **Data Collection:** further study the material, manufacturing and FEA method, design, modeling and static analysis of existing lower control arm suspension system. And collect relevant data from primary and secondary data. Primary data (different organization center) and secondary data (international journals, books, conference paper and others).
2) **Analytical solution**: determine composition ratio Kevlar/E-glass fiber to matrix and determine the maximum vertical force acting on lower control arm suspension system.
3) **Fabrication of hybrid composite plate:** by using hand lay-up process and take different fiber/matrix volume ratio prepared hybrid composite plate. We cut our test piece for testing with the required dimensions.
4) **Experimentation:** tensile, compression and flexural or bending tests are conducted on testing machine and calculated.
5) **Modeling:** modeling of the shape and dimension of steel and composite lower control arm suspension system using SOLIDWORK.
6) **Finite element analysis:** conduct appropriate analysis of lower control arm by finite element analysis (FEA) using ANSYS and obtain the load deflection characteristics and determine the van-miss stress-strain.
7) **Compare result:** finally compare mass, deflection and stress of steel and composite lower control arm.

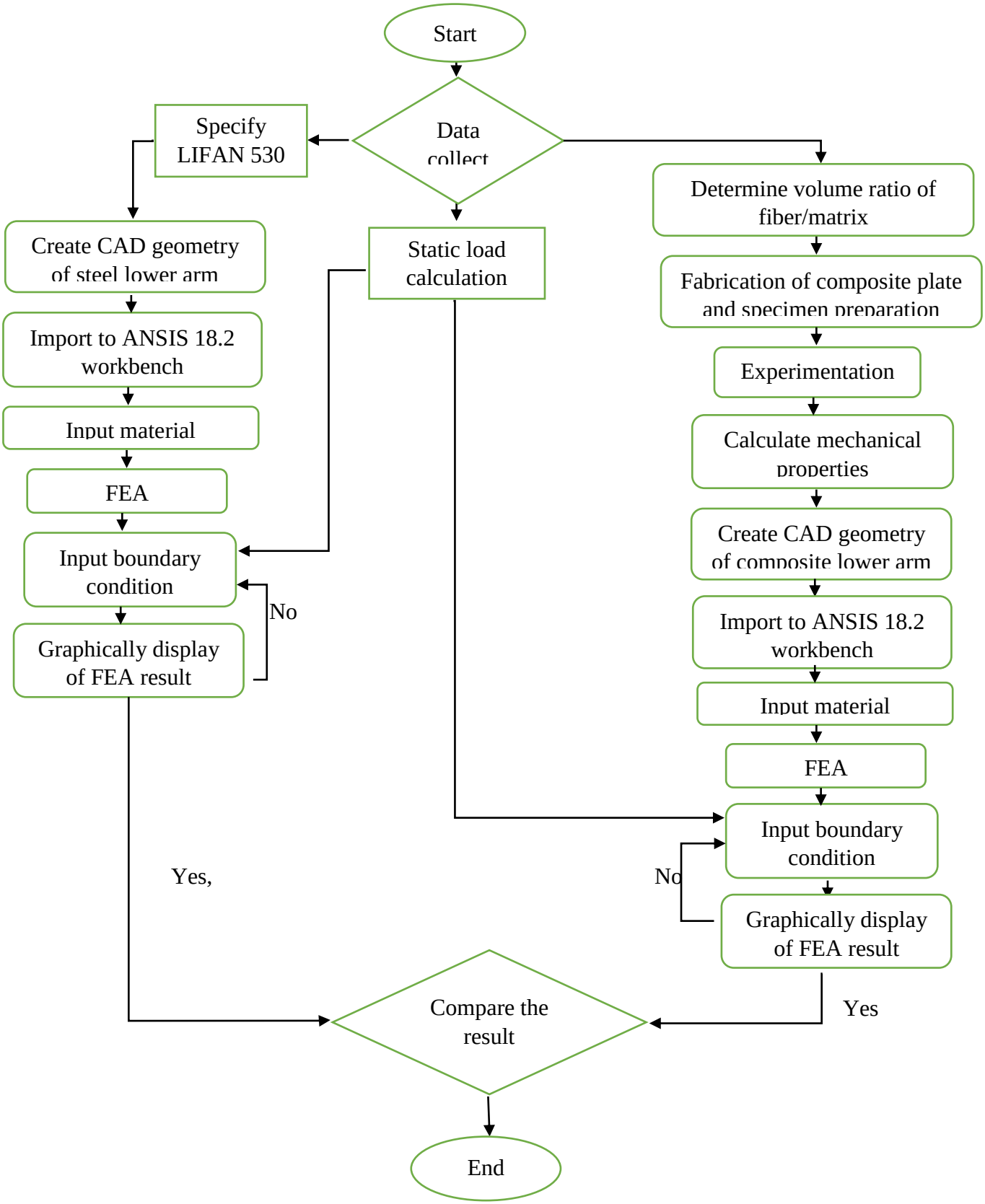


Figure 1.8. Structural development of lower control arm suspension system for light weight vehicle

## 1.6 Organization of the Thesis

This thesis is organized into five chapters.

**In chapter one:** the description of suspension system, problem justification, objectives to be achieved, scope and limitation the methodology are discussed.

**In chapter two:** composite materials are described and literatures relevant to this work are reviewed.

**In chapter three:** focused on selection of materials, specifications/dimensions of lower control arm, statically analysis, modeling, finite element analysis of laminated Kevlar/E-glass hybrid composite and structural steel lower control arm.

**In chapter four**: addresses the results of the analysis are summarized and discussions are made based on the outputs of the FEM.

**In chapter five:** gives a conclusion achieved from this work, recommendation and propose future work.

# CHAPTER TWO

# Literature Review

## 2.1 Composite material

A composite material is made by combining two or more materials to give a unique combination of properties. The constituents are combined at a macroscopic level and are not soluble in each other. One constituent is called the matrix phase and other one in which is embedded in the matrix is called the reinforcing phase. The matrix phase materials are generally continuous. The reinforcing phase material may be in the form of fibers, particles, or flakes [7, 8, 9].

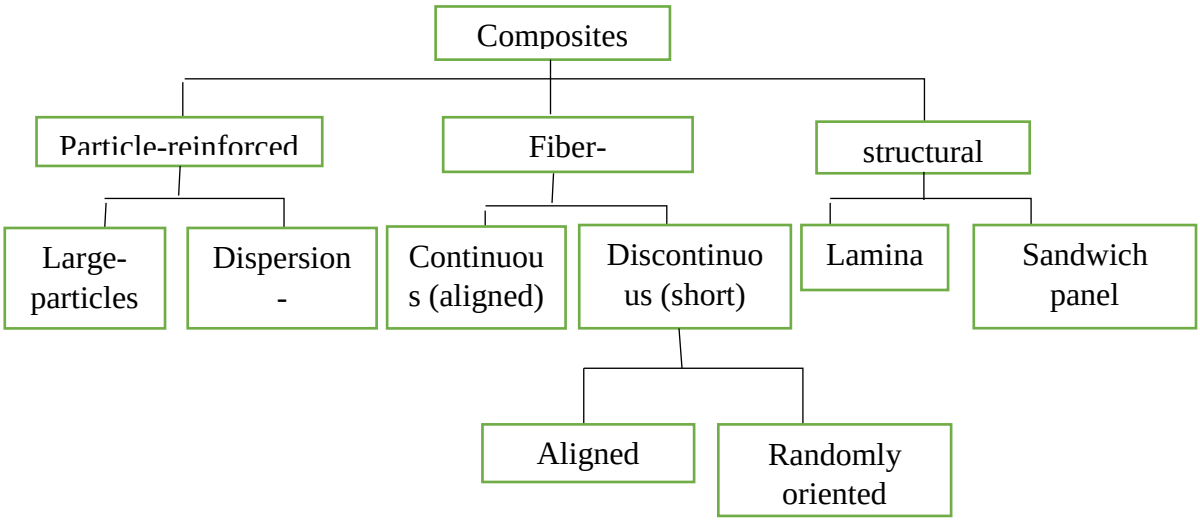


Figure 2.1. Classification of composite materials [10]

In forming fiber reinforcement, the assembly of fibers to make fiber forms for the fabrication of composite material can take the following forms: [9]

- **One-dimensional:** unidirectional tows, yarns, or tapes
- **Bi dimensional:** woven or non-woven fabrics (felts or mats)
- **Tridimensional:** fabrics (sometimes called multidimensional fabrics) with fibers oriented along many directions (>2)

### 2.1.1 Fiber materials

Reinforcements are important constituents of a composite material and give all the necessary stiffness and strength to the composite. These are thin rod like structures. The most common reinforcements are glass, carbon, aramid and boron fibers. Carbon and Kevlar fibers are reserved for high performance components. Typical fiber diameters range from 5 mm to 20mm. In general, fibers are

made into strands for weaving or winding operations. For delivery purposes, fibers are wound around a bobbin and collectively called a "roving." An untwisted bundle of carbon fibers is called "tow." In composites, the strength and stiffness are provided by the fibers. Fibers for composite materials can come in many forms, from continuous fibers to discontinuous fibers, long fibers to short fibers, organic fibers to inorganic fibers. The most widely used fiber materials in fiber-reinforced plastics (FRP) are glass, carbon, aramid, and boron [8, 9].

Following are a few notes on the fibers:

- **Glass fiber:** The filaments are obtained by pulling the glass (silicon + sodium carbonate and calcium carbonate; $T > 1000$℃ through the small orifices of a plate made of platinum alloy.
- **Kevlar fiber:** This is an aramid fiber, yellowish color, made by DuPont de Nemours (USA). These are aromatic polyamides obtained by synthesis at -10℃, then fibrillated and drawn to obtain high modulus of elasticity.
- **Carbon fiber:** Filaments of poly acrylonitrile or pitch (obtained from residues of the petroleum products) oxidize at high temperatures (300 ∞℃), and then heated further to 1500 ∞℃ in a nitrogen atmosphere. Then only the hexagonal carbon chains remain. Black and bright filaments are obtained. High modulus of elasticity is obtained by drawing at high temperature.
- **Boron fiber:** Tungsten filament (diameter 12 mm) serves to catalyze the reaction between boron chloride and hydrogen at 1200℃. The boron fibers obtained have a diameter of about 100 mm (the growth speed is about 1 micron per second).
- **Silicon carbide:** The principle of fabrication is analogous to that of boron fiber: chemical vapor deposition (1200∞℃) of methyl tri-chlorosilane mixed with hydrogen.

### 2.1.2 Matrix materials

Matrix surrounds the fibers and thus protects those fibers against chemical and environmental attack. For fibers carry maximum load, the matrix must have a lower modulus and greater elongation than the reinforcement. Matrix selection is performed based on chemical, thermal, electrical, flammability, environmental, cost, performance, and manufacturing requirements. The matrix determines the service operating temperature of composite as well as processing parameters for part manufacturing [8, 9].

The matrix materials include the following:

- **Polymeric matrix:** Thermoset and thermoplastics.

**Thermoset Curing Process**

Thermoset plastics contain polymers that cross-link together during the curing process to form an irreversible chemical bond. The cross-linking process eliminates the risk of the product re-melting when heat is applied, making thermosets ideal for high-heat applications such as electronics and appliances.

**Features & Benefits**

Thermoset plastics significantly improve the material's mechanical properties, providing enhances chemical resistance, heat resistance and structural integrity. Thermoset plastics are often used for sealed products due to their resistance to deformation.

**Pros**

- More resistant to high temperatures than thermoplastics
- Highly flexible design
- Thick to thin wall capabilities
- Excellent aesthetic appearance
- High levels of dimensional stability
- Cost-effective

**Cons**

- Cannot be recycled
- More difficult to surface finish
- Cannot be remolded or reshaped

Thermoset resins (polyesters, phenolic, melamine's, silicones, polyurethanes, epoxies).

**Thermoplastics Curing Process**

Thermoplastics pellets soften when heated and become more fluid as additional heat is applied. The curing process is completely reversible as no chemical bonding takes place. This characteristic allows thermoplastics to be remolded and recycled without negatively affecting the material's physical properties.

**Features & Benefits**

There are multiple thermoplastic resins that offer various performance benefits, but most materials commonly offer high strength, shrink-resistance and easy bendability. Depending on the resin, thermoplastics can serve low-stress applications such as plastic bags or high-stress mechanical parts.

**Pros**

- Highly recyclable
- Aesthetically-superior finishes
- High-impact resistance
- Remolding/reshaping capabilities
- Chemical resistant
- Hard crystalline or rubbery surface options
- Eco-friendly manufacturing

**Cons**

- Generally, more expensive than thermoset
- Can melt if heated

Thermoplastic resins (polypropylene, poly phenylene sulfate, polyamide, poly ether-ether ketone, etc.).

- **Mineral matrix:** silicon carbide, carbon. They can be used at high temperatures
- **Metallic matrix:** aluminum alloys, titanium alloys, oriented tactics.

### 2.1.3 Hybrid composite material

Hybrid composites contain more than one type of fiber in a single matrix material. In principle, several different fiber types may be incorporated into a hybrid, but it is more likely that a combination of only two types of fibers would be most beneficial. [47] Hybrid composites have more than one kind of fiber embedded in the matrix. They have been developed as a structural material as a logical sequel to conventional composites, which have only one kind of fiber. Hybrid composites have unique features that can be used to meet diverse and competing design requirements in a more cost-effective way than either advanced or conventional composites. Some of the specific advantages of hybrids over conventional composites are-balanced strength and stiffness, balanced bending and membrane mechanical properties, balanced thermal distortion stability, reduced weight and/or cost, improved fatigue resistance, reduced notch sensitivity, improved fracture toughness and/or crack

resisting properties, and improved impact resistance. By using hybrids composite material, it is possible to obtain available compromise between mechanical properties and cost to meet specified design requirements [48].

#### 2.1.3.1 Types of hybrid

There are four general categories of hybrid composite materials [48].

a) **Inter ply (interspersed or core/shell);** the inter ply hybrids consist of plies from two or more different UDC's stacked, in a specified sequence.
b) **Intra ply;** Intra ply hybrids consist of two or more different fibers mixed in the same ply
c) **Inter ply/intra ply;** Inter ply/intra ply hybrids consist of plies of intra ply and Inter ply hybrids stacked in a specified sequence. The Inter ply and intra ply hybrids generally have the same matrix and the laminate is fabricated by the occurring procedure according to specifications provided by the prepreg tape supplier. If the plies: for these hybrids are made from different matrices, the hybrid is fabricated by a curing procedure that is compatible with both systems.
d) **Super hybrid;** the super hybrid is fabricated 6 by adhesively bonding metal foils, boron/aluminum (or other metal matrix) UDC plies, anal resin/fiber prepreg UDC with an adhesive that has the same-curing cycle as the prepreg.

### 2.1.4 Classification of Laminates:

Laminates are classified depending upon the stacking sequence nature. This classification is very helpful in the laminate analysis as some of the coupling terms become zero under specific laminate sequence and their arrangement with respect to the mid-plane [37, 38].

**A. Symmetric Laminates:**

A laminate is called symmetric when the material, angle and thickness of the layers are the same above and below the mid-plane.

B. **Cross-Ply Laminates:**

A laminate is called cross-ply laminate if all the plies used to fabricate the laminate are only 0° and90°.

**C. Balanced laminate**

A laminate is called balanced laminate when it has pairs of plies with the same thickness and material and the angles of plies. Whenever possible, stacking sequences should be balanced, with the same number of $+\theta°$ and $-\theta°$ plies ($\theta \neq 0°$ and $\theta \neq 90°$).

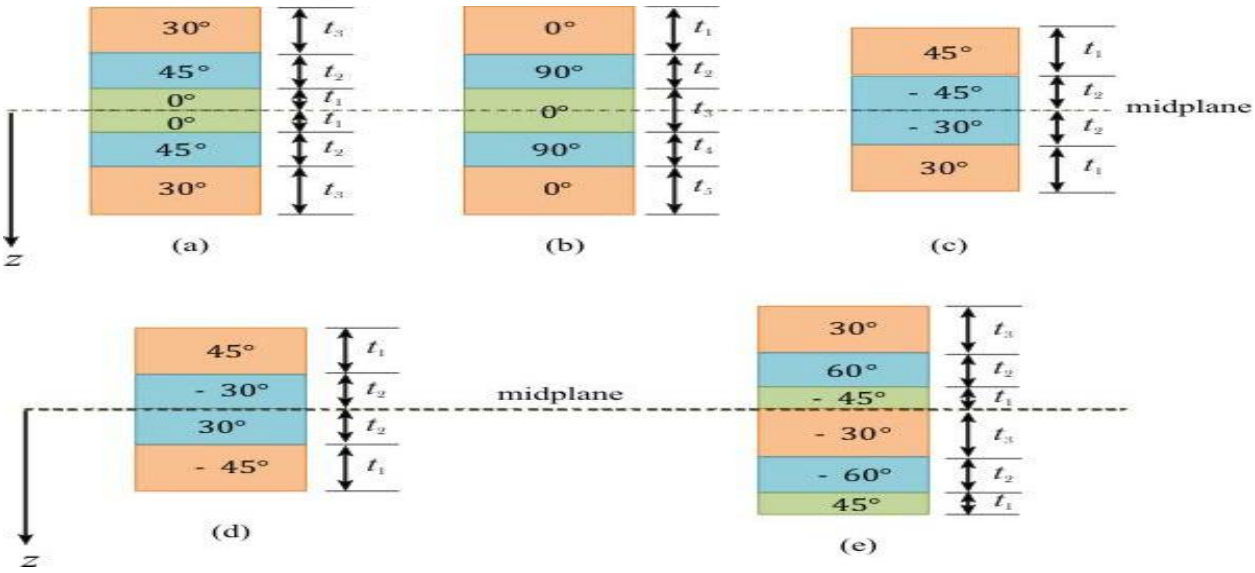


Figure 2.2. Classification of laminates examples (a) Symmetric laminate (b) Cross-ply laminate (c) Angle-ply laminate (d) Anti-symmetric laminate and (e) Balanced laminate [37]

**D. Angle-Ply Laminates:**

A laminate is called angle-ply laminate if it has plies of the same thickness and material and are oriented at $+\theta°$ and $-\theta°$ plies.

**E. Anti-symmetric Laminates:**

A laminate is called anti-symmetric when the material and thickness of the plies are same above and below the mid-plane, but the orientation of the plies at the same distance above and below the mid-plane have opposite signs.

## 2.1.5 Fabrication of Composites plates

FRP fabrication consists of suitably combining reinforcement material (Kevlar fiber, glass fiber or carbon fiber) with a matrix material (resin) by a suitable production process and of curing the resulting molding into the required product. There are many manufacturing methods that could be used to manufacture an advanced composite, these include: [43, 44, 45]

I. **Hand lay-up method:** It is the oldest molding method for making composite products. It requires no technical skill and no machinery. Manual lay-up involves cutting the reinforcement material to size using a variety of hand and power-operated devices. These cut pieces are then impregnated with the wet matrix material, and laid over a mold surface that has been coated with a release agent and then typically a resin gel-coat. The impregnated reinforcement material is then hand-rolled to ensure uniform distribution and to remove trapped air. More reinforcement material is added to the required part thickness has been built-up.

II. **Automated Lay-Up:** The productivity of the manual lay-up can be automated using CNC machines. These machines are used for both prepreg tapes-laying and prepreg fiber-placement primarily in the aerospace industry. There is virtually no limit to the size of the work that can be tape-rolled, but the shape has to be relatively flat to butt each successive row without gaps, overlaps or wrinkles.

III. **Spray-Up:** It is sprayed onto a prepared mold surface using a specially designed spray gun. This gun simultaneously chops continuous reinforcement into suitable lengths as it sprays the resin. After lay-up, the composite parts must be cured. Curing can take place at room temperature, often with heated air assist. A vacuum is slowly created under the bag, forcing it against the lay-up. This draws out entrapped air and excess resin. Vacuum bag molding is effective in producing large, complex shaped parts.

IV. **Filament Winding:** Fulminate winding refers to wrapping a narrow fiber tow or band of tows of resin impregnated fiber around a mandrel of the shape to be produced. When the mandrel is removed, a hollow shape is the result. Uses for filament winding include pipe, tubing, pressure vessels, tanks and items of similar shape. Filament winding is typically applied using either hoop or helical winding.

V. **Pultrusion:** Pultrusion is a continuous process used primarily to produce long, straight shapes of constant cross-section. Pultrusion is similar to extrusion except that the composite material is pulled, rather than pushed, through a die. Pultrusions are produced using continuous reinforcing fibers called 'roving' that provide longitudinal reinforcement, and transverse reinforcement in the form of mat or cloth materials.

VI. **Resin transfer molding:** Resin transfer molding or 'RTM' produces large, complex items such as bath and shower enclosures, cabinets, aircraft parts, and automotive components. In this process, a set of mold halves is loaded with reinforcement material then clamped together. The resin is then pumped or gravity fed into the mold infusing the reinforcement material. Once the mold is filled with resin, it is plugged and allowed to cure. After curing, the mold halves are separated and the part removed for final trimming and finishing.

- Many researchers have been conducted on the analysis of weight, deflection and stiffness of lower control arm suspension system that made up of composite material and other materials. The research work related to lower control arm, which are assisting to introduce the current study. Some of them are direct and the others are indirectly related to the current study. The journals and papers discussed on this subtitle are categorized under the materials, method of manufacturing and conditions.

## 2.2 Previous Work Related with lower control arm using Composite materials, finite element method, fiber to matrix ratio and stacking sequence

**Ramesh et.al [11].** The main objective of this paper is to improve the stability of the Double Wishbone suspension of commercial vehicle. The complete work is done on the left hand Lower Control Arm of the four-wheel drive. This paper focuses on the Finite Element Analysis of the Stress-Strain Analysis of Lower Wishbone arm in aim to improve and modify the existing design. For this work, Carbon Fiber Reinforced Polymer has been deployed in place of Mild Steel that is in use for a considerably longer period in Automobile industry. From this work, it is evident that under the static load conditions, the deflection and the stresses involved with the steel lower wishbone arm and composite lower wishbone arms are found to exhibit great deviation in their performance. Deflection in the Composite lower wishbone arm has been found higher than the steel lower wishbone arm provided the same loading condition environment. The redesigned suspension arms can also achieve an average weight saving of 18% with respect to the baseline Steel Lower Wishbone Arm.

**Władysław et.al [12].** In this paper presents the theoretical discussion on the possibility of replacing the actual design of the steel control arm of the MacPherson column suspension system of the structure made of polymer composite material. Today exist the solutions of the whole suspension using composite materials and it is justified by the synergy effects possible to obtain. The composite control arm was modeled while maintaining the shape and dimensions of the steel control arm. The number of layers and the orientation of the reinforcement were selected following the criterion of maximum allowable stresses and strains. The analysis was performed by MES method in SOLIDWORKS Premium software using a composite module. The analysis was performed for the loads acting on the control arm during braking, acting of the maximum lateral forces and the simultaneous action of lateral forces and braking forces.

**Paolo et.al [13].** This paper focuses on the development of the Forged Composite suspension arms, whose preliminary design, FEA modeling, and testing was performed at the ACSL/ UW. Detailed CAD design of the arms, as well as both Forged Composite and of the control arms manufactured using this technology. The process, which uses high pressures, but conventional temperatures, is used to manufacture parts with complex geometries and subject to combined loadings, which were typically manufactured as aluminum and titanium forgings. The Carbon Fiber Sheet Molding Compound (CFSMC) material is supplied by Quantum Composites. The carbon fiber content is 53% by weight. The paper reviewed the design approach for the lower front suspension arm, which is the most critical of the set. This paper focuses on the development of the suspension control arms, which aim at a 30% weight reduction, as well as a cost and cycle time reduction with respect to the baseline forged aluminum construction.

**Zengfeng et.al [14].** Based on the principle of lightweight design, a method of using carbon fiber reinforced composite instead of traditional metal materials to design automobile carrier can be proposed. In this paper is a typical McPherson suspension arm whose geometry is A-shaped. After measuring the size of the actual swing arm model, the model is simplified. This paper considers three kinds of extreme motion conditions of the suspension, which is the maximum working condition of the vertical force, the maximum working condition of the lateral force and the maximum working condition of the braking force. The type of reinforcement used in this paper is carbon fiber (T300), the matrix is epoxy (5208), their respective volume scores are $V_f = 0.7$ and $V_m = 0.3$. Finally, the carbon fiber swing arm not only meets the strength requirement, but also reduces the weight of 46.8% than the steel swing arm, which is 34.5% lower than that of the aluminum alloy arm.

**Christian et.al [15].** The materials used for the suspension arm were procured from the Advanced International Multi-tech's PPG Division. The part is composed of two distinct phases: a carbon fiber SMC material and a unidirectional prepared. The SMC material consists of 25.4mm long PAN based 12K carbon fiber tows in a vinyl ester matrix. Fiber content is 53%w/w. The unidirectional prepared is a 200gsm 12K standard modulus carbon fiber fabric in a toughened epoxy matrix. Fiber content is 60%w/w. An aluminum suspension control arm was successfully redesigned for composite material substitution. The weight of the composite arm is 40% lower than the baseline, with only marginal increase in deflection. A weight saving of this magnitude is made possible by the effective placement of unidirectional fibers.

**M.Sridharan et.al [17].** The work discusses on the model and to perform structural analysis of a lower control arm used in the front suspension system, which is a sheet metal component. Lower

control arm is modeled in Pro-E software for the given specification. To analyze the lower control arm, CAE software is used. The load acting on the control arm is dynamic in nature, buckling load analysis is essential. First finite element analysis is performed to calculate the buckling strength, of a control arm. The FEA is carried out using Solid works stimulation package. The existing design has been modified, by reducing the thickness of the existing profile and the reinforcement plate has been proposed. The optimization of lower control arm is done by applying the DOE method. For the modified design the structural rigidity has been increased for the LCA, when compared to the existing design. Finally, the mass of the control arm has been reduced up to 13.8 % when compared with existing models.

**SangHyuk et.al [16].** This study shows topology optimization of lower control arm (LCA), made of carbon fiber reinforced plastic (CFRP) that was originally composed of aluminum alloy. T700 carbon fiber (CF) of TORAY and EPOXY 1800 matrix of RESOLTECH is selected as constituent materials of CFRP and their elastic properties are obtained from the material data sheet provided by the company. In composites, CF volumetric portion is fixed at 60 %. The design target is to reduce the LCA weight while satisfying the multiple constraints, including required stiffness and durability conditions at the same time. As a result, the authors propose the new design of CFRP LCA with 30 % weight reduction compared to Al alloy LCA.

**Swapnil et.al [18].** This study deals with Finite Element Analysis of the Lower control arm of Mac-pherson suspension system and it's optimizing under static loading condition. The existing design of lower control arm from one of the light commercial vehicle is selected for the study. In order to determine the deformation and stress distribution in the current design, the finite element analysis is carried out. The baseline model of the lower control arm is created by using solid modeling software viz. CATIA. The present study is used to reduce the weight and cost of the lower control arm by keeping the factor of safety within permissible limits. As deflection and stress of modified LCA is within the range. Thus, the modified design is safe. The weight of the final optimized model is 0.99 kg. The total reduction in mass is observed 17.5% by keeping Factor of safety for optimized design within permissible limits.

**Hardial et.al [2].** This paper deals with the finite element analysis for front lower control arm suspension system of the four-wheel suspension system. Finite element analysis methods are used to predict the structural performance of the design. The linear static structural analysis has been carried out for a given model to determine the maximum deflection, stress distribution and its location in the

front lower control arm. It has been observed that stresses, displacements found well within safe limits and structure could withstand the given load. The FEA predictions are validated with experimental data. A bunch of nodes is selected and a rigid element is created. Then load is applied to this rigid element which distributes the load equally on all these nodes. The FEA results have been compared with the experimental results to ensure the feasibility of the model. The results obtained after solving and post processing shows that the model is safe for static loading conditions. Maximum value of von miss's stress and displacement are within safe limits & less than experimental results.

**Vinayak et.al [19].** The key objective of this effort is to carry out static and modal analysis of lower control arm using different materials and also perform topology optimization for achieving weight reduction. This paper deals with calculating the forces acting on lower wishbone arm while vehicle subjected to critical loading conditions. The lower arm suspension has been modeled using Pro-Engineer. Von misses stress –strain is carried out in order to find out maximum induced stress and strain. These analyses were carried using Altair Hyper works and solver used is Radios. From the analyzed results, design parameters were compared for two different materials and best on was taken out. From result obtained it was found that the current design is safe and somewhat overdesign. Optimization reduces weight, product design cycle, time and cost.

**Tilottama et.al [20].** This paper presents the design, modeling and analysis of car front suspension lower arm to study the stress condition and to select the suitable materials for the front suspension lower arm. The main objective of this study was to determine critical locations and strain distributions of the component. The paper aims to complete Finite Element Analysis of the front suspension lower arm, which consist the stress optimization loadings and analysis of deformation. From the review of the literature on structural analysis the lower suspension arm it is seen that there is a scope for research work in the area of stress analysis of the lower suspension arm. As such, it is proposed to carry out theoretical and experimental studies on stress analysis of the lower suspension arm used in light commercial vehicles. These force and torque values are mentioned in the load case. So in this analysis the main concern is to find out the maximum stress region and stress value in control arm and compare this value with tensile yield strength of material and results of the experimental testing of control arm at the same load which are mentioned in load case of control arm.

**Dattatray et.al [3].** This paper describes an analysis of the lower suspension arm using F.E.A. Approach. This paper deals with finite element analysis for MacPherson type suspension system lower control arm (LCA) of 4W suspension system. This paper was prepared CAD Model using

PRO-E Software & finite element analysis using ANSYs software. This paper studies to calculate various dynamic loads like road bump, kerb strike, braking, cornering & acceleration load case. By applying all these forces in X, Y and Z directions perform non-linear static analysis using ANSYs software. It will be going to save the testing as well as validation cost. This paper showed the validation of finite element analysis results with actual physical sample testing. In this Study they concluded that a how much the results by using analysis software as well as physical testing of the model are similar or not.

**Mr. Balasaheb et.al [1].** This paper describes Design, analysis of A-type front lower suspension arm in commercial vehicle. The main objective of this study was to calculate working life of the component under static loading. The A-type lower suspension arm was developed by using CAD software. This paper result was this model imported in the hyper mesh. After meshing apply load on hub bush they found the weaker section in the model. To validate the FEA results we create a typical A-type suspension arm of same material of AISI 1040 as per the consideration in FEA we constraint two bushes and load apply on remaining wheel hub bush on universal testing machine. After trails it is seen that theoretical results agree with the actual test experiments. FEA analysis or software calculations give maximum stress at the contact point with wheel hub is about 280 MPa, and actual experimental tests give maximum stress value of 254 MPa. This shows the fit of the model designed under actual working conditions. The load goes on increasing and at last they found the stress in material at maximum stressed area.

**R. Prashanthasamy et.al [21].** This paper describes Design and analysis of lower wishbone suspension arm using FE approach and the main objective is prepared the existing design of wishbone suspension arm. In this study is made on existing design with aluminum alloy. The 3D model was generated CATIA V5, the FE model will be generated by Hyper Mesh and the Static and dynamic analysis was conducted by Abacus. 3D Cad Model of the design created and FE model of the design was created. Analysis under Static and modal condition was done. They concluded that the stresses and deformation for the existing design with an aluminum alloy is almost maximum compare to AISI 1040 of 218 MPa and 2.062 mm respectively. New Design was developed to reduce stress and deformation existing in the current design with aluminum alloy. Finally, they were concluded that from the FE analysis the new design 1 and new design 2 can be replaced with aluminum alloy existing design with AISI 1040 for Wishbone Suspension System, the stresses are almost reduced to 30% compare to existing design.

**Prof. A. M. et.al [6].** This paper describes Experimental & Finite Element Analysis of Left Side Lower Wishbone Arm of Independent Suspension System. Hence it is essential to focus on the stress, strain analysis study of lower wishbone arm to improve and modify the existing design. Also current conventional material (mild steel) is replaced by composite materials (Carbon fiber polymer). Under the static load conditions deflection and stresses of steel lower wishbone arm and composite lower wishbone arm are found with the great difference. Carbon fiber suspension control arms that meet the same static requirements of the steel ones they replace. Deflection of Composite lower wishbone arm is high as compared to steel lower wishbone arm with the same loading condition. The redesigned suspension arms achieve an average weight saving of 27% with respect to the baseline steel arms.

**Muhamad et.al [22].** The aim of the paper is to FEM analysis of the lower arm, Design the lower arm using CATIA model, making a 3D solid parametric model of suspension link in CATIA software, Meshing the model by 10 nodded tetrahedral elements in ANSYS, Static analysis to find Von-Misses stresses, Static analysis deformation plot in ANSYS and If fails corrective actions for design improvement of suspension link. In this study CAD model was prepared using CATIA v5 software and finite element analysis was done using ANSYS 14.5 software by importing the par solid file to ANSYS. The result obtained from the analysis was studied to check whether the design is safe or not. In some cases, the stresses become more than safe limit. In that case optimization approach is carried out to increase the structural strength of the component.

**Miss. P. B. et.al [4].** In this paper, lower control arm of Indic Vista car is used for analysis. Modal analysis is done on the control arm to find its natural frequency. Modes of vibration that lie within the frequency range of the operational forces always represent potential problems. Mode shapes are the dominant motion of a structure at every of its natural or resonant frequencies. Modes are an inherent property of a structure and do not depend upon the forces that act on it. Existing model is taken and optimized by removing material from high stressed region. Modal analysis is carried out in ANSYS. This optimized model is fabricated and tested on the FFT analyzer for validation.

**A. Kalaiyarasan et.al [23].** The main objective involved is to reduce the un-sprung mass of the vehicle, thereby obtaining a better ride and stability by application of Aluminum alloy. The weight reduction helps to solve the existing problem of increase in weight due to Global standards and Safety norms. Aluminum alloys [Al6065] have high Strength to weight ratio. The recent manufacturing processes have solved the misery of manufacturing using aluminum alloys. This resulted in a strong, eager for Aluminum alloy application in all the fields of engineering. The development stages started in aerospace and aircraft in earlier stages itself. The adaptation into road

vehicle is a subject of study. The project here deals with application of Aluminum alloy with suspension components replacing steel with design change accompanying that can improve the material change aggressively.

**Jagwinder et.al [5].** The aim of the project is to FEM analysis of the lower arm. Hence it essential to focus on the stress and deformation study of the lower suspension arm to develop and the changes in existing designs. CAD model was prepared using CATIA v5 software and finite element analysis was done using ANSYS 14.5 software by importing the para solid file to ANSYS. The static structural analysis was done to find out the stress, deformation and safety factor of the component. The model was meshed using 10-nodes tetrahedral elements. The result obtained from the analysis were studied to check whether the design is safe or not. In some cases, the stresses become more than safe limit. In this case maximum von-misses stress is 211 MPa which is below the yield strength of the material. In stress analysis, the stresses of the material for the given loading condition fall well in within the yield stress i.e. 211.06 MPa. The total deformation due to the force applied on the suspension arm was 0.65515 mm which is maximum was at the ball bearing of the suspension arm. The minimum safety factor was 1.1845 which shows the component is safe.

**Gururaje et.al [26].** Here in this analysis the main concern is to find out the maximum stress region and stress values in the control arm and compare these values with yield strength of materials and the result of experimental testing of control arm at the same load are mentioned in the load case of the control arm. To study the structural stability of lower control arm under turning conditions. The structural strength of lower control arm is good and safe to manufacture with either steel or aluminum. To study the behavior of the structure with different material properties. Strength wise both the materials are better, but if the design is based on the elastic limit (i.e. if the deflection is design criteria) than steel is a better choice. Currently the analysis is done on the topology optimization, but this will only reduce the weight of the component still there is a chance of getting stress concentration.

**Hemin M. et.al [28].** The thesis describes the analysis of lower automobile suspension arm using stochastic design improvement technique. The objectives of this study are to characterize the dynamic behavior, to investigate the influencing factors of lower suspension amusing FEM incorporating the design of experiment (DOE) and artificial neural network (ANN) approach and to analysis the lower suspension arm using the robust design method. The structural 3-D solid modelling

of lower arm was developed using the Solid works computer-aided drawing software. The results can significantly reduce the cost and time to market, improve product reliability and customer confidence.

**Patik S. et.al [29].** The main objective this paper is the complete work of the left hand Lower Control Arm of the four-wheel drive. During the testing force measurement has been done, which is the basis of stress limit check of the Independent Suspension Link in actual working environment. The paper aims at a complete FEM analysis of a suspension link for bending vibrations, pitching, bouncing and combined mode dynamic analysis of deformation and stresses. For these a 3-D solid parametric model of a suspension link is uses for this. As they have studied the result from ANSYs the safe mode by considering the result obtained in step 5, so the method they have used to add U shaped plate for our component to make it stiff and reduce the failure at the chassis connection point is a valid one. Then the study includes the corrective action and implementation by providing an extra you shape bracket for the complete to decrease the stress and deformation limit, concludes our aim of the paper.

**Subhan Ali et.al [39].** In this paper studied that Evaluation of Impact Strength of Epoxy Based Hybrid Composites Reinforced with E-Glass/Kevlar 49. Lay-up placement of Glass fibers/ Kevlar at $0°/90°$ , $45°/45°$ and $30°/60°$ were set for this work. Experimental investigations were conducted to enhance the impact toughness of glass/epoxy and glass/Kevlar epoxy composites. From Dart impact test, it was concluded that orientation GFK $0°/90°$ and $30°/60°$ have improved impact toughness than $45°/45°$ whereas GF $0°/90°$ have the lowest value. But the surface and fracture study suggest that at $0°/90°$ orientation has better fracture strength than other orientations. Therefore, it can conclude that best results can be obtained for designing the structures at $0°/90°$ lay-up placement.

**Sandesh K.J. et.al [40].** In this study observed that, Mechanical characterization of glass/Kevlar - epoxy laminates are done by conducting impact, flexural (3-point bending) test, inter laminar shear strength test and tensile test as per respective ASTM standards. The three types of hybrid composites with different stacking sequence have prepared and tested for mechanical characterization and vibration analysis. The flexural strength is the maximum in the glass fiber reinforced composite and minimum in the Kevlar reinforced composite. Among the hybrid composites the specimen with two-on-two Glass/Kevlar layers gives the good flexural strength. The tensile strength is found to be maximum in the hybrid composite with one-on-one layers and minimum in the glass fiber reinforced

composite. The hybrid composite with stacking sequence one-on-one Glass/Kevlar layers can be rated as the best hybrid composite specimen produced in this work.

**Yash M. et.al [41].** The main aim of the study, the hybrid composite material is prepared by combining Glass and Kevlar fibers with different combination. The characterization in terms of tensile stress and shear stress is determined for all combinations. The Glass fiber and the Kevlar fiber laminates having epoxy resin as the matrix material were prepared using the hand-lay-up method and compression molding process and the dimension of the laminates was 30cmX30cmX3mm**.** After conducting various tests on the Glass-Kevlar hybrid composite following can be concluded that the combination of Glass fiber and Kevlar fibers have led to making of composite that has higher tensile and shear strength also lowering of the cost of composite requiring high strength for primary applications.

**LEVENT et.al [42].** In this study effect of stacking sequence of mechanical properties of stitched composites is studied for low velocity impact damages. Tests were performed for the same volume fraction $(V_f)$ with different hybrid sequence and ply angle. The stacking sequence was proved to be significant for all of the mechanical properties either individually or as an interaction with ply angle using ANOVA analysis. In particular, the tensile behavior of the samples had the strongest contribution from ply order. Volume fraction of glass fibers affected the material properties in different ways. Mechanical properties of the composite were better under low velocity impact, as the glass percentage was higher. The tensile failure behavior of impacted reinforced composites was affected by the interaction of reinforcement property, hybrid order and ply angle.

**GURU RAJA et.al [46].** For the study of the potential of these materials, in this work specimens were prepared with different angle ply orientation of Kevlar/glass hybrid with epoxy resin as an adhesive. Three orientations$0°/90°$, $45°/-45°$and $30°/60°$ were considered for studies. Mechanical properties such as tensile strength, tensile modulus, & peak load of the hybrid composites were determined as per ASTM standards. Vacuum bagging technique was adopted for the fabrication of hybrid specimens. It was observed that angle ply orientation at $0°/90°$showed significant increase in tensile properties as compared to other orientation. Finally, the failure analysis of hybrid composites is also discussed. Experiments were conducted on Glass fiber/ Kevlar fiber/Epoxy resin hybrid angle ply laminates with different fiber orientation to characterize the tensile properties. It is analyzed from the result, those tensile properties for $0°/90°$is more than$45°/-45°$and $30°/60°$ orientation composites. Hence it is preferred orientation with $0°/90°$is best suitable for designing of structures in the field of Aerospace, Marine and Automobile.

# CHAPTER THREE

# Materials, Methods and Conditions

In this work, manufactured Kevlar/E-glass hybrid composite material (in the form lower control arm) is modeled and analyzed using ANSYS 18.2 Workbench Software to meet the final goal of the study that is; the weight of the composite lower control arm is much lower than that of the current conventional steel and the strength to weight ratio is higher for composite lower arm than current steel lower arm with the same design. Then to meet the objective of the study, the details of the materials and methods applied are discussed below.

## 3.1 material

Composite materials were made to reduce the weight of the lower control arm suspension system without any reduction on load carrying capacity [8, 9]. To select the best composite material for the lower control arm suspension system, the tensile strength, compressive strength, bending strength, density, modulus of elasticity and adhesion to the matrix of the material should be investigated.

### 3.1.1 Fiber selection of lower control arm

Fiber reinforcement (FR) composites materials offer a combination of strength and elasticity that are better than conventional metallic materials. Composites are superior because of their low specific-density, strength to weight ratios. Reinforcements are important constituents of a composite material and give all the necessary stiffness and strength to the composite [8, 9]. These are thin rod like structures. The most common reinforcements are glass, carbon, aramid and boron fibers. Aramid fibers provide the highest tensile strength-to-weight ratio among reinforcing fibers. They provide good impact strength. Aramid fibers are light weight, strong, and tough. An advantage of aramid fibers is their high resistance to impact damage, so they are often used in areas prone to impact damage. Service reports have indicated that some parts made from Kevlar absorb up to 8 percent of their weight in water. Therefore, parts made from aramid fibers need to be protected from the environment. It has a natural yellow color and is available as dry fabric and prepare material. Bundles of aramid fibers are not sized by the number of fibers like carbon or fiberglass but by the weight. Glass is an amorphous a material composed of a silica network. There are four main classes of glass used commercially: High alkali (A glass), electrical grade E glass), chemically-resistant modified E glass grade and high strength grade (S glass). E glass fiber is the one most widely-used for reinforcement purposes**.**

Table 3.1. Properties of Kevlar 49 (Composite Materials) [9, 35, 36]

| Reinforcement | E- glass | Kevlar 49 |
|---|---|---|
| Fiber Dia d($\mu m$) | 16 | 12 |
| Density $\rho(kg/m^3)$ | 2600 | 1440 |
| Modulus of Elasticity E(Mpa) | 85,000 | 141,000 |
| Shear Modulus G(Mpa) | 36,000 | 12,000 |
| Poisson Ratio v | 0.25 | 0.4 |
| Tensile strength $\sigma_{Ult}$(Mpa) | 2050 | 3,600 |
| Compressive strength $\sigma_{Ult}$(Mpa) | 4000-5000 | 582.7 |
| Strain to failure or Elongation E(%) | 3.5 | 2.8 |
| Coefficient of Thermal Expansion $\alpha(℃^{-})$ | -0.5× $10^{-5}$ | -0.2× $10^{-5}$ |
| Coefficient of Thermal Conductivity $(W/M\infty C)$ | 1 | 0.03 |
| Heat Capacity $c(J/kg°C)$ | 800 | 1400 |
| Useful Temperature Limit $T_{max}$ (℃) | 700 | >1500 |
| Price 1993 ($/kg) | 2 | 70 |

### 3.1.2 Resin selection of lower control arm

Matrix selection is performed based on chemical, thermal, electrical, flammability, environmental, cost, performance, and manufacturing requirements. The matrix determines the service operating temperature of a composite as well as processing parameters for part manufacturing. Epoxy is a very versatile resin system, allowing for a broad range of properties and processing capabilities. Epoxies are the most widely used resin materials and are used in many applications. By changing the formulation, properties of epoxies can be changed; the cure rate can be modified, the processing temperature requirement can be changed, the cycle time can be changed, the drape and tack can be varied, the toughness can be changed, the temperature resistance can be improved. Epoxy-based composites provide good performance at room and elevated temperatures. Epoxies can operate well up to temperatures of 200 to 250°F, and there are epoxies that can perform well up to 400°F. For high-temperature and high-performance epoxies, the cost increases, but they offer good chemical and corrosion resistance [7, 8, 9].

In general, epoxy resins have the following advantages over the other resin types [34]:

- They have better adhesive properties.

- They have superior mechanical properties, i.e. strength and stiffness.
- They have better resistance to fatigue and micro cracks.
- They have well resistant to water penetration.
- Increased resistance to osmosis (surface degradation due to water permeability) Quantity of resin required.
- Faster cures at room temperature.
- Good chemical resistance properties.

Table 3.2. Epoxy Properties [9]

| Reinforcement | Epoxy |
|---|---|
| Fiber Dia d($\mu m$) | — |
| Density $\rho(kg/m^3)$ | 1200 |
| Modulus of Elasticity E(Mpa) | 4500 |
| Shear Modulus G(Mpa) | 2,260 |
| Poisson Ratio v | 0.37 |
| Tensile strength $\sigma_{Ult}$(Mpa) | 130 |
| Flaxural Modules (MPa) | 125 |
| Compressive strength $\sigma_{Ult}$(Mpa) | 190 |
| Elongation E(%) | 2(100℃) |
| Coefficient of Thermal Expansion $\alpha(℃^{-})$ | $11\times 10^{-5}$ |
| Coefficient of Thermal Conductivity $(W/M\infty C)$ | 0.2 |
| Heat Capacity $c(J/kg°C)$ | 1000 |
| Useful Temperature Limit $T_{max}$ (℃) | 90 to 200 |
| Price 1993 ($/kg) | 6 to 20 |

## 3.2 Specification of lower control arm suspension system

### 3.2.1. Specification from LIFAN 530 VIP data

The main objective of this research paper is development of lower control arm for light weight vehicle using composite material. Chinese vehicle manufacturing lifan motors has a long term vision to invest in new assembly plant in Ethiopia. This move is aimed at expanding lifan's sales and it is making only from the after-sale service it offers to customers [53]. The parts to be assembled are not manufactured here rather imported from china. However, these can lead the company to extra

expense and deny the country's resource. Production of an automotive components indirectly to Ethiopia's ability to generate or save hard currency and provides expanded opportunities for the people can be produced domestically in Ethiopia. Lower control arm is one of the components of the vehicle and to input this industry. Data collect from LIFAN Motors Company of LIFAN 530 VIP specification and listed using table 3.3.

Table 3.3. LIFAN 530 VIP specification

| | |
|---|---|
| Vehicle model | LF7133 |
| Dimension parameter | |
| $L \times W \times H(mm)$ | $4300 \times 1690 \times 1490$ |
| Wheel base (mm) | 2550 |
| Tread(front/rear) (mm) | 1465/1460 |
| Min. Turning radius (m) | 4.8 |
| Min. Ground clearance (empty load mm) | 180 |
| Front/Rear suspension (mm) | 810/940 |
| Curb mass (Kg) | 1140 |
| Gross weight (Kg) | 1515 |
| Trunk volume (L) | 475 |
| Power train system | |
| Engine | LF479Q3-B |
| Displacement (L) | 1.3 LVVT |
| Max. power [Kw/(r/mm)]: | 69KW/600rpm |
| Max. torque [Nm/(r/mm)]: | 119N.m/400rpm |
| Max. speed (Km) | ≥ 170 |
| 100 Km fuel consumption (L) | 6.4 |
| Oil tank volume (L) | 42 |
| Emissions standards | National IV emission |
| Gear box | 5MT |
| Steering gear type | Electric power steering / hydraulic steering |
| Front overhanging | McPherson independent suspension |
| Rear overhanging | Composite semi-trailing arm independent suspension |

### 3.2.2 The current LIFAN 530 VIP lower control arm suspension system specification

Material : stractural steel

Total Mass of lower control arm (including bush and connecting rods): its total wieght is 4.76 Kg

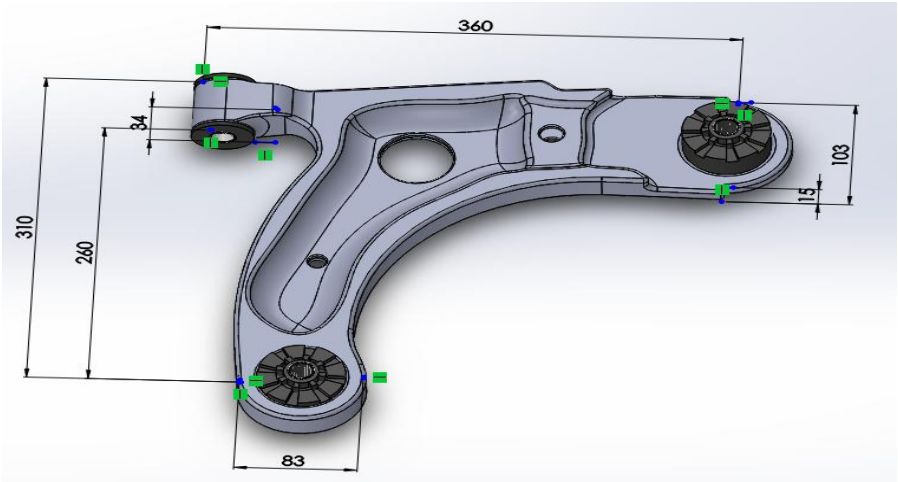


Figure 3.1. Lower control arm of LIFAN 530 VIP (all dimension in mm)

### 3.2.3 Static Load calculation of Lower Control Arm:

Figure 3.2 shows the schematic diagrams of the car and the forces distribution.

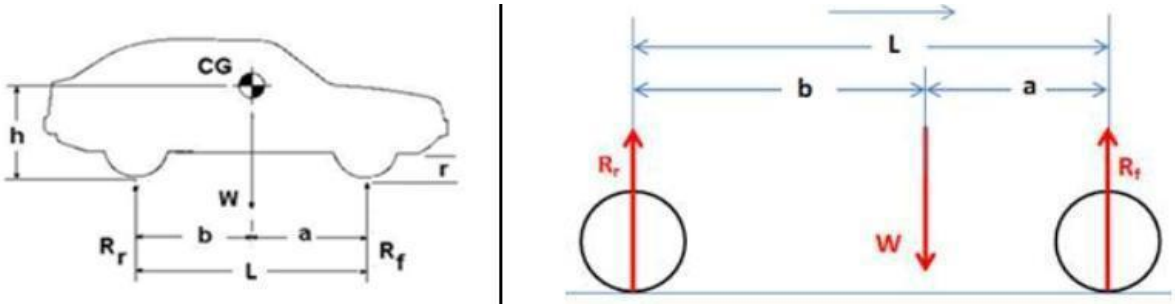


Figure 3.2. Forces on Stationary Car [18]

The weight (W = mg) acts through the center of gravity, and the reaction acts through the contact patches between the tires and the road. The vectors shown represent the combined reactions at both front wheels ($R_f$) and both rear wheels($R_r$) .

The Kerb or curb weight = 1140 Kg

The gross weight (the cars includes the cargo and passengers) = 1515 Kg

Total Weight $W = 1515 \times 9.81 = 14862.15$ N..... (3.1)

Weight must be divided into front axle weight and rear axle weight. It is assumed that 52% of weight taken by front axle, due to mounting of engine on front side and remaining 48% weight taken by the rear axle [18].

Therefore,

Weight on Front axle $(F_1) = 0.52 \text{ x } 14862.15 \text{ N} = 7728.31 \text{ N}$ ..... (3.2)

Weight on Rear axle $F_2 = 0.48 \text{ x } 14862.15 \text{ N} = 7133.83\text{N}$ ..... (3.3)

$$\text{Reaction at each front wheeler} = \frac{\text{Weight on Front axle}}{2} \quad \text{..... (3.4)}$$

$$\text{Reaction at each front wheeler} = \frac{7728.31\text{N}}{2}$$

$$\text{Reaction at each front wheeler} \approx 3850 \text{ N}$$

## 3.3 Analytical solution

### 3.3.1 Rule of mixtures

The rule of mixtures can predict the properties of the particulate composite material because the particulate composite materials depend on relative amount and properties of the individual constituents [9]. Properties that obey rule of mixture can be calculated as the sum of the value of the property of each composite constituent multiplied by its respective volume fraction or weight fraction in the composite mixture. In order to calculate composite properties using the rule of mixtures, the volume and weight fraction of each constituent must be determined. We denote as ply the semi-product "reinforcement + resin" in a quasi-Bi dimensional form. This can be

- A fabric + matrix, or
- woven + matrix.

The ratio of the resin in the laminate can be determined based on literatures or by experience. Then for this study 50-60% volume fraction of fiber and 40-50% volume fraction of matrix is selected. The selection is done by considering the following factors:

- To minimize the cost of the fiber.
- Increase strength of lower control arm
- To minimize the overall weight of the lower control arm suspension system.
- To minimize the brittle of the lower control arm suspension system. Generally, the selected fiber and matrix volume fraction is a good selection to making the composite material for lower control arm.

The formula used to calculate the weight fraction and the volume fraction of fiber and matrix was discussed below using the rule of mixture. According to [9], The Engineering constants of fiber reinforced composites can be determined using the following expressions.

The weight fraction of the fiber is defined as$(W_f)$:

$$W_f = \frac{weight\ of\ fiber}{total\ weight} = \frac{W_f}{W_t} = \frac{W_f}{W_f + W_m} \quad \text{..... (3.5)}$$

Weight fraction of matrix is defined as $(W_m)$:

$$W_m = \frac{weight\ of\ matrix}{total\ weight} = \frac{W_m}{W_t} = \frac{W_m}{W_f + W_m} \quad \text{..... (3.6)}$$

$$W_f + W_m = W_c = 1$$

Volume fraction of the fiber component is defined as $(V_f)$:

$$V_f = \frac{volume\ of\ fiber}{volume\ of\ composite} = \frac{V_f}{V_c} \quad \text{.....(3.7)}$$

Volume fraction of the matrix component is defined as $(V_m)$:

$$V_m = \frac{volume\ of\ matrix\ component}{volume\ of\ composite} = \frac{V_m}{V_c} \quad \text{..... (3.8)}$$

The sum of the volume fractions of all constituents in a composite must be equal to one. In the two component system consisting of one fiber and one matrix, then, the total volume of the composite is:

$V_f + V_m = V_c$, hence $V_m = 1 - V_f$ ..... (3.9)

Similarly the weight fractions $W_f$ and $W_m$ of the fiber and matrix respectively can be defined in terms of the fiber weight$W_f$ , the matrix weight, $W_m$ and the composite weight. $W_c$. Hence,

$W_f = \frac{W_f}{W_c}$ ..... (3.10)

$W_m = \frac{W_m}{W_c}$ ..... (3.11)

$W_m = 1 - W_f$ ..... (3.12)

### 3.3.2 Composite Density

The density of the composite in terms of volume fraction can be found by considering the weight of the composite to be composed of the weights of their constituent,

$W_f + W_m = W_c$ ..... (3.13)

The weights can be expressed in terms of their respective densities and volumes,

$\rho_f V_f + \rho_m V_m = \rho_c V_c$ ……..……..……..... (3.14)

Applying the definitions of volume fraction the density of the composite, $\rho c$ can be expressed in terms of the fiber density $\rho f$ and the matrix density $\rho m$ as:

$\rho_f v_f + \rho_m v_m = \rho_c$ ……..…… (3.15)

We know that the result of volume fraction of fiber = 0.50, 0.55 and 0.60 volume fraction of matrix material (epoxy) = 0.50, 0.45 and 0.30 density of Kevlar 49 fiber = 1.45 $\frac{g}{cm^3}$, density of E-glass fiber = 2.6 $\frac{g}{cm^3}$ and density of epoxy = 1.2 $\frac{g}{cm^3}$ from table.

Now calculate the density of composite Kevlar/epoxy material ($\rho c$):

$\rho_{c1} = \rho_f v_f + \rho_m v_m = 1.45 \frac{g}{cm^3} \times 0.25 + 2.6 \frac{g}{cm^3} \times 0.25 + 1.2 \frac{g}{cm^3} \times 0.5$

$= 0.349 \frac{g}{cm^3} + 0.65 \frac{g}{cm^3} + 0.624 \frac{g}{cm^3}$

$= 1.61 \frac{g}{cm^3}$

$\rho_{c2} = \rho_f v_f + \rho_m v_m = 1.45 \frac{g}{cm^3} \times 0.275 + 2.6 \frac{g}{cm^3} \times 0.275 + 1.2 \frac{g}{cm^3} \times 0.45$

$= 0.399 \frac{g}{cm^3} + 0.715 \frac{g}{cm^3} + 0.54 \frac{g}{cm^3}$

$= 1.673 \frac{g}{cm^3}$

$\rho_{c3} = \rho_f v_f + \rho_m v_m = 1.45 \frac{g}{cm^3} \times 0.3 + 2.6 \frac{g}{cm^3} \times 0.3 + 1.2 \frac{g}{cm^3} \times 0.4$

$= 0.435 \frac{g}{cm^3} + 0.78 \frac{g}{cm^3} + 0.48 \frac{g}{cm^3}$

$= 1.695 \frac{g}{cm^3}$

### 3.3.3 Volume fraction of the fiber and matrix component of the composite

$$\boldsymbol{V_m} = \frac{volume\ of\ matrix\ component}{volume\ of\ composite} \quad \text{…….. (3.16)}$$

$$\boldsymbol{V_f} = \frac{volume\ of\ fiber}{volume\ of\ composite}$$

The pattern is made up of mild steel. The pattern size is $229mm \times 229mm \times 20mm$

Total sample composite Volume $V = L \times W \times t$ ……..……..…… (3.17)

Take $t = 4\ mm$

$$V = 229mm \times 229mm \times 4\ mm = 209764\ mm^3 = 209.76\ cm^3$$

Mass fraction of Kevlar 49 with epoxy resin

$$\frac{M_{fiber}}{M_{epoxy\ resin}} = \frac{\rho_{fiber} \times v_{fiber}}{\rho_{epoxy\ resin} \times v_{epoxy\ resin}} \text{……..……..…… (3.18)}$$

Take, volume fraction of fiber = 50% and volume fraction of matrix material (epoxy resin) = 50%.

$$\frac{\%50}{\%50} = \frac{2025^{(\text{kg}}{}_{\text{m}^3)\times \text{v}_{\text{fiber}}}}{1200^{(\text{kg}}{}_{\text{m}^3)\times \text{v}_{\text{epoxy resin}}}} \quad \text{(3.19)}$$

$$v_{epoxy} = 1.2083 \times v_{\text{fiber}}$$

$$v\text{fiber} + vepoxy = 209.76\ cm3$$

$$v_{\text{fiber}} + 1.2083 \times v_{\text{fiber}} = 209.76\ cm^3$$

$$2.2083 \times v_{\text{fiber}} = 209.76\ cm^3$$

$$v_{\text{fiber}} = \frac{209.76\ \text{cm3}}{2.2083} = 94.0871 cm^3$$

$$M_{fiber} = \rho_{fiber} \times v_{fiber} = 2.025\ ^{(g}{}_{cm^3}) \times 94.0871 cm^3 = 136.4263 g$$

$$v_{fiber}\ v_{epoxy} = 209.76\ cm^3 - v_{fiber}$$

$$v_{fiber}\ V_{epoxy} = 209.76\ cm^3 - 94.0871 cm^3 = 115.673 cm^3$$

$$Mepoxy = \rho epoxy \times vepoxy = 1.2\ g/cm3 \times 115.673 cm3 = 138.8976\ g$$

$$total\ mass = M_{\text{fiber}} + M_{epoxy} = 136.4263 g + 138.8976\ g = 275.234\ g$$

Take, volume fraction of fiber = 55% and volume fraction of matrix material (epoxy resin) = 45%.

$$\frac{\%55}{\%45} = \frac{2025^{(kg}{}_{m^3)\times v_{fiber}}}{1200^{(kg}{}_{m^3)\times v_{epoxy\ resin}}} \quad \text{(3.20)}$$

$$vepoxy = 0.806 \times v_{fiber}$$

$$v_{fiber} + vepoxy = 209.76\ cm3$$

$$v_{fiber} + 0.806 \times v_{fiber} = 209.76\ cm^3\ \ 1.806 \times v_{fiber} = 209.76\ cm^3$$

$$v_{\text{fiber}} = \frac{209.76\ \text{cm3}}{1.806} = 116.1462 cm^3$$

$$M\text{fiber} = \rho\text{fiber} \times v\text{fiber} = 1.45\ g/cm3 \times 116.1462 cm3 = 168.412 g$$

$$V\text{fiber}\ Vepoxy = 209.76\ cm^3 - Vkevlar\ 49$$

$$V_{\text{fiber}}\ V_{epoxy} = 209.76\ cm^3 - 116.146 cm^3 = 93.614 cm^3$$

$$Mepoxy = \rho epoxy \times vepoxy = 1.2\ g/cm3 \times 93.614 cm3 = 112.337\ g$$

$$total\ mass = M_{\text{fiber}} + M_{epoxy} = 168.412g + 112.337\ g = 280.75\ g$$

Take, volume fraction of fiber = 60% and volume fraction of matrix material (epoxy resin) = 40%.

$$\frac{\%60}{\%40} = \frac{2025^{(kg}{}_{m^3)\times v_{fiber}}}{1200^{(kg}{}_{m^3)\times v_{epoxy\ resin}}} \quad \text{..... (21)}$$

$$vepoxy = 0.518 \times v\text{fiber}$$

$$v\text{fiber} + vepoxy = 209.76\ cm3$$

$$v_{\text{fiber}} + 0.518 \times v_{kevlar}\ 49 = 209.76\ cm^3$$

$$1.518 \times v_{\text{fiber}} = 209.76\ cm^3$$

$$v_{\text{fiber}} = \frac{209.76\ \text{cm3}}{1.518} = 138.182cm^3$$

$$M_{fiber} = \rho_{fiber} \times v_{fiber} = 2.025\ ^{(g}{}_{cm^3}) \times 138.182cm^3 = 200.364g$$

$$V\text{fiber}\ Vepoxy = 209.76\ cm^3 - V\text{fiber}$$

$$V_{\text{fiber}}\ 49\ V_{epoxy} = 209.76\ cm^3 - 138.182cm^3 = 71.578cm^3$$

$$Mepoxy = \rho epoxy \times vepoxy = 1.2\ g/cm3 \times 71.578cm3 = 85.894\ g$$

$$total\ mass = M_{\text{fiber}} + M_{epoxy} = 200.364g + 85.894\ g = 286.2576\ g$$

## 3.4. Experimental procedure

### 3.4.1. Fabrication of Hybrid Composites plates

Fiber reinforcement polymer (FRP) fabrication consists of suitably combining reinforcement material (Kevlar fiber, glass fiber or carbon fiber) with a matrix material (resin) by a suitable production process and of curing the resulting molding into the required product. There are many manufacturing methods that could be used to manufacture an advanced composite, and these are shown using figure 3.3 [43, 44, 45].

Figure 3.3. (a) Plain woven Kevlar 49 fiber

figure 3.3 (b) Plain woven E-glass fiber

### 3.4.2 Sample Preparation

A mold is prepared for fabrication of the test pieces. The pattern is made up of mild steel. The pattern size is$229mm \times 229mm \times 20mm$. The process used is Hand Lay-up processed. Figure 3.4 Illustrate the work bench. The mold should be in such a way that the thickness of the test pieces should be 3-4mm as per the ASTM D 638-02a standards. GP RESIN a type of epoxy and BUTANOX M-50 a type of hardener used.

Figure 3.4. Kevlar and E-glass cut with dimension is229mm×229mm×20mm

**a) <u>First Sample:</u>**

The type of Kevlar fiber used is Kevlar 49 and the type of glass fiber used E-glass. The volume fraction of fiber (Kevlar/glass fiber) = 50% and volume fraction of matrix material (epoxy resin) = 50%. Then the Kevlar and E-glass fibers was cut and kept ready. Cross ply laminated used for this paper Kevlar 49 fiber (five layer) and E-glass (four layers) cloths are used for fabrication. As per

ASTM 638-02a Standards and the requirement of 4mm thickness, Kevlar type is found to have 58.4 g and E-glass 89.63g in weight. The five types of Kevlar fibers and four types of E-glass fiber should be cut with a dimension of is$229mm \times 229mm \times 20mm$. These Kevlar and E-glass fibers types should be placed in a specific order as per ASTM D638-02a standards [40, 41]. For embedding reinforcing fibers, 157.08 g of Epoxy resin and mixed thoroughly with 5% (8g) of Hardener. In a mixing jar pot, the mixture should be mixed thoroughly with a long stick. It should be mixed completely so that the resin is uniform in every part of the mixture. The order is represented using figure 3.5:

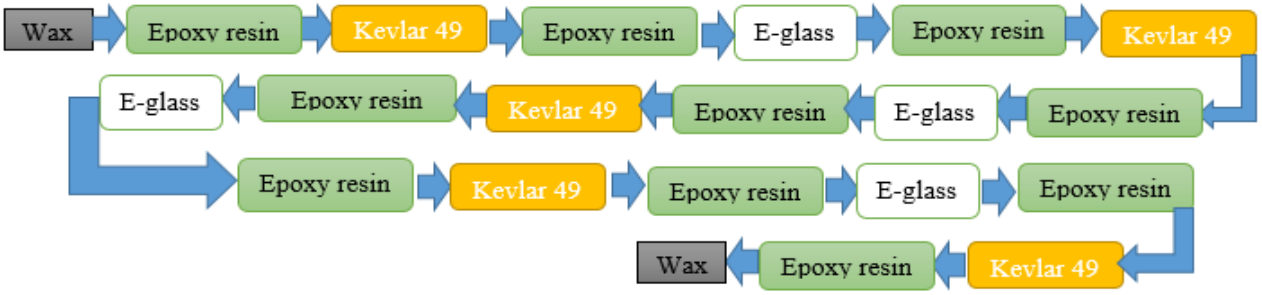


Figure3.5. Plate preparation procedure of fiber 50% and matrix 50%.

The mold is cleaned with Wax so that the epoxy resin will not stick to the mold. After applying Wax, the mold surface should be cleaned with fresh cotton. It should be waited from 15 to 20 min, that before the Epoxy resin mixture is applied on the surface of the mold with the dimensions of$229mm \times 229mm \times 20mm$. First, Kevlar plain weave was placed on the mold surface and Epoxy resin was added over the fiber, on which the E-glass plain weave fiber was applied, subsequently. The sequence was repeated again and again, apply the resin again until the last Kevlar type (see the above order) is layered up. After the last Kevlar type is placed, the epoxy resin is applied on it and quickly the mold is closed. Then apply 50 tons on the upper mold to get the required dimension. It will take nearly some hours for this test piece to dry completely. After six hours the test piece is fully dried, and then should remove our test specimen from the mold.

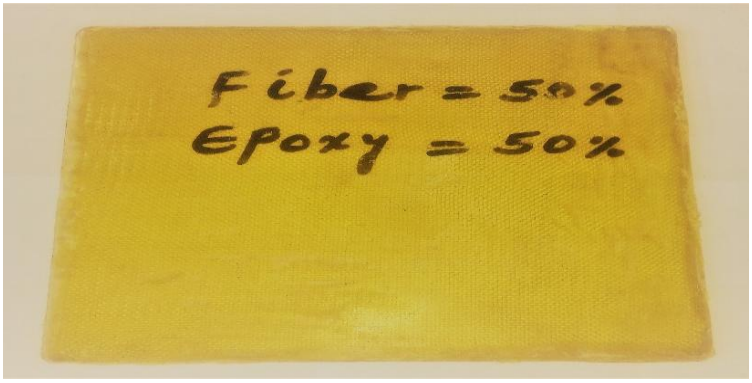

Figure 3.7. Hybrid composite plate of fiber 50% and matrix 50%.

**b) Second Sample:**

The volume fraction of fiber (Kevlar/glass fiber) = 55% and volume fraction of matrix material (epoxy resin) = 45%. Then the Kevlar and E-glass fibers was cut and kept ready. Cross ply laminated used for this paper Kevlar 49 fiber (six layer) and E-glass (five layers) cloths are used for fabrication. Kevlar type is found to have 72.64 g and E-glass 109.83g in weight. The six types of Kevlar fibers and five types of E-glass fiber should be cut with a dimension of is$229mm \times 229mm \times 20mm$. For embedding reinforcing fibers, 145.12 g of Epoxy resin and mixed thoroughly with 5% (7.25g) of Hardener. In a mixing jar pot, the mixture should be mixed thoroughly with a long stick. It should be mixed completely so that the resin is uniform in every part of the mixture. The order is represented using figure 3.7:

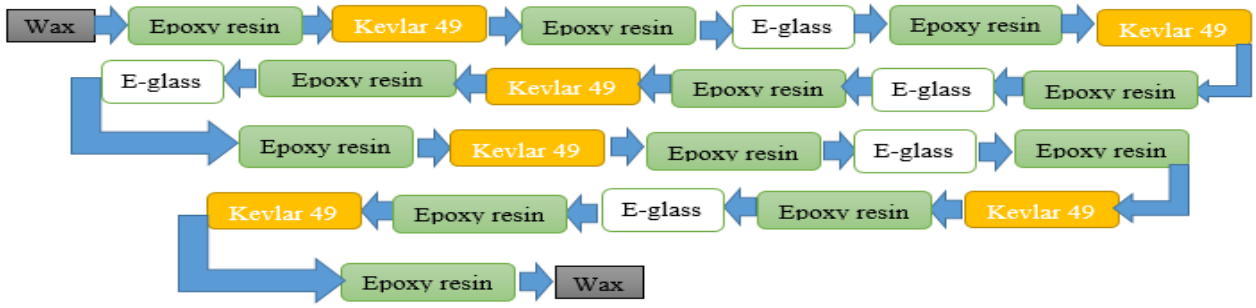


Figure3.7. plate preparation procedure of fiber 55% and matrix 45%.

And it was prepared using the same procedure as first sample.


Figure3.8. Hybrid composite plate of fiber 55% and matrix 45%.

**c) Third Sample:**

The volume fraction of fiber (Kevlar/glass fiber) = 60% and volume fraction of matrix material (epoxy resin) = 40%. Cross ply laminated used for this paper Kevlar 49 fiber (seven layer) and E-glass (six layers) cloths are used for fabrication. plain weave fiber of Kevlar and E-glass are 208.4g in weight. The seven types of Kevlar fibers and six types of E-glass fiber should be cut with a

dimension of is$229mm \times 229mm \times 20mm$. For embedding reinforcing fibers, 132.2 g of Epoxy resin and mixed thoroughly with 5% (6.61g) of Hardener. The order is represented using figure 3.9:

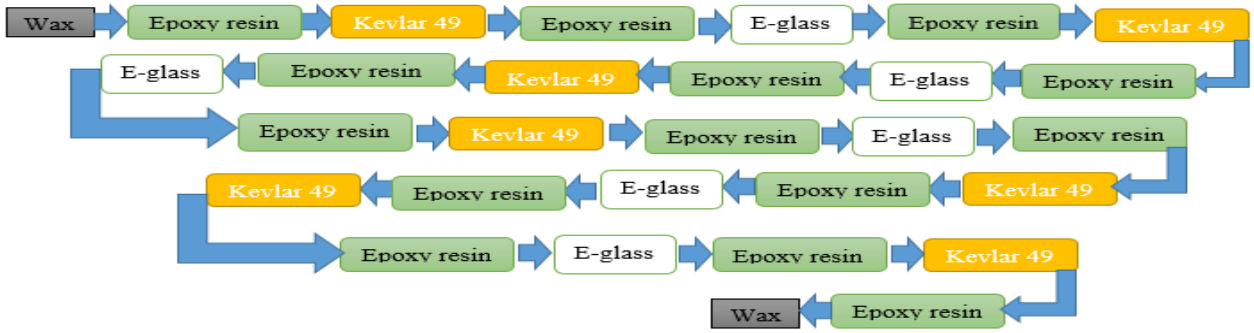


Figure 3.9. plate preparation procedure of fiber 60% and matrix 40%.

And it was prepared using the same procedure as first sample.

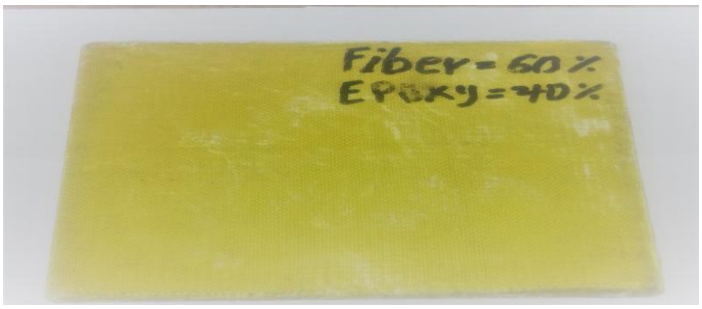


Figure 3.11. hybrid composite material Plate of fiber 40% and matrix 60%.

### 3.4.3 Specimen pieces preparing procedure

The test used in this research required five specimens per test conditions, unless invalid results can be gained through the use of fewer specimens, a total of about 45 specimens for both tensile, compression and flexural taste Kevlar with E-glass fiber. Band saw as shown in figure 3.22 was used to cut each laminate into the required dimension of pieces, the band saw cutter has a speed of 850m/minute and power 1100w:

Figure 3.12. cutting taste pieces using band saw machine.

### 3.4.3.1 Specimen pieces Geometry and Dimensions

American Society of Testing & Materials (ASTM) test method D3039 method for determination of tensile properties of isotropic and orthotropic fiber reinforced composite materials was selected for tensile tests [44]. And the constant rectangular cross section specimen was used. As it is shown in figure 3.13, 20 mm wide, 200 mm length and 4 mm thick by 88 mm gage length woven Kevlar with E-glass/ epoxy.


Figure3.13. Tensile taste specimen

Taste pieces and composition ratio of 60%/40%, 55%/45% and 50%/50% of fiber/epoxy for testing after cutting with required dimensions shows below in figures 3.14.

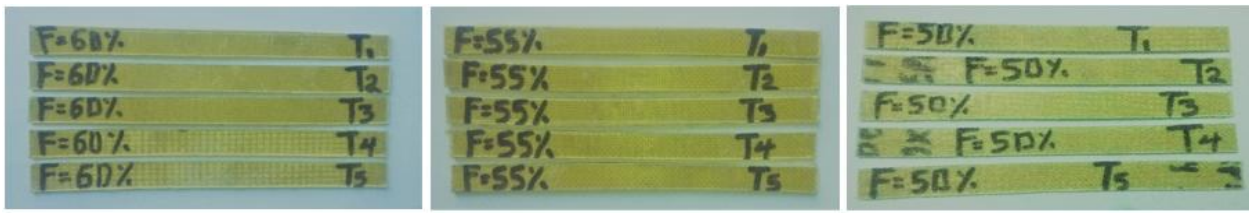

Figure 3.14. Before tensile taste pieces' different composition ratio of fiber/epoxy for tensile taste

For compressive properties of resin-matrix composites reinforced with oriented continuous or cross-ply reinforcement fibers on a universal testing machine according to ASTM standard ASTM D3410/D 3410M-03 [52]. According to ASTM D3410/D 3410M-03 the specimen dimensions are 80 mm length, thickness of 4 mm and 20mm width with composite tab is prepared which is depicted below in figure 3.15.

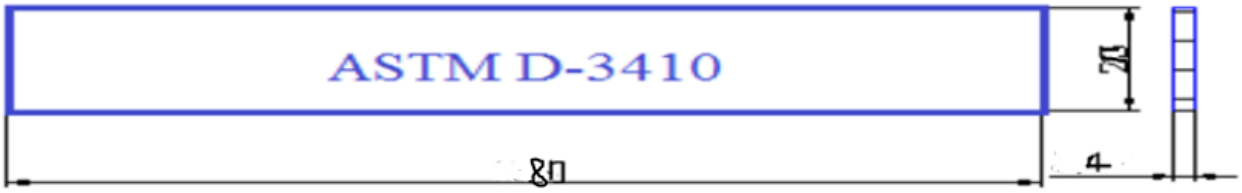


Figure 3.15 Compression taste specimen

Taste pieces and composition ratio of 60%/40%, 55%/45% and 50%/50% of fiber/epoxy for testing after cutting with required dimensions shows below in figure 3.16.

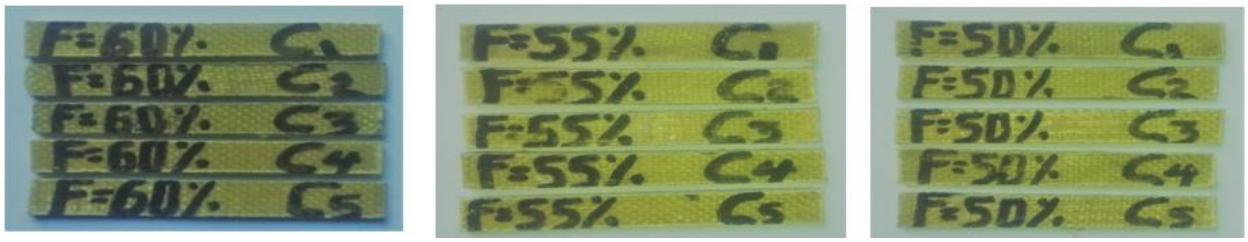


Figure3.16 Taste pieces' different composition ratio of fiber/epoxy for compression taste

Three-point flexure testing of polymer matrix composites per ASTM D7264 is done to determine the relevant property data for flexural tests [46]. And the constant rectangular cross section specimen was used. As it is shown in figure 3.17, 13 mm wide, 200 mm length and 4 mm thick by 128 mm span support length woven Kevlar with E-glass/ epoxy.

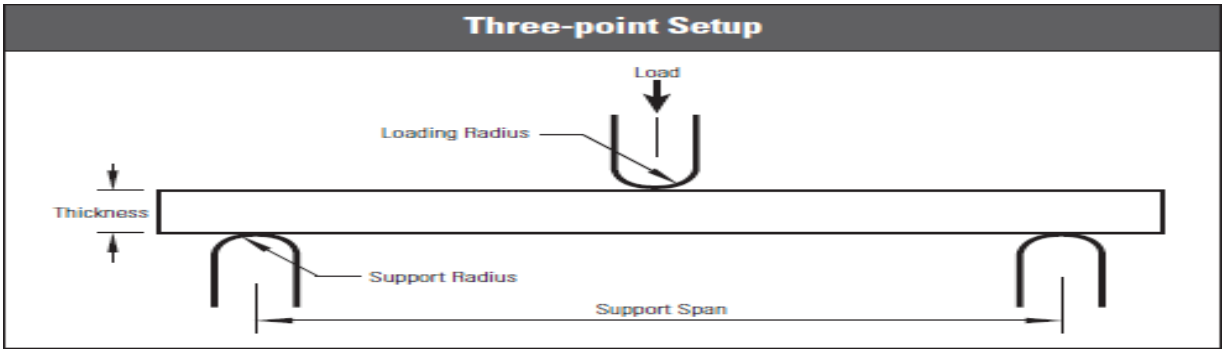


Figure 3.17 Three-point setup flexural tests

| Width | Thickness | Support span |
|---|---|---|
| 13mm | 4mm | 128mm |

Taste pieces and composition ratio of 60%/40%, 55%/45% and 50%/50% of fiber/epoxy for testing after cutting with required dimensions shows in figure 3.18.


Figure 3.18 Taste pieces' different composition ratio of fiber/epoxy for flexural taste

## 3.5 Introduction to taste apparatus

YF Zhejiang TugongPN0206000031 WAW- 1000B microcomputer controlled UTM is a superior version UTM. It is suitable to test various metallic & non-metallic materials for tensile, compressive and bending strength. The capacity of the machine is 1000 $KN$ at a load rating of 0.05kN/s which is found in the Bahir Dar University institute of technology, school of Civil and Water Resource Engineering at the material laboratory. The machine is computer integrated time, load, displacement, deflection, expansion 1 and expansion 2 were generated directly from the machine.

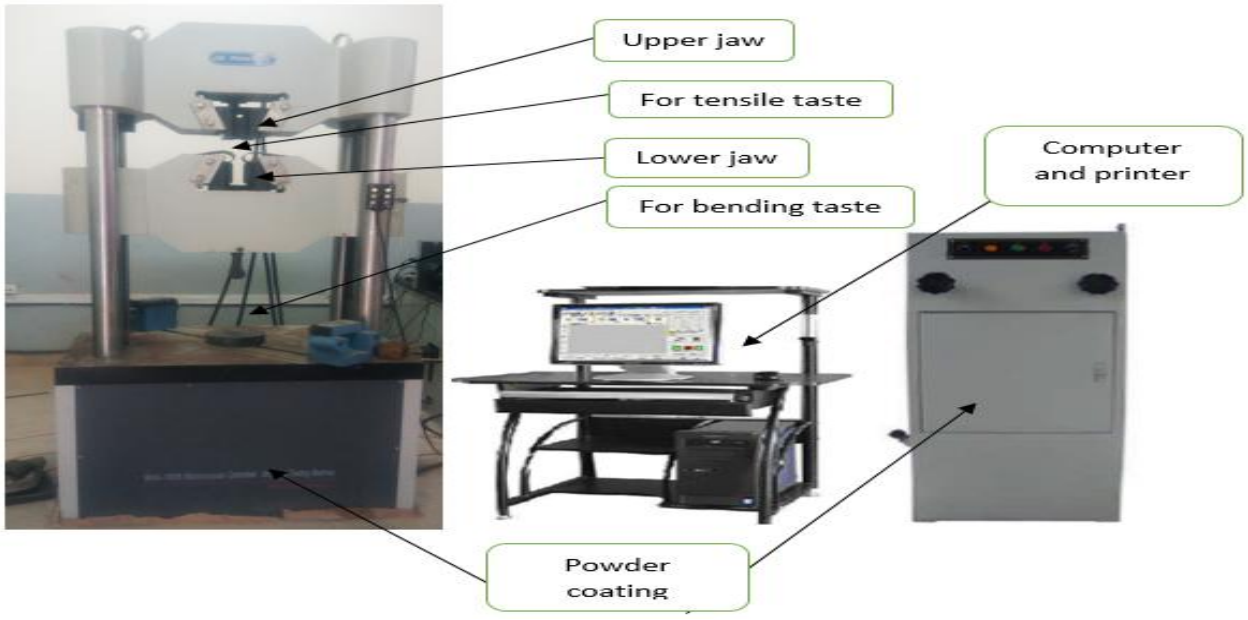


Figure 3.19. WAW- 1000B microcomputer controlled UTM is a superior version UTM.

## 3.6 Testing the Mechanical Properties of Kevlar/E-glass hybrid composite

### 3.6.1 Tensile strength taste

Tensile test is the most commonly used methods to evaluate the mechanical properties of materials. These properties can be used for the design and analysis of engineering structures, and for developing new materials that best suit a specified application [47].

**Stress-strain curve:** an x-y plot of stress vs strain through the entire range of loading of the specimen until its failure. See in the appendix.

***Stress (engineering):*** Engineering stress($\sigma$) is obtained by dividing the load (F) at any given time by the original cross sectional area ($Ao$) of the specimen [49].

$$\sigma = \frac{F}{Ao} \quad \text{..... (3.22)}$$

**Strain (engineering):** the unit deformation of the material under load. The strain is not normally measured directly [49].

$$\epsilon_l = \frac{lo}{l} \quad \text{..... (3.23)}$$

Where

ε= Engineering strain

Lo= elongation the specimen

L= original gage length

Tensile Modulus of Elasticity[E]: [49] $E = \frac{\sigma}{\epsilon_l}$ ..... (3.24)

Poisson's Ratio [v]**:** [49] $v = \frac{\epsilon_t}{\epsilon_l}$ ..... (2.25)

$\epsilon_t$ =difference in lateral strain between the two longitudinal strain points.

For each sample, 5 specimens were tested in each machine and cross-machine direction each specimen was 20mm by 200 mm. The test was done based on the following steps:

1) Samples have to be prepared as stated in Fig 13a).
2) Make ready the UTM for testing.
3) Samples specimens were placed in the grips of UTM.

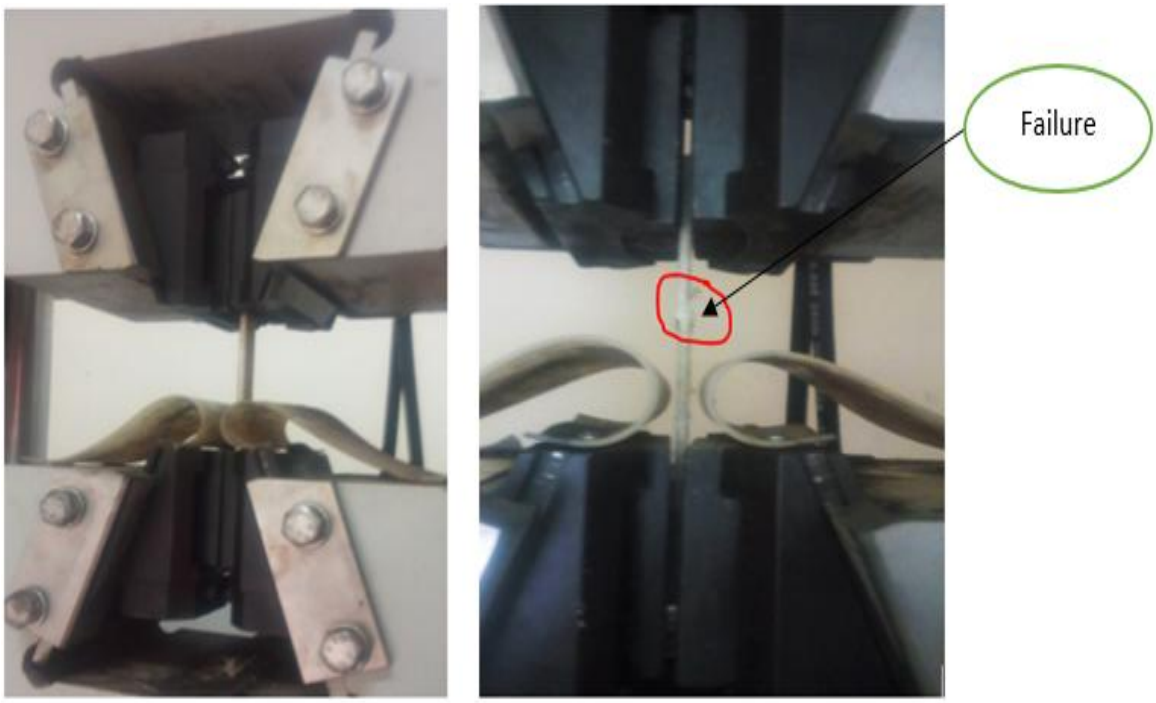


Figure3.20. Tensile strength taste set up

4) After positioning the sample specimens, click the run button on the desktop.
5) Save the test files to the appropriate place on the desktop.
6) Repeat steps, 2 to 15 until the end of the all sample of specimen's test

As the same repeat these steps up to all finishing the sample. After an axial load is applied through both the ends of the specimens looks like as following bellows.

Figure 3.21. After tensile taste pieces' different composition ratio of fiber/epoxy for tensile taste

### 3.6.1.1 Result of Tensile Strength

Values of Ultimate maximum Stresses, Yield Stresses, deflection at maximum Stress and Young Modulus for F=50%, 55%and 60% and Ep=50%, 45% and 40% hybrid composites are reported using table 3.4.

Table 3.4. Experimental result of tensile test F=50%, 55% and 60% and Ep=50%, 45% and 40% hybrid composites.

| Specimen | | Y.Modulus (E)Gpa | Max. load (KN) | Poisons ratio | Max. stresses (MPa) | Yield Stresses | Change of length (mm) |
|---|---|---|---|---|---|---|---|
| F=50% and Ep=50% | Trail 1 | 15.64 | 20.466 | 0.355 | 258.38 | 204.12 | 5.283 |
| | Trail 2 | 14.79 | 19.388 | 0.365 | 242.35 | 198.73 | 5.84 |
| | Trail 3 | 16.65 | 20.82 | 0.365 | 260.26 | 211.12 | 4.42 |
| | Trail 4 | 17.845 | 22.38 | 0.3657 | 279.78 | 245.01 | 4.35 |
| | Trail 5 | 16.61 | 19.85 | 0.362 | 248.92 | 207.75 | 4.11 |
| | ẋ | 16.4 | 20.98 | 0.365 | 265.2 | 222.35 | 4.7 |
| | S | 16.31 | 20.63 | 0.3625 | 264.88 | 220.4 | 4.8 |
| F=55% and Ep=45% | Trail 1 | 23.74 | 29.27 | 0.354 | 370.93 | 253.12 | 4.37 |
| | Trail 2 | 26.01 | 25.89 | 0.355 | 323.58 | 255.44 | 3.23 |
| | Trail 3 | 25.14 | 25.69 | 0.355 | 321.083 | 245.45 | 3.62 |
| | Trail 4 | 24.48 | 27.32 | 0.357 | 341.72 | 230.70 | 2.56 |
| | Trail 5 | 21.85 | 29.72 | 0.359 | 371.56 | 222.53 | 5.71 |
| | ẋ | 24.43 | 28.25 | 0.367 | 351.4 | 234.27 | 4.1 |
| | S | 24.25 | 27.98 | 0.357 | 349.73 | 232.53 | 3.9 |
| F=60% and Ep=40% | Trail 1 | 34.4 | 31.27 | 0.345 | 390.93 | 259.64 | 3.04 |
| | Trail 2 | 32.74 | 31.89 | 0.355 | 393.67 | 229.13 | 5.46 |
| | Trail 3 | 35.75 | 33.19 | 0.365 | 414.89 | 246.45 | 5.32 |
| | Trail 4 | 36.58 | 35.68 | 0.357 | 445.61 | 253.70 | 3.2 |
| | Trail 5 | 38.68 | 34.48 | 0.352 | 430.98 | 258.53 | 1.16 |
| | ẋ | 35.87 | 32.7 | 0.36 | 420.5 | 246.39 | 3.6 |
| | S | 35.62 | 32.567 | 0.355 | 419.198 | 244.76 | 3.64 |

Average value, standard deviation, and coefficient of variation for each property determined calculated from for each series [51].

$$S = \sqrt{(x^2 - n\dot{x}^2)/(n-1)} \quad \text{(3.26)}$$

$$CV = 100.s/\dot{x} \quad \text{(3.27)}$$

S = estimated standard deviation

$X$ = value of single observation

n = number of observations, and

ẋ = arithmetic mean of the set of observations

CV= sample coefficient of variation, in %

The average tensile test results for F=50% and Ep=50% hybrid composites are tabulated and presented in the figure 3.22 and 3.23 based on the five tensile test result.

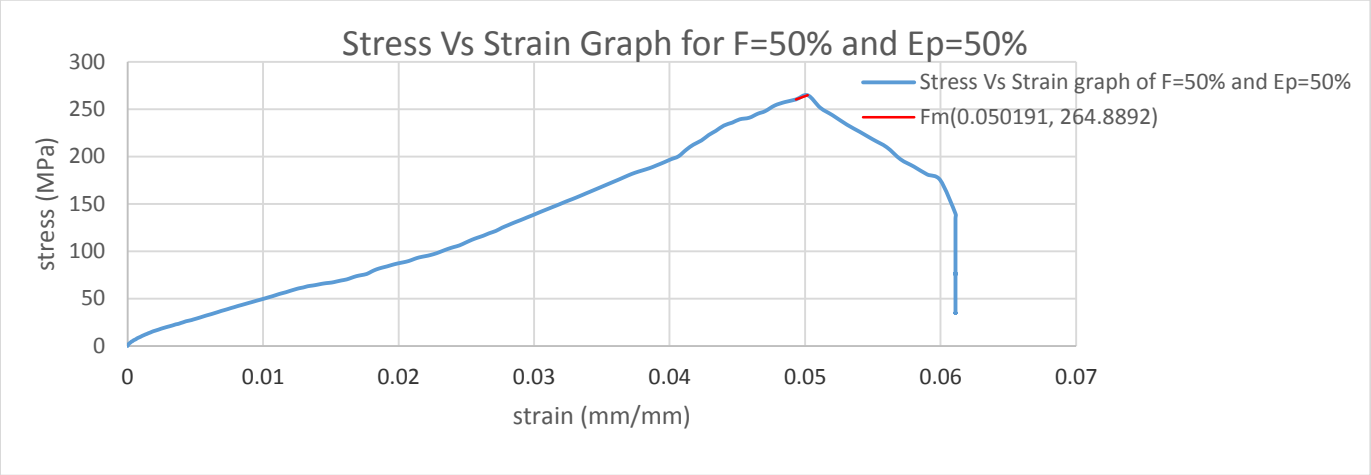


Figure 3.22. Stress Vs Strain Graph for F=50% and Ep=50%

The tensile strength of composite with fiber to matrix ratio of 50/50 about 265 MPa.

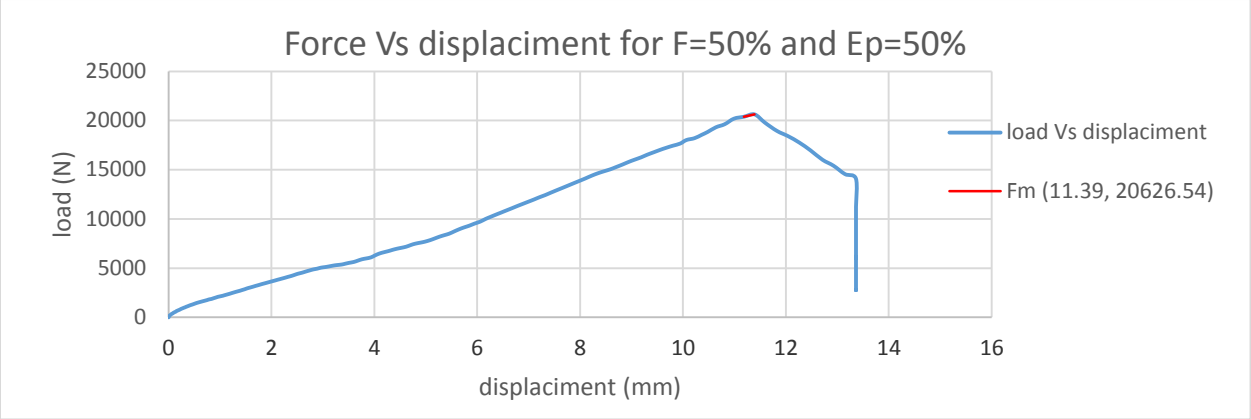


Figure 3.23. Force Vs displacement for F=50% and Ep=50%

The peak load applied on the composite with fiber to matrix ratio of 50/50 about 20.6 KN.

The average tensile test results for F=55% and Ep=45% hybrid composites are presented in the fig. 3.24 and 3.25 based on the five tensile test result.

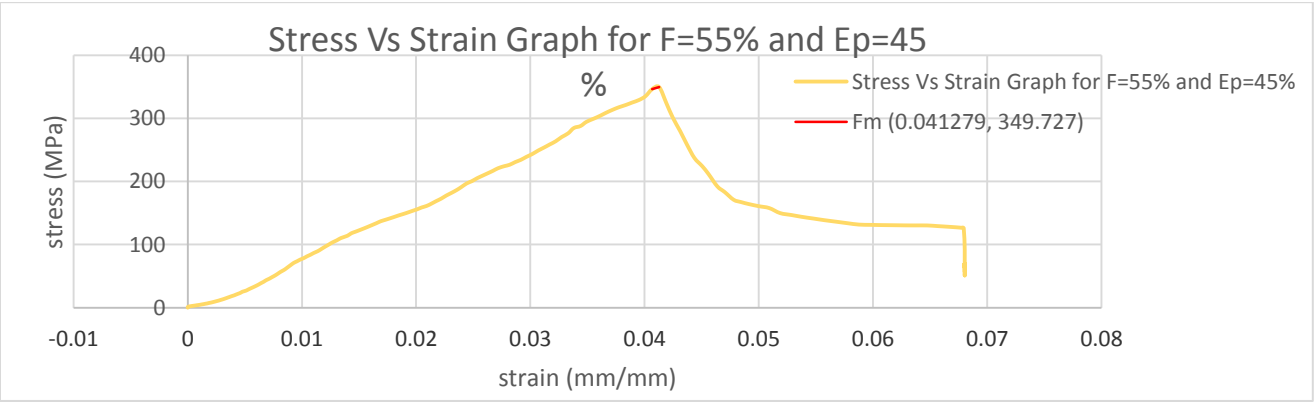


Figure 3.24. Stress Vs Strain Graph for F=55% and Ep=45

The tensile strength of composite with fiber to matrix ratio of 55/45 about 350 MPa.

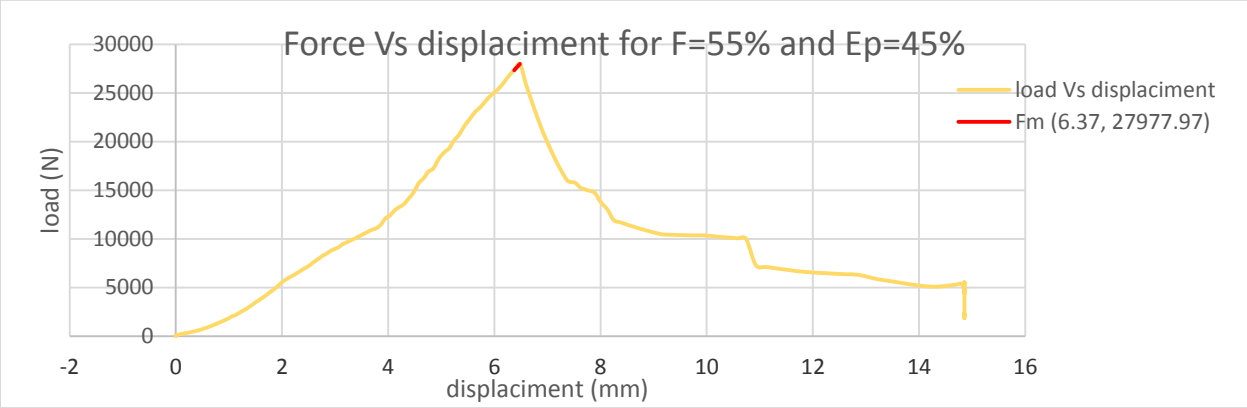


Figure 3.25. Force Vs displacement for F=55% and Ep=45%

The peak load applied on the composite with fiber to matrix ratio of 55/45 about 28 KN.

The average tensile test results for F=60% and Ep=40% hybrid composites are tabulated and presented in the figure 3.26 and 3.27 based on the five tensile test result.

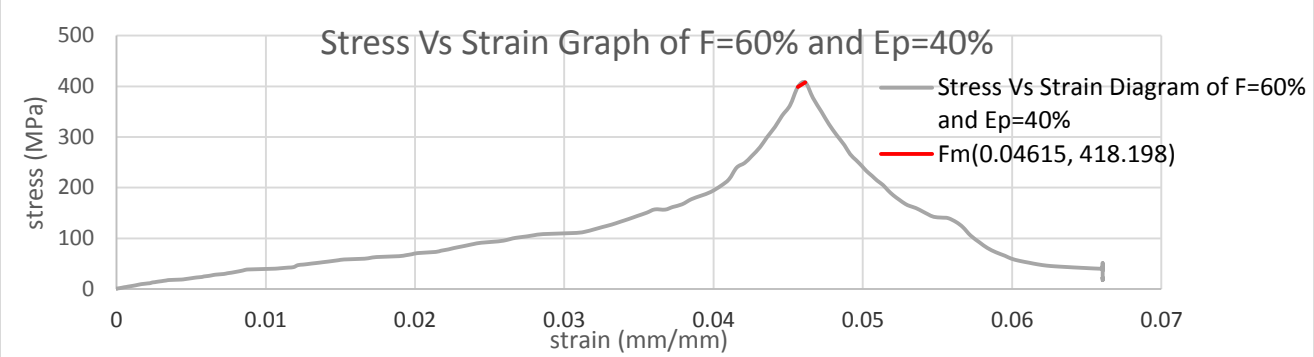


Figure 3.26. Stress Vs Strain Graph of F=60% and Ep=40%

The tensile strength of composite with fiber to matrix ratio of 60/40 about 419 MPa.

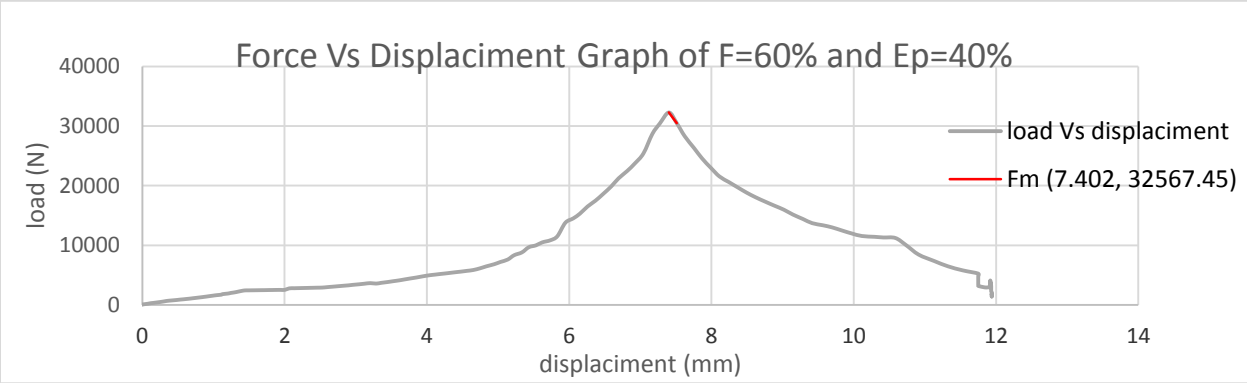


Figure 3.27. Force Vs Displacement Graph of F=60% and Ep=40%

The peak load applied on the composite with fiber to matrix ratio of 60/40 about 33 KN.

The average tensile test results for F=50% and Ep=50%, F=55% and Ep=45% and F=60% and Ep=40% hybrid composites are tabulated and presented in the figure 3.28 and 3.29

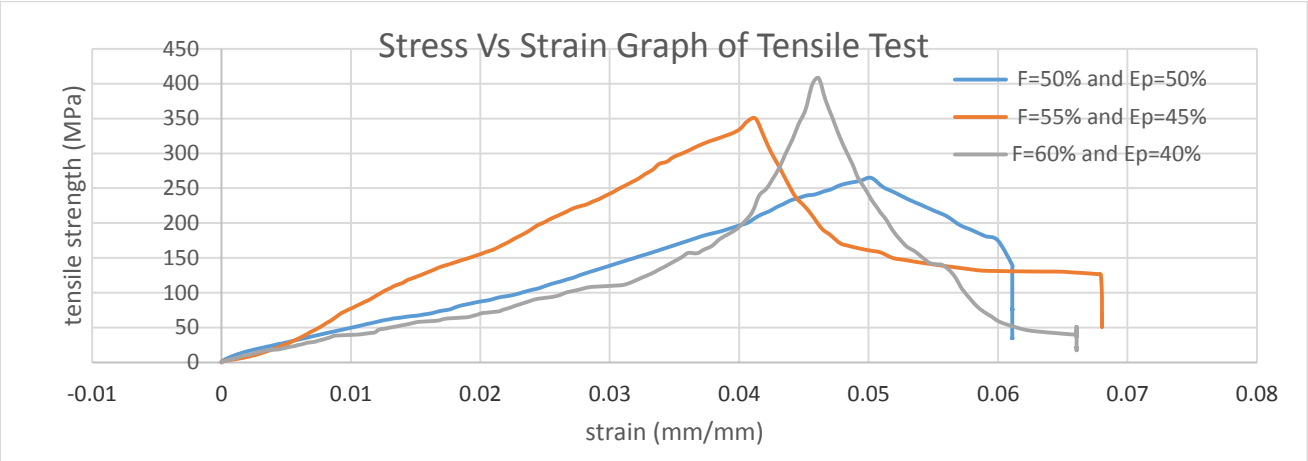


Figure 3.28. Stress Vs Strain Graph of Tensile Test

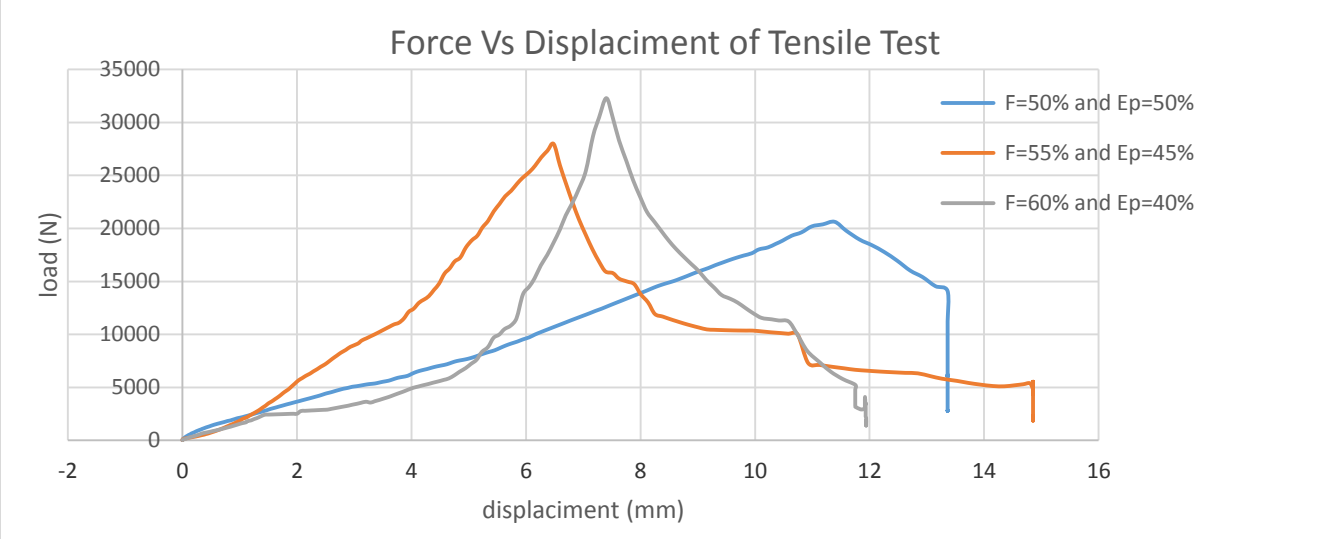


Figure 3.29. Force Vs Displacement of Tensile Test

### 3.6.1.2 Observation of Tensile Strength

1) Comparing the maximum tensile strength of fiber/epoxy composition ratio of 50%/50%, 55%/45% and 60%/40%. The tensile strength of hybrid composite shows an increase by 10.92% the ratio changes from 50/50 to 55/45, and increase by 15% when the ratio changes from 55/45 to 60/40. According to this variation and in figure 3.28 the fiber matrix ratio significantly affects tensile strength with increasing the fiber and also increase tensile strength.
2) The effect of fiber to matrix content change on the applied load. Figure 3.29 shows an increase by About 10.92% the ratio changes from 50/50 to 55/45, and increase by 15% when the ratio changes from 55/45 to 60/40.

### 3.6.2 Flexural Strength Taste

Flexural strength is defined as a material's ability to resist deformation under bending load. The structural member has larger length as compared to its cross-sectional area, which is loaded in the transverse direction. Lateral loads acting on the beam causes the beam to bend or flex, then deforming the axis of the beam into a curved line. In this study, three points bending test was carried out. The three-point flexure test produces peak stress at midpoint the sample. The stress at any point may be calculated using the following equations [48].

$$\sigma = \frac{3PL}{2bh^2} \quad \text{(3.27)}$$

where:

$\sigma$ =stress at the outer surface at mid-span, [MPa],

P= applied force, [N],

L= support span, [mm],

b= width of beam, [mm], and

h= thickness of beam, [mm].

Elasticity modulus was calculated according to

$$E = \frac{L^3 m}{4bh^2} \quad \text{(3.28)}$$

Where:

m= is the slope of the tangent to the initial straight line portion of the force deflection curve.

The maximum strain at the outer surface also occurs at mid-span, and it may be calculated as follows [48].

$$\varepsilon = \frac{6Dh}{L^2} \quad \text{(3.29)}$$

D= is the deflection beam at a given point in the load –deflection data.

The procedures of bending/ flexural test from sample preparation to testing of the sample are as follows:

1) Samples have to be prepared as stated in Fig 14a).
2) Clearly marked each specimen in the center and span length.
3) Make ready the machine for bending test.
4) Place the loading point on the center mark on the top of the sample.


Figure 3.30. Flexural/ bending strength taste set up

5) Center the test jig in the testing machine and apply the loading at the indicated rate until failure occurs.
6) Save the result displayed.
7) Repeat steps, 2 to 15 until the end of the all sample of specimen's test.

The test was a three-point test in which the load is applied at the center. The samples for bending test of Kevlar/E-glass hybrid composite material is prepared according to the standard stated and failure of Kevlar/E-glass hybrid composite material was shown in the figure 3.31.

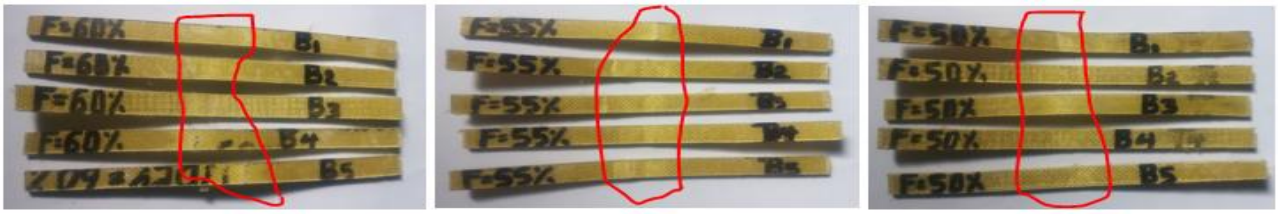

Figure 3.31. After flexural/bending taste that show pieces of failure for different composition ratio of fiber/epoxy

### 3.6.2.1 Result of Flexural Strength

Bending stresses are important in structure tests because of variety of loading situations in service. The mechanical properties of the materials are affected by many factors, including: fiber type, volume fraction and direction of the fiber.

The flexural test results are presented in the table 3.5. The most exaggerated result obtained from among the five specimen from each batch were omitted.

Table 3.5. experimental result of flexural test F=50%, 55% and 60% and Ep=50%, 45% and 40% hybrid composites.

| Specimen | | Y.Modulus (E)Gpa | Max. load (KN) | Max. stresses (MPa) | Change of length (mm) |
|---|---|---|---|---|---|
| F=50% and | Trail 1 | 17.76 | 432.83 | 290 | 15.99 |
| | Trail 2 | 15.04 | 438.54 | 294.54 | 17.1 |
| | Trail 3 | 16.64 | 441.08 | 296.92 | 20.43 |
| | Trail 4 | 14.71 | 398.54 | 267.68 | 14.38 |
| | Trail 5 | 16.76 | 432.83 | 290 | 15.99 |

| | | | | | |
|---|---|---|---|---|---|
| | ẋ | 16.3 | 438.1 | 294.09 | 16.9 |
| | S | 16.2 | 436.36 | 293.06 | 16.78 |
| F=55% and | Trail 1 | 23.11 | 527.79 | 345.79 | 21.25 |
| | Trail 2 | 24.71 | 470.83 | 317.45 | 24.81 |
| | Trail 3 | 22.96 | 517.02 | 340.89 | 13.78 |
| | Trail 4 | 24.77 | 484.7 | 325.84 | 17.74 |
| | Trail 5 | 23.38 | 430.85 | 298.38 | 16.03 |
| | ẋ | 23.91 | 489.74 | 326.9 | 18.8 |
| | S | 23.76 | 487.47 | 325.85 | 18.72 |
| F=60% and | Trail 1 | 34.38 | 560.1 | 376.19 | 18.65 |
| | Trail 2 | 36.72 | 549.33 | 368.18 | 17.84 |
| | Trail 3 | 34.38 | 560.1 | 376.19 | 18.65 |
| | Trail 4 | 36.45 | 576.1 | 386.93 | 18.65 |
| | Trail 5 | 35.15 | 539.1 | 362.08 | 18.65 |
| | ẋ | 36.43 | 559.45 | 376.56 | 18.61 |
| | S | 36.22 | 558.98 | 375.32 | 18.49 |

The average flexural test results for F=50% and Ep=50% hybrid composites are tabulated and presented in the figure 3.32 and 3.33 based on the five flexural test results.

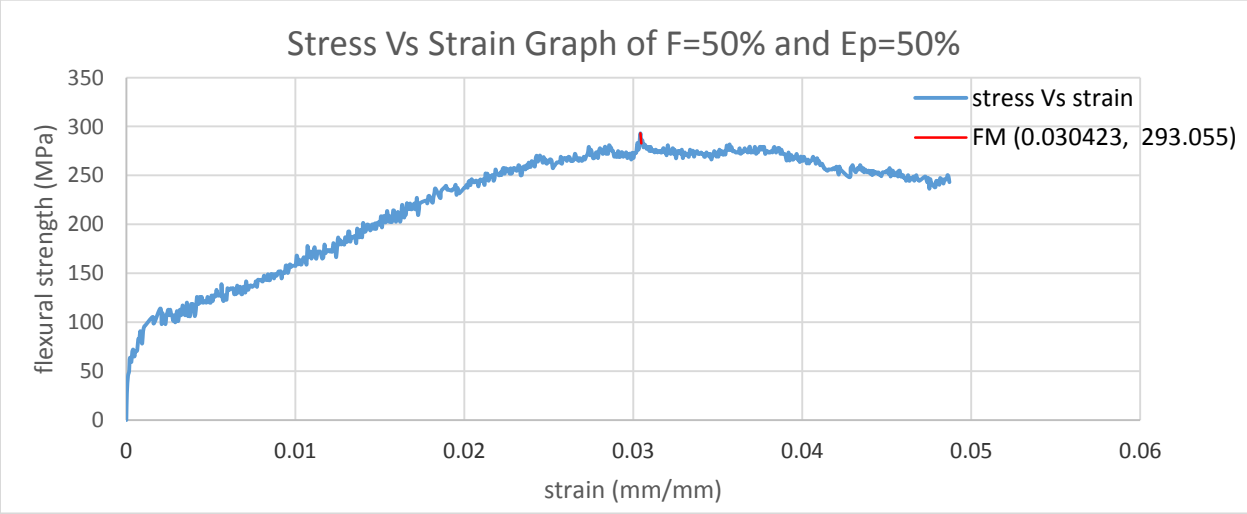


Figure 3.32. Stress Vs Strain Graph of F=50% and Ep=50%

The flexural strength of composite with fiber to matrix ratio of 50/00 about 293 MPa.

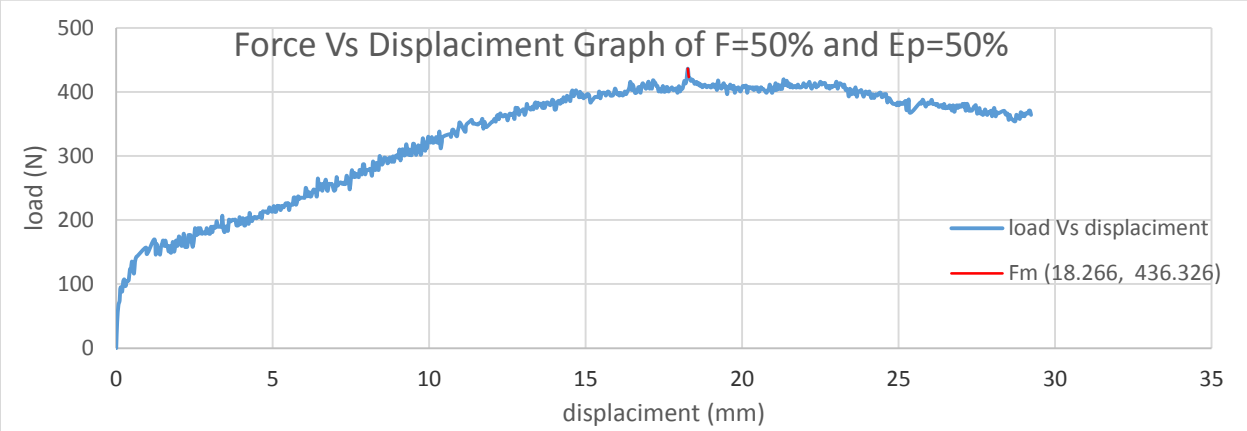


Figure 3.33. Force Vs Displacement Graph of F=50% and Ep=50%

The average flexural test results for F=55% and Ep=45% hybrid composites are tabulated and presented in the figure 3.34 and 3.35 based on the five flexural test result.

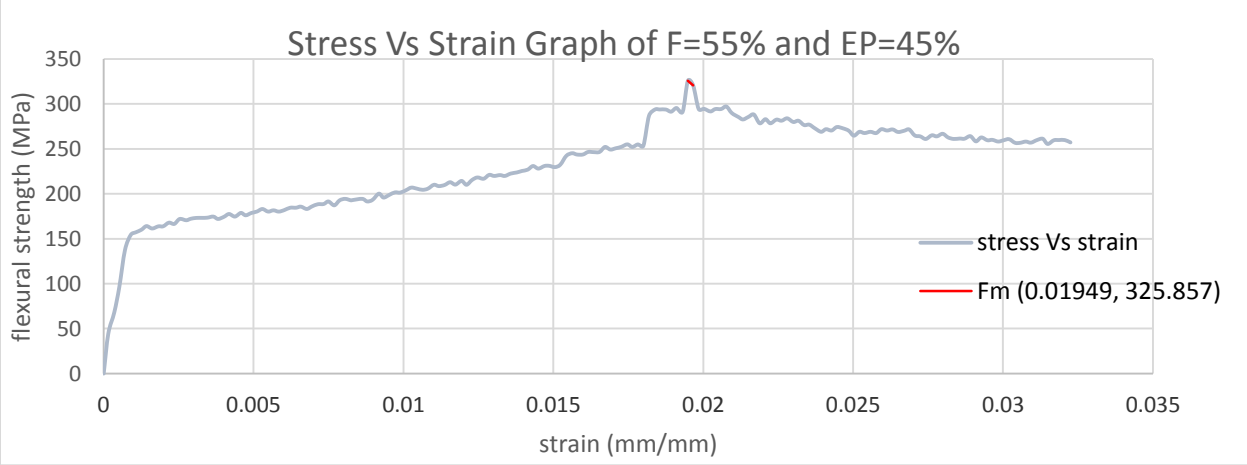


Figure 3.34. Stress Vs Strain Graph of F=55% and EP=45%

The flexural strength of composite with fiber to matrix ratio of 55/45 about 326 MPa.

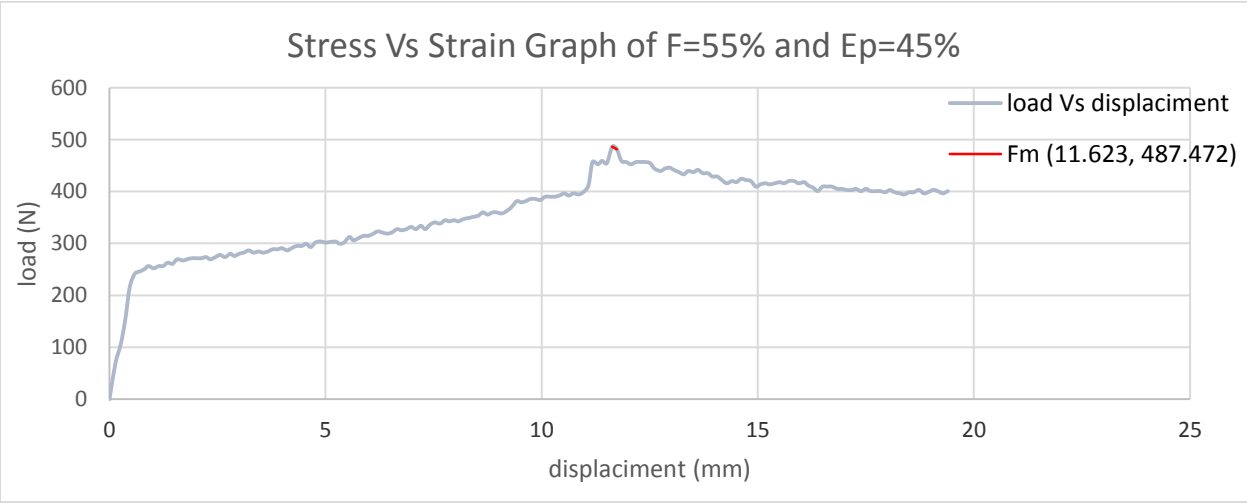


Figure 3.35. Stress Vs Strain Graph of F=55% and Ep=45%

The average flexural test results for F=60% and Ep=40% hybrid composites are tabulated and presented in the figure 3.36 and 3.37 based on the five flexural test result.

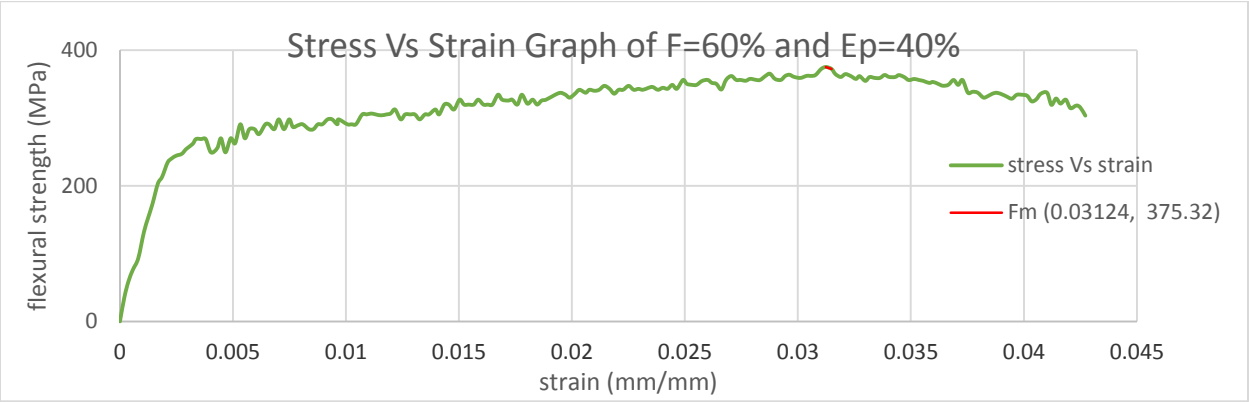


Figure 3.36. Stress Vs Strain Graph of F=60% and Ep=40%

The flexural strength of composite with fiber to matrix ratio of 60/40 about 375 MPa.

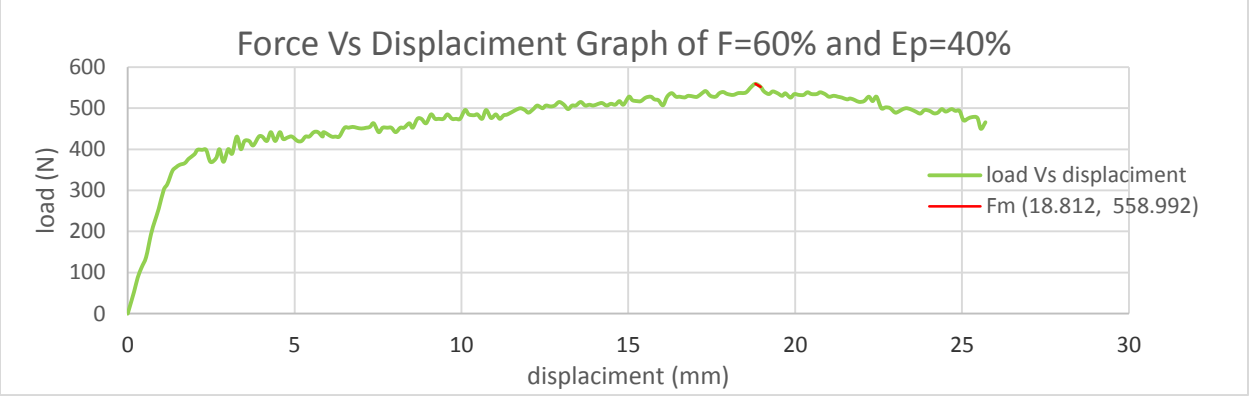


Figure 3.37. Force Vs Displacement Graph of F=60% and Ep=40%

The average flexural test results for F=50% and Ep=50%, F=55% and Ep=45% and F=60% and Ep=40% hybrid composites are tabulated and presented in the figure 3.38 and 3.39.

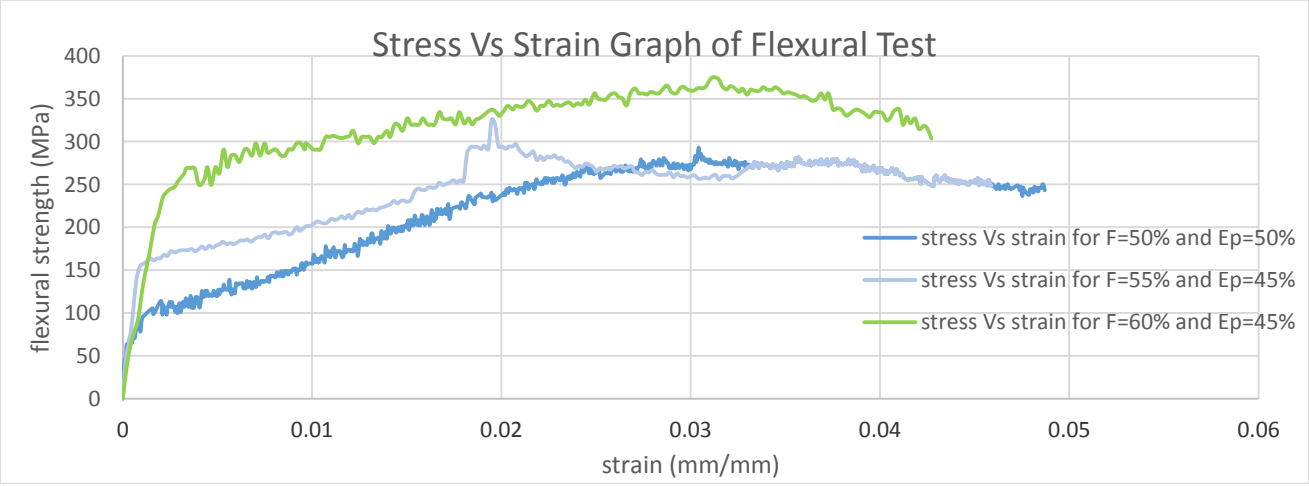


Figure 3.38. Stress Vs Strain Graph of Flexural Test

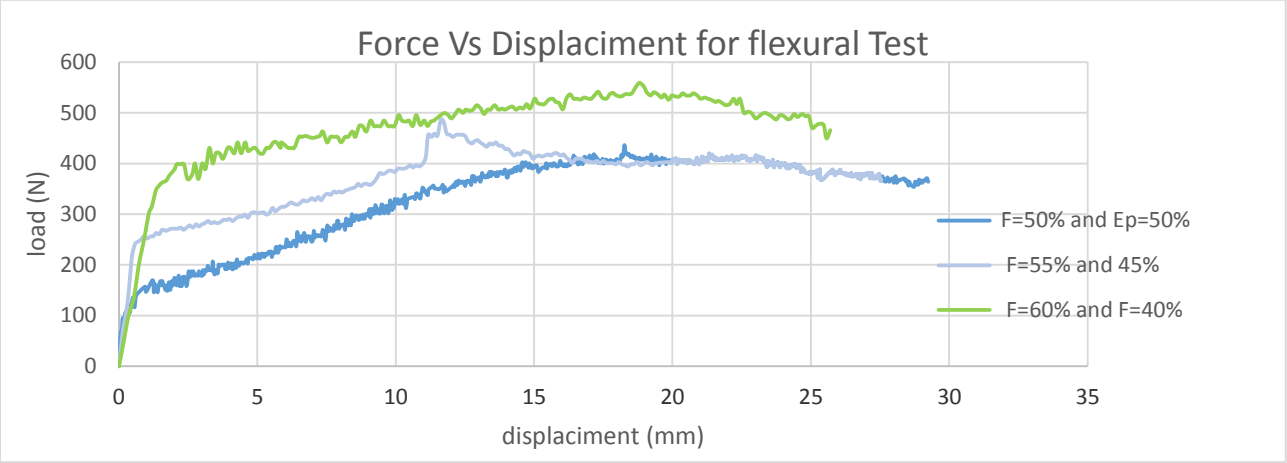


Figure 3.39. Force Vs Displacement for flexural Test

### 3.6.2.2 Observation of Flexural Strength

1) In figure 3.38 compared flexural strength of a composite with F=50% and Ep=50%, F=55% and Ep=45% and F=60% and Ep=40% the fiber to matrix ratio. As fiber composition ratio decreases the flexural strength of hybrid composite decreases.
2) Flexural modulus increase when the weight of fiber increase. For flexural strength of hybrid composite shows an increase by 9.92% the ratio changes from 50/50 to 55/45, and increase by 13.38% when the ratio changes from 55/45 to 60/40. Increased fiber in fiber to matrix ratio, especially greatly improved flexural strength and flexural modulus.
3) The effect of fiber/matrix content change on the applied load. Increased by 9.92% the ratio changes from 50/50 to 55/45, and increase by 15% the ratio changes from 55/45 to 60/40.

## 3.6.3 Compressive strength taste

A compression test is used to determine the behavior of materials under a compressive load. Compression tests are conducted by applying a compression load on the samples. The experiment of the compressive test was carried out in order to check the strength of Kevlar/E-glass hybrid composite material for compressive load along the grain direction. During the test, the maximum load, displacement and deformation was a record, And the stress and strain were calculated.

Compressive Stress: determine the compressive stress at each required data point using. [52]

$$F_{cu} = \frac{P_{Max}}{A} \quad \text{..... (3.30)}$$

Where:

$F_{cu}$ =compressive strength, MPa

$P_{Max}$ =maximum force before failure, N

$A$ =cross-sectional area at test section, $mm^2$

Compressive Strain: If compressive modulus or ultimate compressive strain is to be calculated, determine the average compressive strain at each required data point using,

$$\epsilon_{ci} = \frac{\epsilon_{1i}+\epsilon_{2i}}{2} \quad \text{(3.31)}$$

$$\epsilon_{cu} = \frac{\epsilon_{1cu}+\epsilon_{2cu}}{2} \quad \text{(3.32)}$$

Where:

$\epsilon_{cu}$ =average ultimate compressive strain

$\epsilon_{ci}$ =average compressive strain at $i^{th}$ data point

$\epsilon_{1i}$ and$\epsilon_{2i}$ =gage 1and 2 compressive strain at $i^{th}$ data point respectively,

$\epsilon_{1cu}$ and $\epsilon_{2cu}$ = gage 1 and 2 ultimate compressive strain respectively.

Compressive Modulus of Elasticity**:** Calculate the compressive chord modulus of elasticity from the stress-strain data using,

$$E_{chord} = \frac{\Delta\sigma}{\Delta\epsilon} \quad \text{(3.33)}$$

Where:

$E_{chord}$ =chord modulus of elasticity, MPa

$\Delta\sigma$ =difference in applied compressive stress between the two strain points

$\Delta\epsilon$ =difference in the average compressive strain between the two strain points

Testing was done based on the following steps:

1) Be sure that all samples are prepared and check the levelness of the end of the sample.
2) Make ready the Compressive Tester.


Figure 3.40. Compressive strength taste set up

3) Position the specimen under the crosshead of the testing machine, and apply load continuously at a loading rate of 0.5 KN/min.
4) Keep it until the material would be failed

5) Record the peak load when the material failed.
6) Measure the final length of the sample.
7) Calculate the stress and stain analytically.
8) Repeat, step 2 to 15 until the end of all sample taste the experiment.

The failure of the samples of Kevlar/E-glass hybrid composite material is shown in Figure 41.

Figure 3.41. after compression taste sample pieces of failure for different composition ratio of fiber/epoxy

### 3.6.3.1 Result of Compressive strength

Values of Ultimate maximum Stresses, Yield Stresses, deflection at maximum Stress and Young Modulus for a composite with F=50%, 55% and 60% and Ep=50%, 45% and 60% fiber to matrix ration are reported using table 3.6.

Table 3.6. experimental result of compressive test F=50%, 55% and 60% and Ep=50%, 45% and 40% hybrid composites.

| Specimen | | Max. load (KN) | Max. stresses (MPa) | Yield force (N) | Yield Stresses (MPa) | Change of length (mm) |
|---|---|---|---|---|---|---|
| F=50% and | Trail 1 | 10.4 | 200 | 7222 | 138.88 | 11.24 |
| | Trail 2 | 11.04 | 212.31 | 8792 | 169.08 | 7.27 |
| | Trail 3 | 10.75 | 206.73 | 8100 | 155.77 | 6.07 |
| | Trail 4 | 11.675 | 224.52 | 8478 | 163.04 | 9.3 |
| | Trail 5 | 10.97 | 210.93 | 8510 | 163.65 | 5.7 |
| | ẋ | 10.98 | 210.9 | 8220.4 | 158.08 | 7.92 |
| | S | 10.53 | 207.98 | 8218.1 | 157.32 | 7.8 |
| F=55% and | Trail 1 | 13.47 | 258.96 | 11600 | 223.08 | 10.15 |
| | Trail 2 | 14.79 | 284.42 | 11890 | 228.65 | 5.902 |
| | Trail 3 | 14.85 | 285.66 | 11510 | 221.34 | 10.8 |
| | Trail 4 | 14.78 | 284.15 | 12470 | 239.81 | 10.23 |
| | Trail 5 | 14.66 | 281.92 | 12600 | 242.31 | 6.15 |
| | ẋ | 14.51 | 279.022 | 12014 | 231.03 | 8.65 |
| | S | 14.43 | 277.88 | 12000 | 230.1 | 7.8 |
| F=60% and | Trail 1 | 18.25 | 350.96 | 13000 | 250 | 7.71 |
| | Trail 2 | 18.45 | 354.81 | 11750 | 225.96 | 9.46 |
| | Trail 3 | 19.96 | 383.85 | 11000 | 211.53 | 9.26 |
| | Trail 4 | 19.35 | 372.15 | 10250 | 197.11 | 8.85 |
| | Trail 5 | 19.6 | 376.92 | 11500 | 221.15 | 9.74 |
| | ẋ | 19.12 | 374.78 | 11500 | 221.15 | 9.004 |
| | S | 19.3 | 372.69 | 11490 | 220.5 | 8.97 |

The average compressive test results for F=50% and Ep=50% hybrid composites are presented in the figure 3.42 and 3.43 based on the five compressive test results.

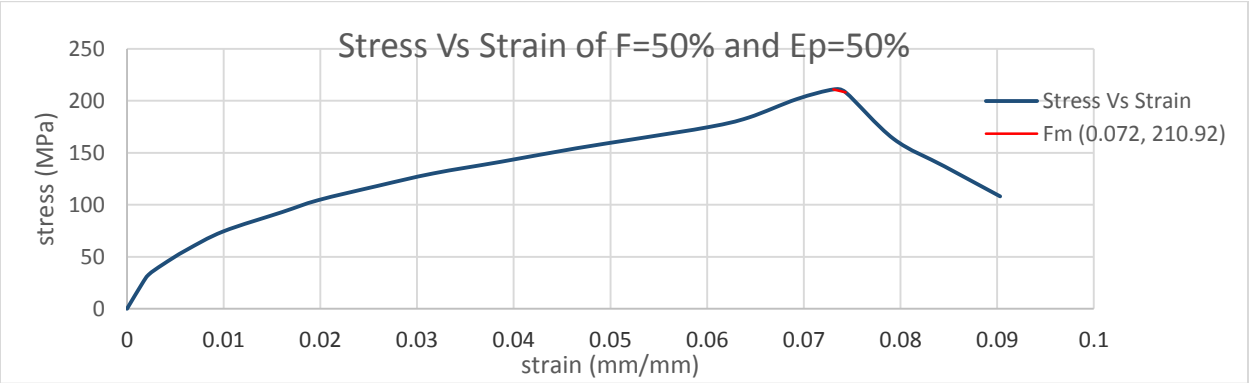


Figure 3.42. Stress Vs Strain Graph of F=50% and Ep=50%

The compressive strength of composite with fiber to matrix ratio of 50/50 about 211 MPa.

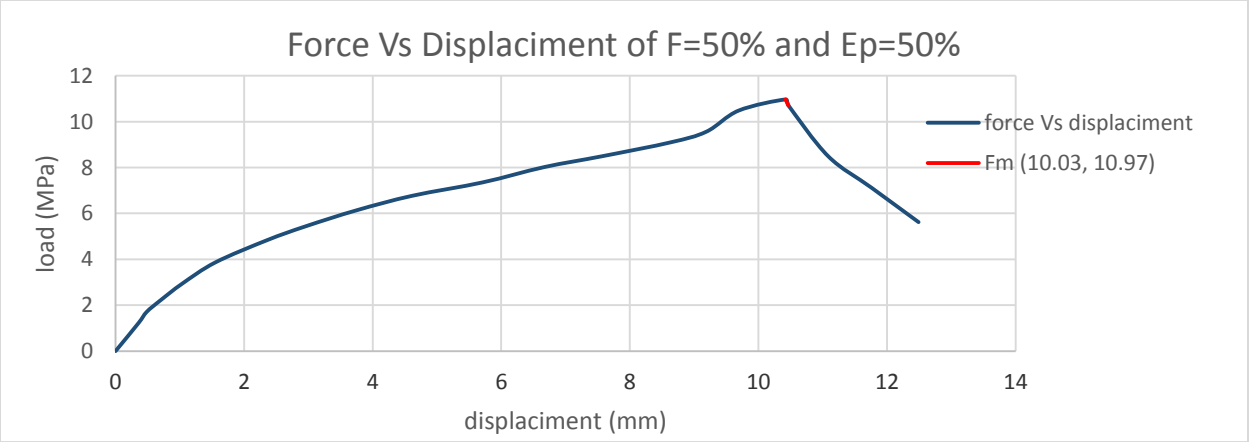


Figure 3.43. Force Vs Displacement Graph of F=50% and Ep=50%

The average compressive test results for F=55% and Ep=45% hybrid composites are presented in the figure 3.44 and 3.45 based on the five compressive test results.

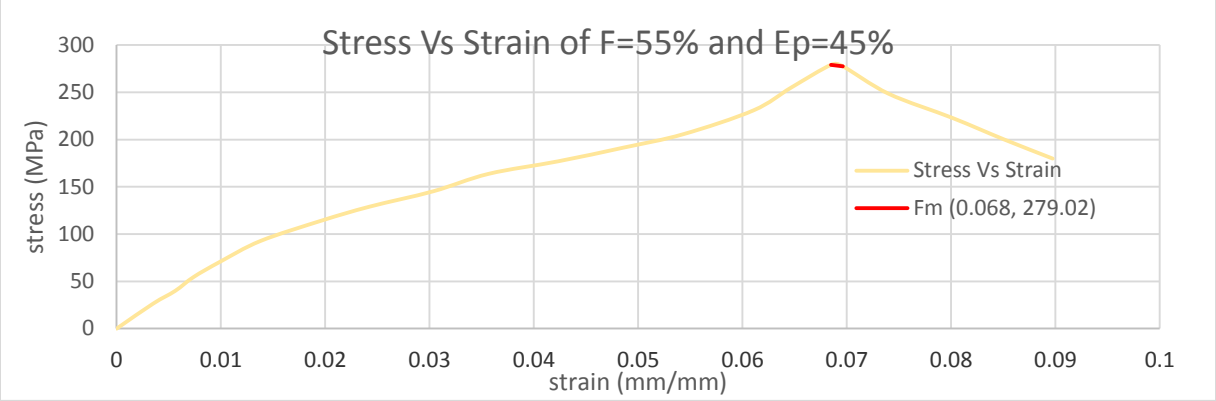


Figure 3.44. Stress Vs Strain Graph of F=55% and Ep=45%

The compressive strength of composite with fiber to matrix ratio of 55/45 about 279 MPa.

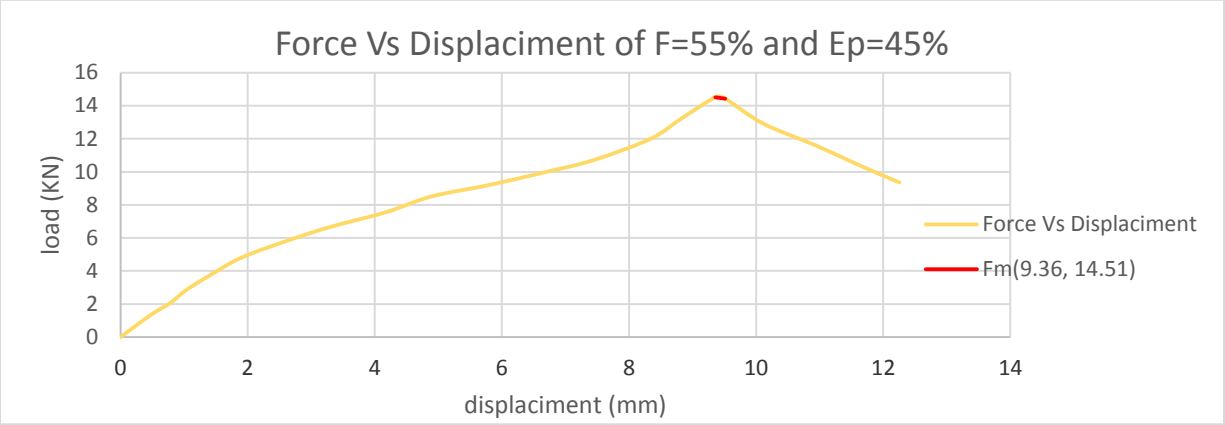


Figure 3.45. Force Vs Displacement Graph of F=55% and Ep=45%

The average compressive test results for F=60% and Ep=60% hybrid composites are presented in the figure 3.46 and 3.47 based on the five flexural test results.

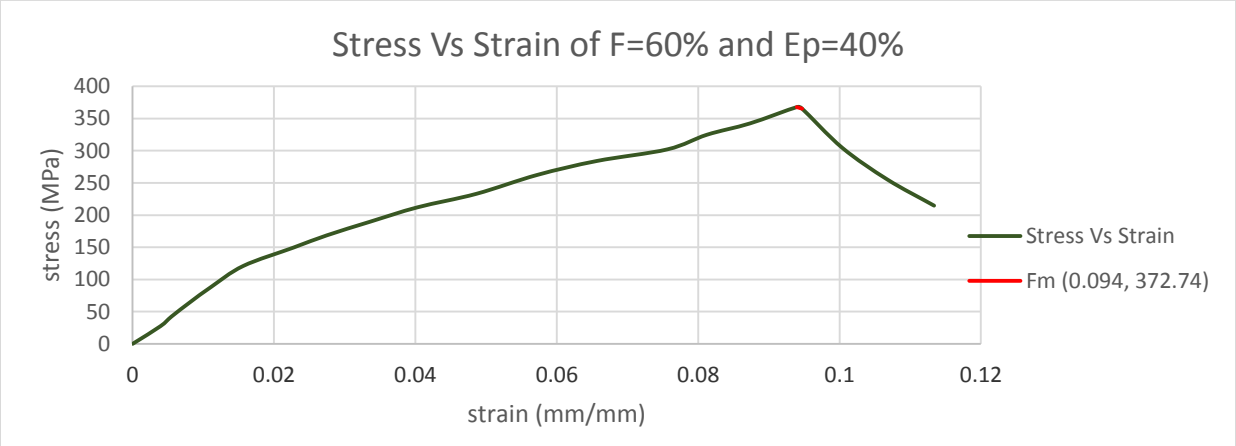


Figure 3.46. Stress Vs Strain Graph of F=60% and Ep=40%

The compressive strength of composite with fiber to matrix ratio of 60/40 about 372 MPa.

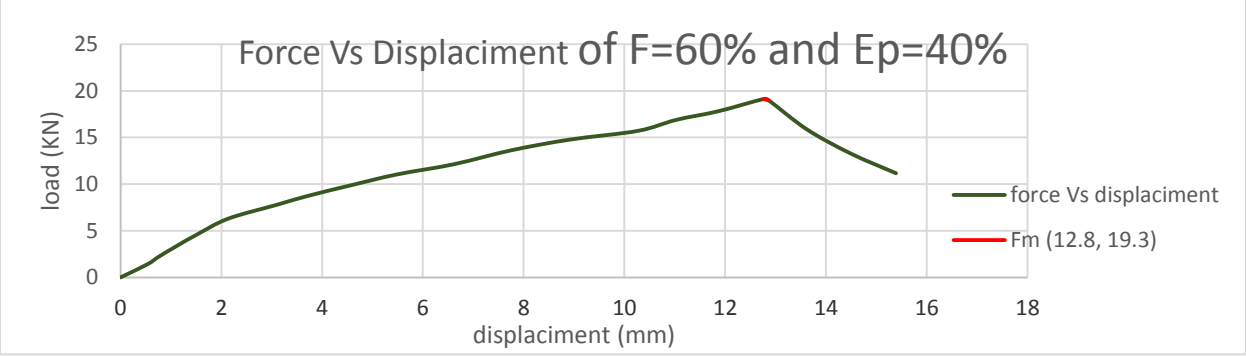


Figure 3.47. Force Vs Displacement Graph of F=60% and Ep=40%

The average compressive test results for F=50% and Ep=50%, F=55% and Ep=45% and F=60% and Ep=40% hybrid composites are tabulated and presented in the figure 3.48 and 3.49 based on the five flexural test results.

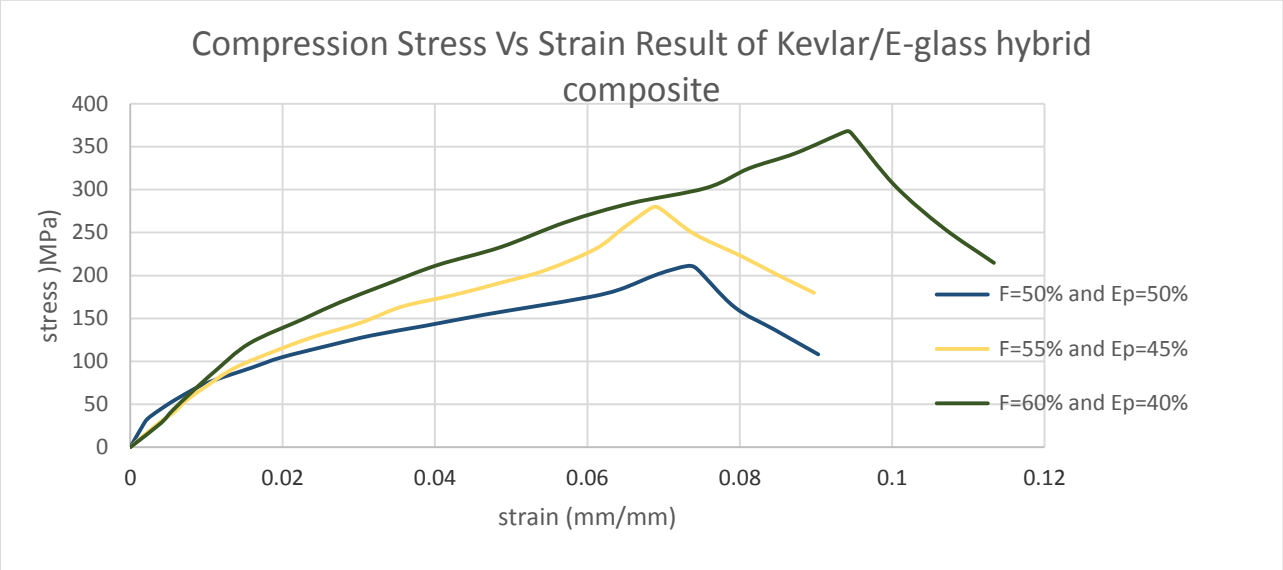


Figure 3.48. Stress Vs Strain Graph of compressive Test

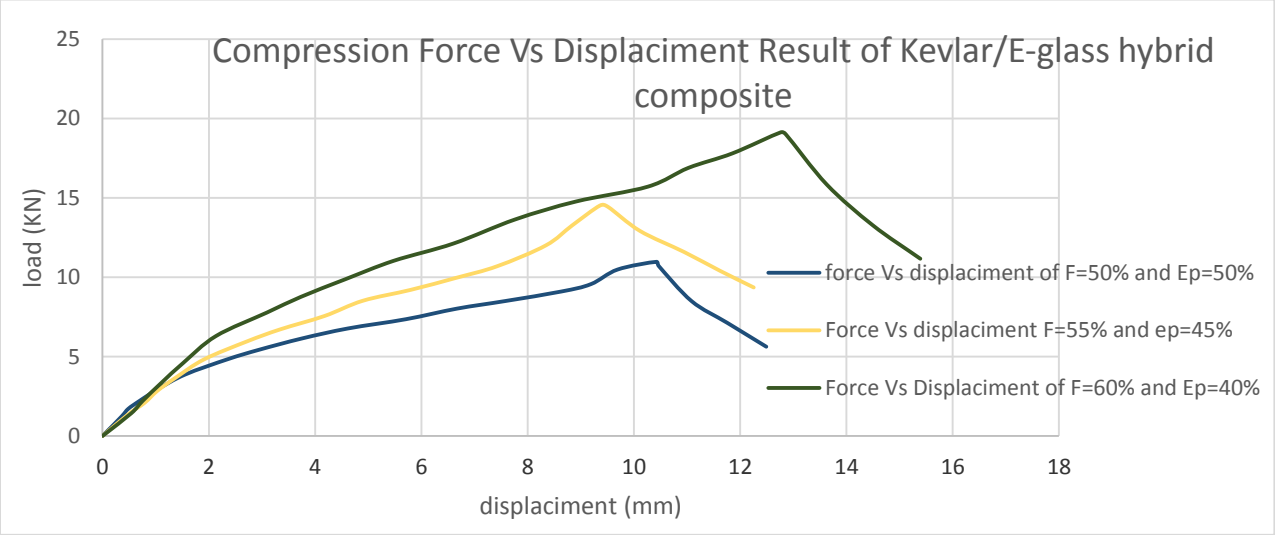


Figure 3.49. Force Vs Displacement for compressive Test

### 3.6.3.2 Observation of Compressive strength

1) The compressive strength of fiber/epoxy composition ratio of 50/50, 55/45 and 60/40 is 210.5Mpa, 279.02Mpa and 372.69Mpa respectively as above figure 3.48. It is clearly shown that when the weight of the fiber is increased in hybrid composite material there is an increase in compressive strength.
2) The effect of fiber/matrix content change on the applied load. The load is increase by 29.62% the ratio changes from 50/50 to 55/45, and increase by 25% when the ratio changes from 55/45 to 60/40.

## 3.7 Analysis using Finite element method (FEM)

Here the procedures used in the in the analysis of finite element method will be discussed.

### 3.7.1 Modeling of Lower Control Arm

3D Modeling is a geometrical representation of a real object without losing information which the real object has various mechanical design and manufacturing operations modeled using SOLID WORK.

The 3D-model used in this paper is a typical McPherson suspension lower arm. After measuring the size of the actual swing arm model, the model is simplified and the principle is:

1) The composite lower control arm model was simplified from the original design of the conventional structural steel lower arm in order to maintain the outline of design geometry and avoid interference with exterior geometric constraints.
2) As only using LIFAN 530 VIP lower control arm suspension system**,** so ignore the lower control arm of the process structure, to use of the original lower control arm model.
3) The geometrical complexity (holes for assembly guide) was removed to save computing time in simulation and for the composite manufacturing process.

After the simplification and processing of the model, the final use of the lower control arm SOLID WORK analysis model as shown Figure 3.50:

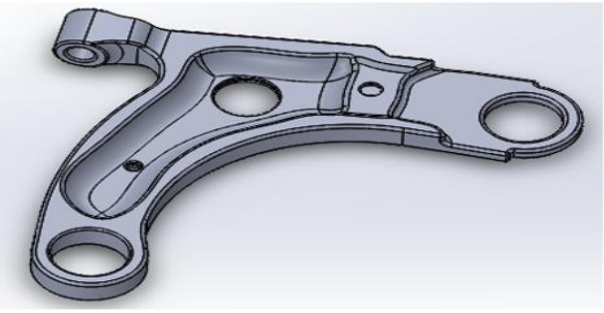

Figure 3.50. (a) Conventional structural steel lower arm model.

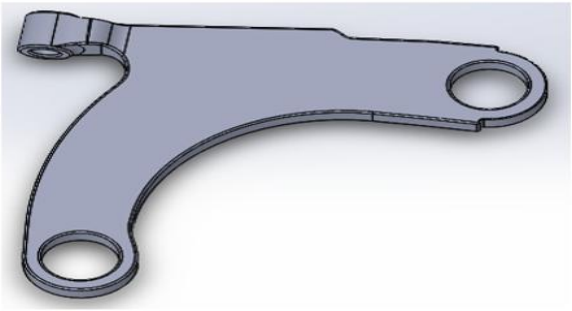

Figure 3.50 (b) simplified composite lower arm model.

This new model is suitable for the composite laminated lower arm structure and for the finite element analysis.

### 3.7.2 Analysis of Lower Control Arm Using ANSYS 18.2 Workbench

Finite Element Analysis is a numerical method of deconstructing a complex system into very small pieces called elements. The software implements equations that govern the behavior of these elements and solves them all creating a comprehensive explanation of how the system acts as a whole [50]. These results then can be displayed in tabulated, or graphical forms. This type of analysis is

typically used for the design and optimization of a system that is too complex to Analyze manually. Systems that may fit into this category are too complex due to their geometry, scale, or governing equations [24].

### 3.7.3 Static structure analysis

A static structural analysis determines the displacements, stresses, and forces in structures or components caused by loads that do not induce significant inertia and damping effects. Steady loading and response conditions are assumed; that is, the loads and the structure's response are assumed to vary slowly with respect to time. The types of loading that can be applied in a static analysis include:

- Externally applied forces and pressures
- Total load is applied to the wheel hub ball joint in a downward direction.
- The displacement and rotation between each reference point and the inside face of each bush was constrained.

#### 3.7.3.1 Define Engineering Data

The specific material property of the selected Kevlar/E-glass hybrid composite and structural steel materials are reported using table 3.7:

Table 3.7. workbench material properties of laminated Kevlar/E-glass hybrid composite

Outline of Schematic A2: Engineering Data

| | A | B | C | D | E |
|---|---|---|---|---|---|
| 1 | Contents of Engineering Data | | | Source | Description |
| 2 | Material | | | | |
| 3 | Kevlar/E-glass hybrid composite material | | | General_Materials.xml | Fatigue Data at zero mean stress comes from 1998 ASME BPV Code, Section 8, Div 2, Table 5 -110.1 |
| * | Click here to add a new material | | | | |

Properties of Outline Row 3: Kevlar/E-glass hybrid composite material

| | A | B | C | D | E |
|---|---|---|---|---|---|
| 1 | Property | Value | Unit | | |
| 2 | Material Field Variables | Table | | | |
| 3 | Density | 1695 | kg m^-3 | | |
| 4 | Isotropic Secant Coefficient of Thermal Expansion | | | | |
| 6 | Orthotropic Elasticity | | | | |
| 7 | Young's Modulus X direction | 3.622E+10 | Pa | | |
| 8 | Young's Modulus Y direction | 3.622E+10 | Pa | | |
| 9 | Young's Modulus Z direction | 9.64E+09 | Pa | | |
| 10 | Poisson's Ratio XY | 0.05 | | | |
| 11 | Poisson's Ratio YZ | 0.355 | | | |
| 12 | Poisson's Ratio XZ | 0.355 | | | |
| 13 | Shear Modulus XY | 1.4266E+10 | Pa | | |
| 14 | Shear Modulus YZ | 4.02E+09 | Pa | | |
| 15 | Shear Modulus XZ | 4.02E+09 | Pa | | |
| 16 | Orthotropic Stress Limits | | | | |
| 17 | Tensile X direction | 4.192E+08 | Pa | | |
| 18 | Tensile Y direction | 4.192E+08 | Pa | | |
| 19 | Tensile Z direction | 3.9E+07 | Pa | | |
| 20 | Compressive X direction | -3.9269E+08 | Pa | | |
| 21 | Compressive Y direction | -3.9269E+08 | Pa | | |
| 22 | Compressive Z direction | -1.05E+08 | Pa | | |
| 23 | Shear XY | 1.25E+08 | Pa | | |
| 24 | Shear YZ | 5.5E+07 | Pa | | |
| 25 | Shear XZ | 5.5E+07 | Pa | | |

Table 3.8. workbench material properties of structural steel

Outline of Schematic B2: Engineering Data

| | A | B | C | D | E |
|---|---|---|---|---|---|
| 1 | Contents of Engineering Data | | | Source | Description |
| 2 | Material | | | | |
| 3 | Structural Steel | | | General_Materials.xml | Fatigue Data at zero mean stress comes from 1998 ASME BPV Code, Section 8, Div 2, Table 5 -110.1 |

Properties of Outline Row 3: Structural Steel

| | A | B | C | D | E |
|---|---|---|---|---|---|
| 1 | Property | Value | Unit | | |
| 2 | Material Field Variables | Table | | | |
| 3 | Density | 7850 | kg m^-3 | | |
| 4 | Isotropic Secant Coefficient of Thermal Expansion | | | | |
| 5 | Coefficient of Thermal Expansion | 1.2E-05 | C^-1 | | |
| 6 | Isotropic Elasticity | | | | |
| 7 | Derive from | Young's Modulus and... | | | |
| 8 | Young's Modulus | 2E+11 | Pa | | |
| 9 | Poisson's Ratio | 0.3 | | | |
| 10 | Bulk Modulus | 1.6667E+11 | Pa | | |
| 11 | Shear Modulus | 7.6923E+10 | Pa | | |
| 12 | Alternating Stress Mean Stress | Tabular | | | |
| 16 | Strain-Life Parameters | | | | |
| 24 | Tensile Yield Strength | 2.5E+08 | Pa | | |
| 25 | Compressive Yield Strength | 2.5E+08 | Pa | | |
| 26 | Tensile Ultimate Strength | 4.6E+08 | Pa | | |
| 27 | Compressive Ultimate Strength | 0 | Pa | | |

### 3.7.3.2 Export Geometry

The browsed solid model of the composite and conventional steel lower control arm are done on SOLID WORK, saved as "IGS". That is possible to create the geometry of the composite and conventional steel lower control arm using design model in ANSYS workbench, beyond this from a CAD system supported by workbench that can export a file that is supported by ANSYS workbench form looks like in the following figure 3.51.

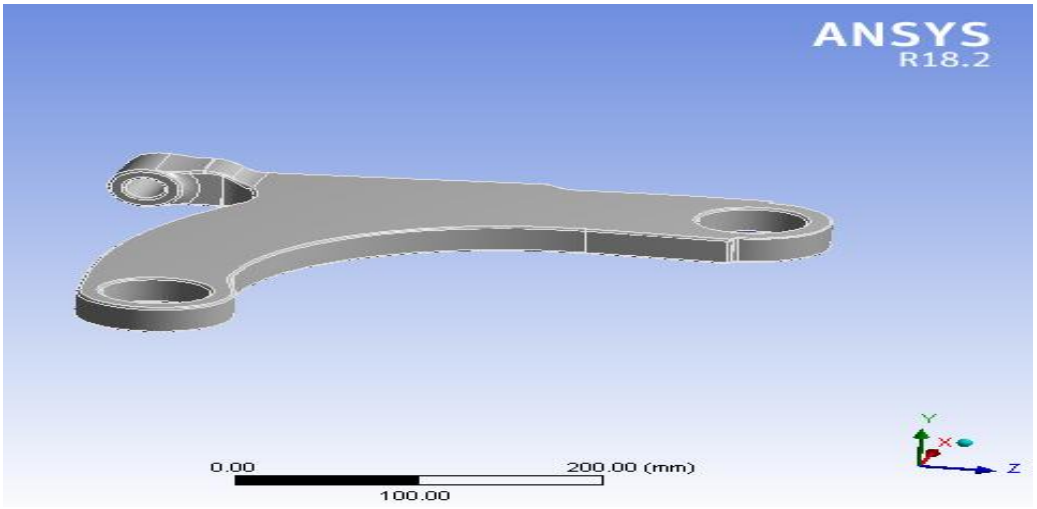


Figure 3.51. The browsed 3D model of Kevlar/E-glass hybrid composite lower control arm.

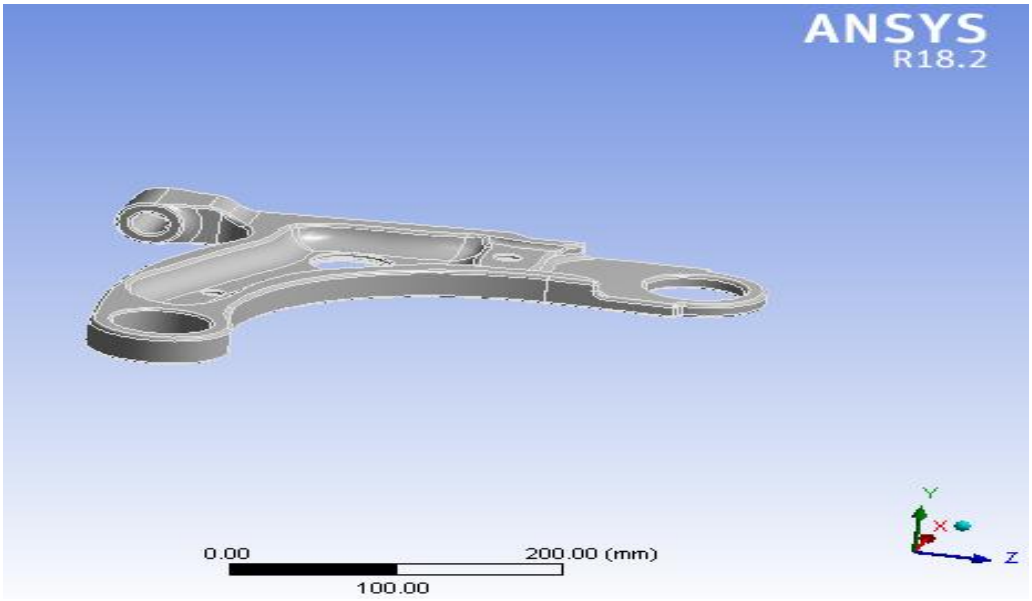


Figure 3.52. The browsed 3D model of conventional steel lower control arm.

### 3.7.3.3 Apply Mesh Controls/Preview Mesh

Meshing is done to reduce the degree of freedom from infinite to finite. The geometric surfaces of all the components of the front lower control arm are meshed using 10 nodes (quadratic tetrahedron), In this analysis mesh generation is an auto mesh generation with an element lengths edge is 5 mm**.**

Then the meshed model of the Kevlar/E-glass hybrid composite material looks like in the figure below with Number of Nodes and Elements- 64634 and 41666 respectively and Element Type – Tetrahedral (10 node).

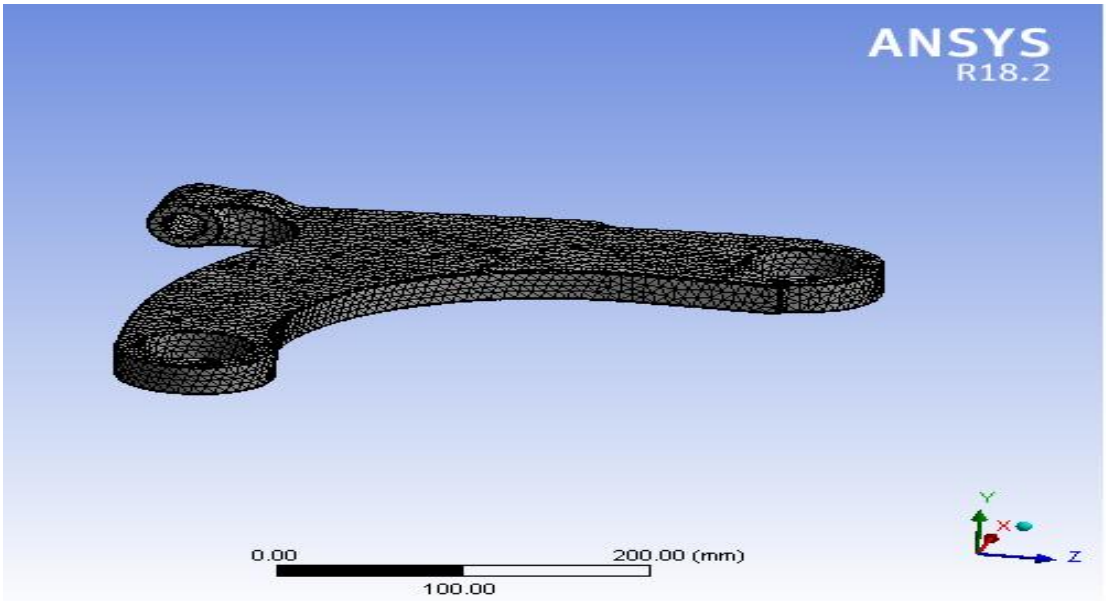


Figure 3.53. meshed model of Kevlar/E-glass hybrid composite lower control arm.

Then the meshed model of the conventional structural steel material looks like in the figure below with No, of Nodes – 52349, No, of Elements- 26981 and Element Type – Tetrahedral (10 node).

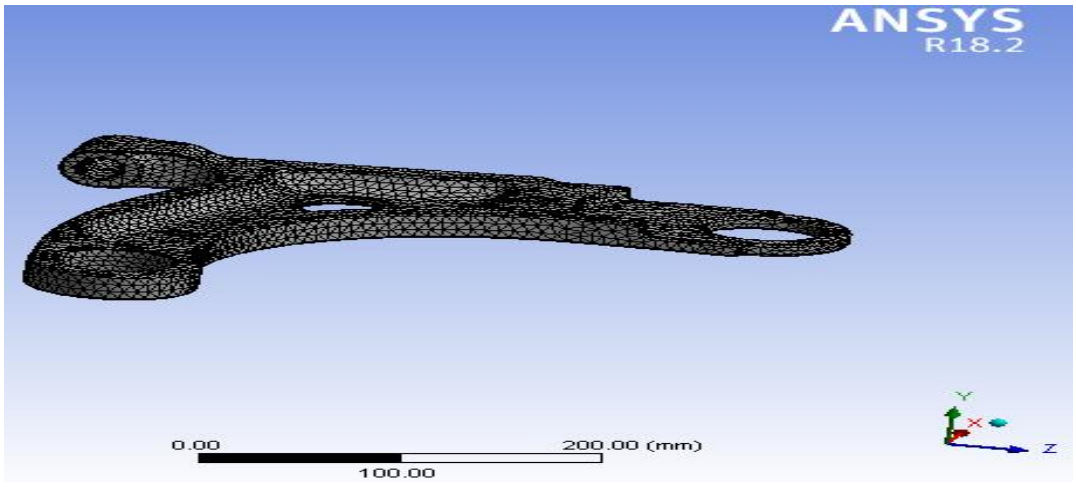


Figure 3.54. meshed model of conventional steel lower control arm.

### 3.7.3.4 Loading and Boundary Conditions

The boundary condition is the collection of boundary conditions, i.e. different forces, pressure, velocity, supports, constraints and any other condition required for a complete analysis. Applying the boundary condition is one of the most typical processes of analysis. A special care is required while assigning loads and constraints to the elements. From above study in theoretical analysis, import the 3D model of the lower suspension arm in hyper mesh for analysis under 3850 N load. The bush connected to the chassis is considered as the constraint and the total load is applied to the wheel hub bush in downward direction.

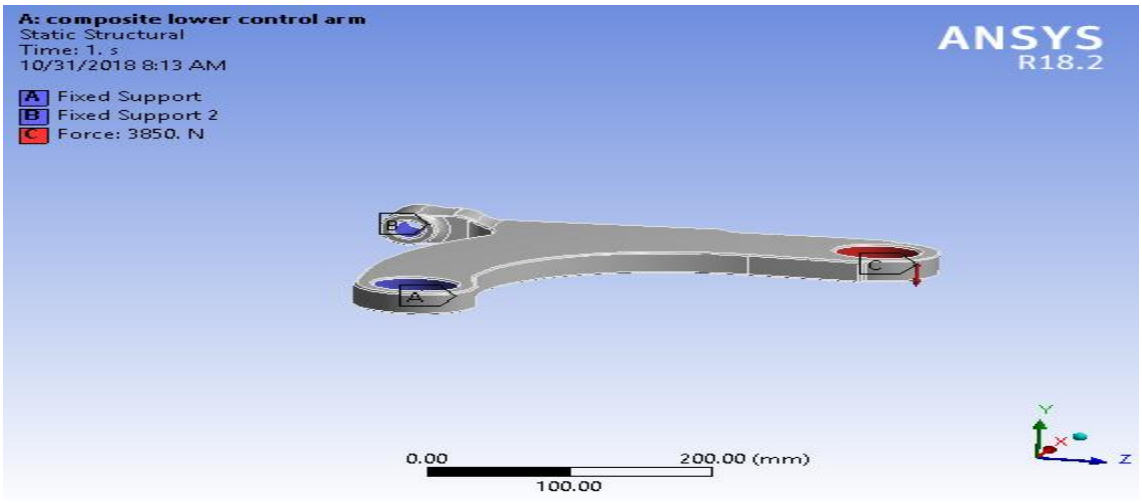


Figure 3.55. loading and boundary condition of Kevlar/E-glass hybrid composite lower control arm

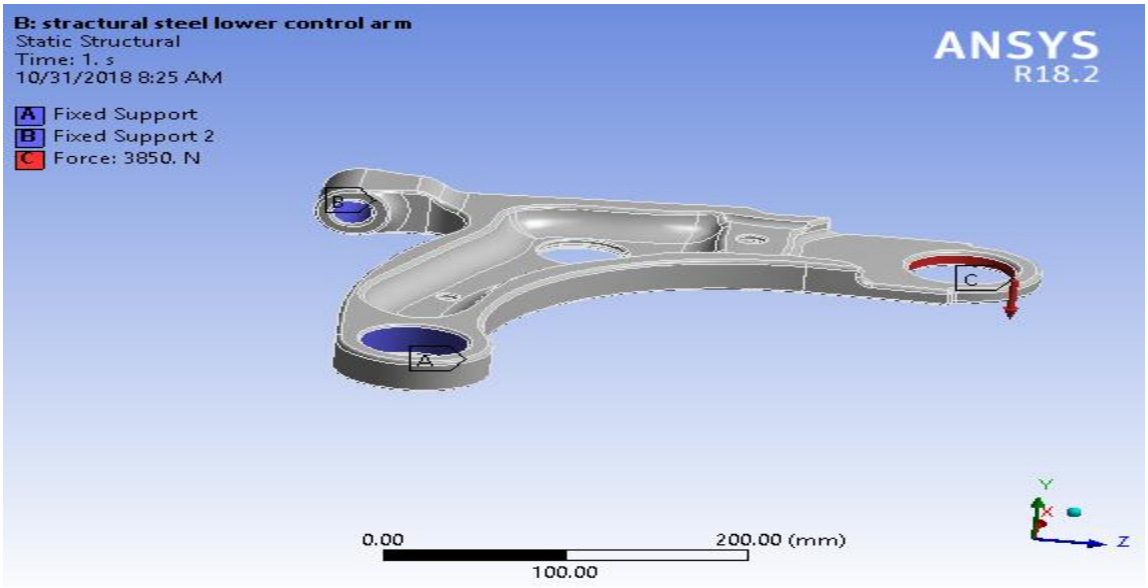


Figure 3.56. loading and boundary condition of conventional steel lower control arm

### 3.7.3.5 Generating solution

The solution is generated from the above input parameters of the project. The total deformation, equivalent (Von Misses) stress and safety factor are the basic variables to be solved by this software analysis. Solution Output continuously updates any listing output from the solver and provides valuable information on the behavior of the structure during the analysis.

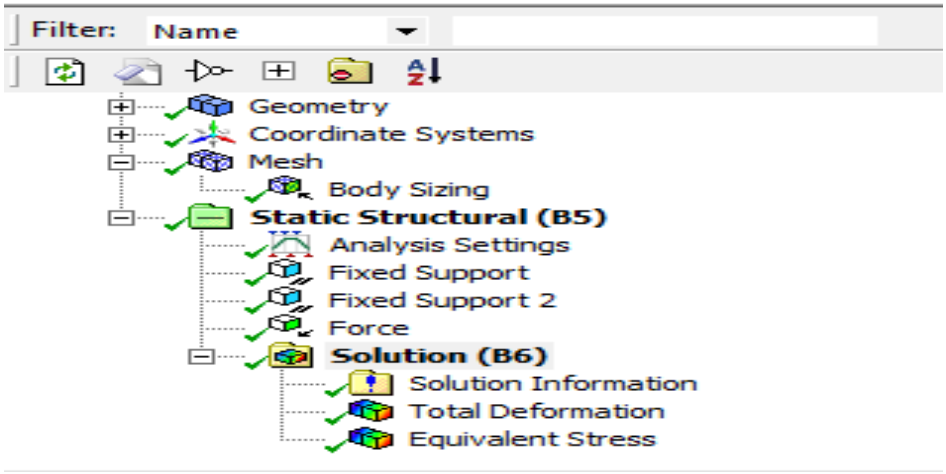


Figure 3.57. generating solution of lower control arm.

# CHAPTER FOUR

# Result and Discussion

In this chapter the results of both laminated Kevlar/E-glass hybrid composite and structural steel materials obtained from the static structural analysis clearly stated. Then the results presented here are the two lower control arm materials, namely laminated Kevlar/E-glass hybrid composite and structural steel materials of; total deformation and equivalent (Von Misses) stress. The most important step of finite element analysis procedure is the physically realistic interpretation of the results of the analysis.

For this study, the lower control arm static structural analysis is performed using finite element method by using ANSYS 18.2 workbench, that consist of a static structure. The static structural analysis determines the characteristics of the stress and deformation of the structure caused by the applied static loading systems and boundary conditions. The following typical static structural analysis system of ANSYS 18.2 workbench could be performed analysis and get an appropriate solution of the problem.

## 4.1. Results

### 4.1.1. Equivalent (von misses) stress

The equivalent (Von Misses) stress values of both the composite and conventional structural steel of lower control arm of FEA respectively looks like in the following figures.

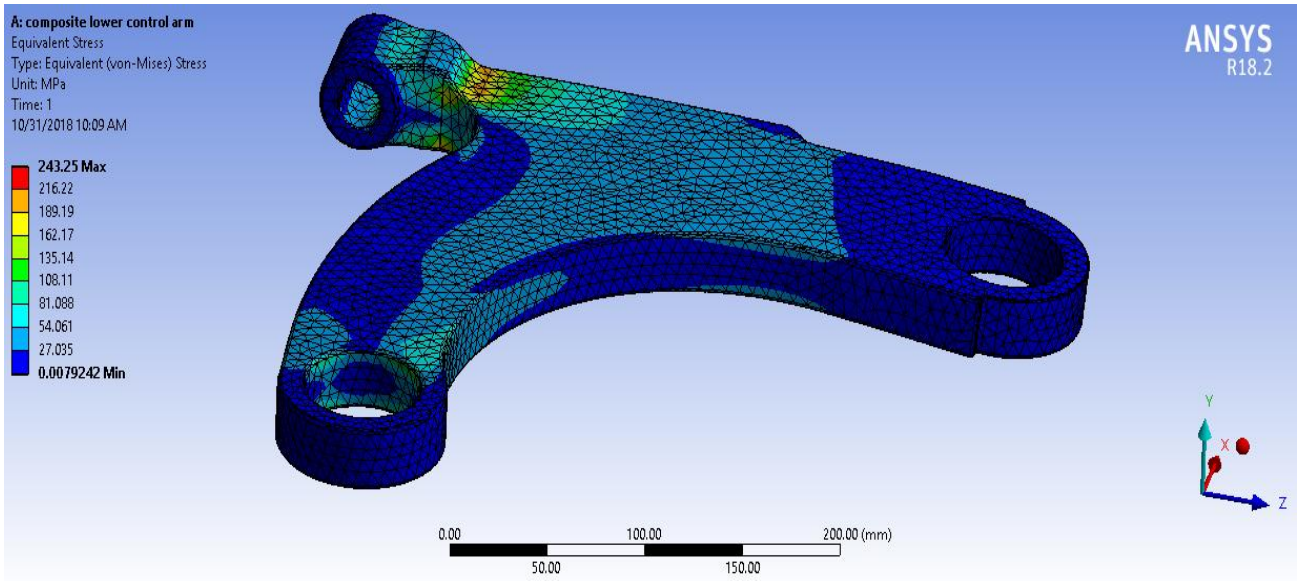


Figure 4.1. Equivalent (Von Mises) stress of Kevlar/E-glass hybrid composite of lower control arm.

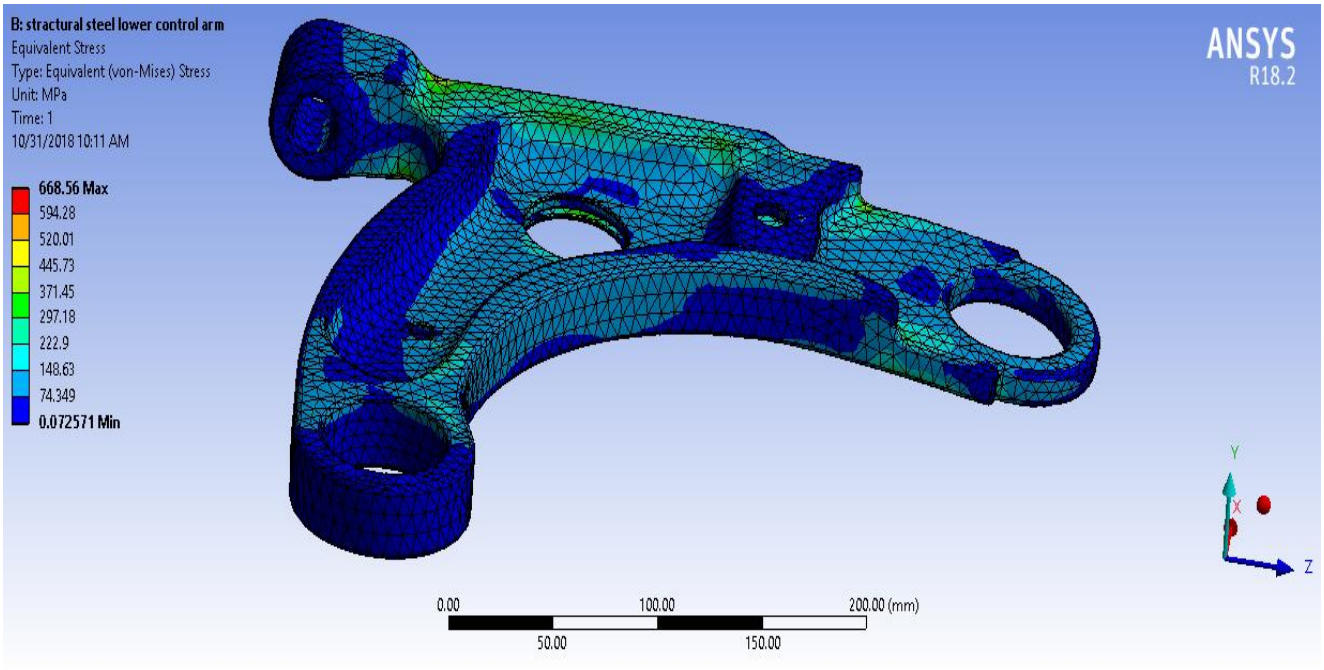


Figure 4.2. Equivalent (Von Mises) stress of conventional steel lower control arm.

## 4.1.2. Deformation

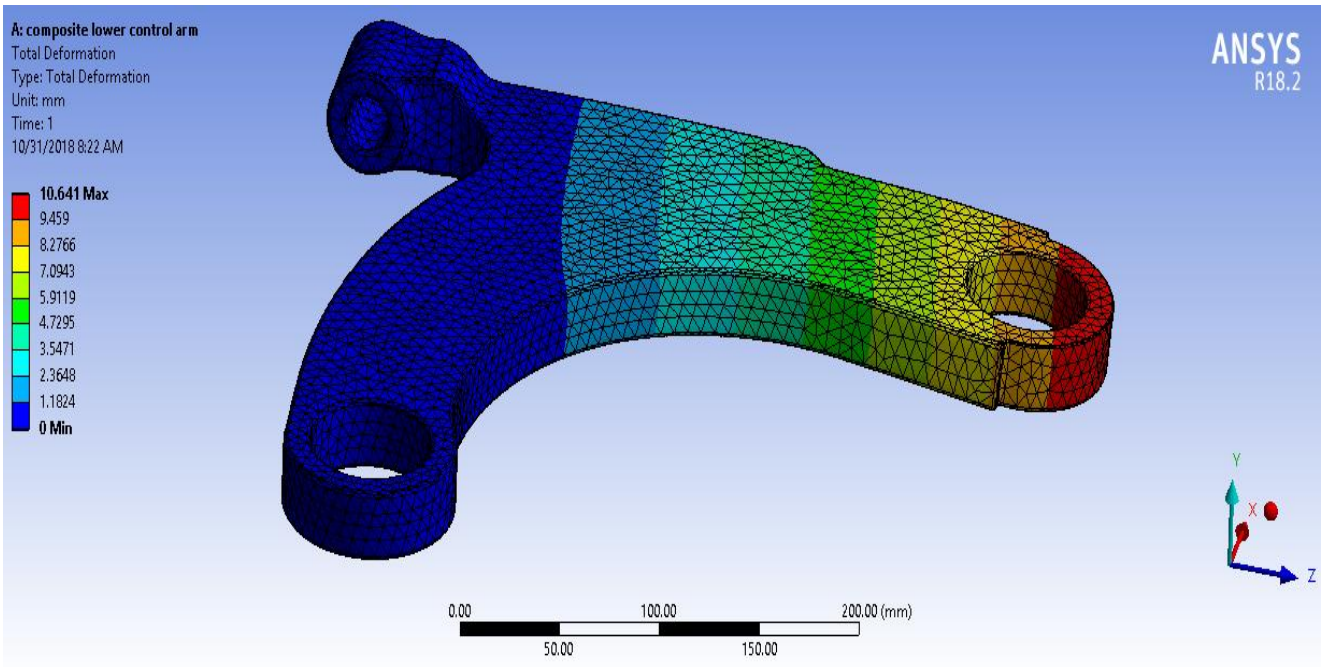


Figure 4.3. Total deformation of Kevlar/E-glass hybrid composite lower control arm.

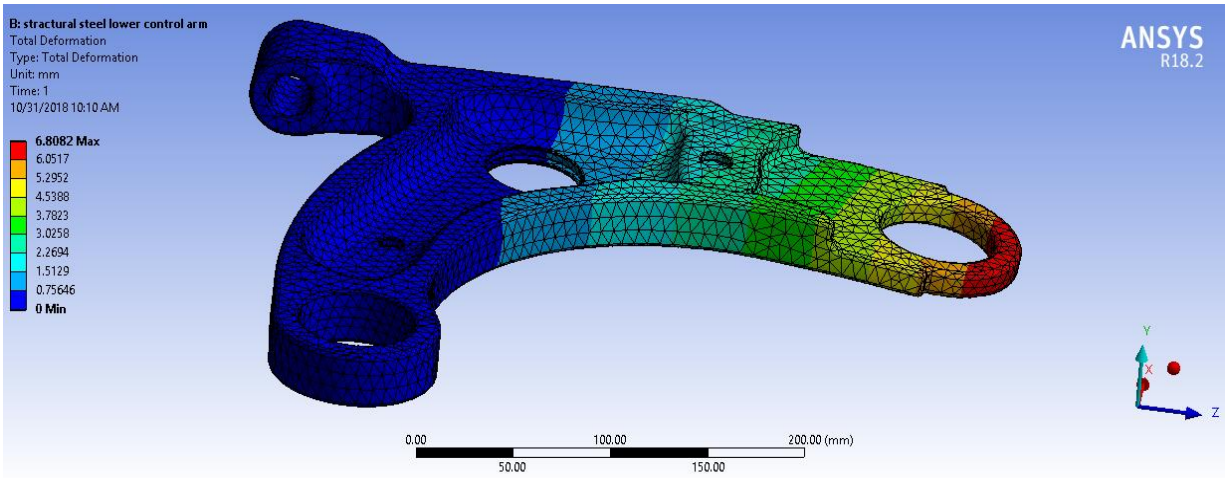


Figure 4.4. Total deformation of conventional steel lower control arm.

## 4.2. Discussion

The static structural analysis of a lightweight vehicle of lower control arm using laminated Kevlar/E-glass hybrid composite and structural steel material was performed for applying a static load of 3850 N on a ball joint of the lower arm. When comparing the results obtained from FEA of the designed laminated Kevlar/E-glass hybrid composite and structural steel lower arm, the newly designed laminated Kevlar/E-glass hybrid composite lower arm has light weight and less stressed than that of the current structural steel lower arm. In this specific research the comparison between the results of the FEA of these laminated Kevlar/E-glass hybrid composite and structural steel lower arm is carried out by making everything the same, except the geometry and material properties; i.e. at the same loading type and magnitude, the same boundary condition and the same method of FEM analysis.

### 4.2.1. Equivalent (Von-Misses) stress

Using the ANSYS 18.2 workbench software, the values of equivalent (Von-Misses) stress found along with the given boundary conditions and applied load of 3850 N. Then the maximum equivalent (Von-Misses) stress values of laminated Kevlar/E-glass hybrid composite lower arm has been found 243.25MPa. so, the value of stress is well below the max stress, which is 419.2 MPa for laminated Kevlar/E-glass hybrid composite. And then the maximum equivalent (Von-Misses) stress values of structural steel lower arm has been found 668.56MPa so, the value of stress is above the max stress, which is 460 MPa structural steel material. The results of this static structural analysis show that the equivalent (Von-Misses) stress of the laminated Kevlar/E-glass hybrid composite material lower control arm is the smallest one as compared to that of the current conventional structural steel lower control arm under the same load and boundary conditions. This implies that laminated Kevlar/E-glass hybrid composite lower control arm is less stressed.

### 4.2.2. Deformation

From this static structural analysis ANSYS 18.2 workbench software, the maximum deformation observed is 10.641mm for laminated Kevlar/E-glass hybrid composite material and 6.8082mm conventional structural steel material in the lower control arm at the free end. This show that, the maximum displacements of the laminated Kevlar/E-glass hybrid composite lower control arm has higher than the current conventional steel lower control arm.

Table 4.1. Comparison of the FEA results of the Kevlar/E-glass hybrid composite and conventional steel lower control arm

| Parameters | Composite lower control arm | Conventional steel lower control arm | Variation |
|---|---|---|---|
| Displacement | 10.641 | 6.8082 | 36.02% |
| Von Misses Stress | 243.25 | 668.56 | 63.62% |
| mass | 2.42 | 4.36 | 44.5% |

The graph below shows that the comparisons of FEA values of equivalent stress of for both laminated Kevlar/E-glass hybrid composite lower control arm and current structural steel lower control arm**.**

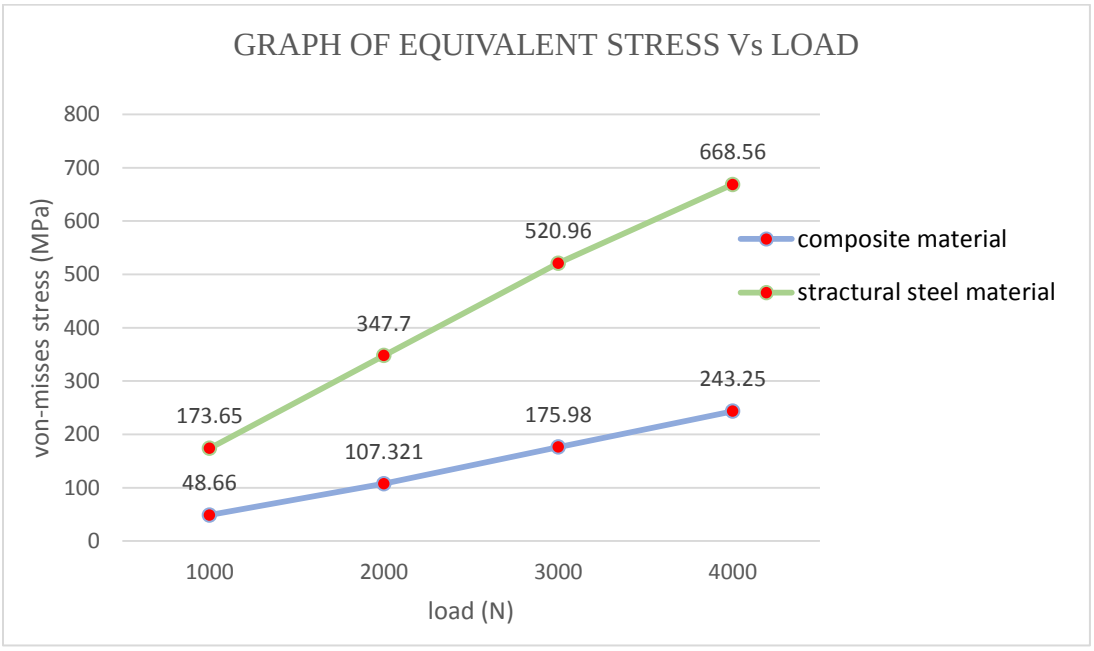


Figure 4.5. Comparison of equivalent stress of Kevlar/E-glass hybrid composite and structural steel lower control arm.

Figure 4.6 below shows that the comparison of deformation between the current conventional steel lower control arm of LIFAN 530 VIP automobile and the newly designed laminated Kevlar/E-glass hybrid composite lower control arm.

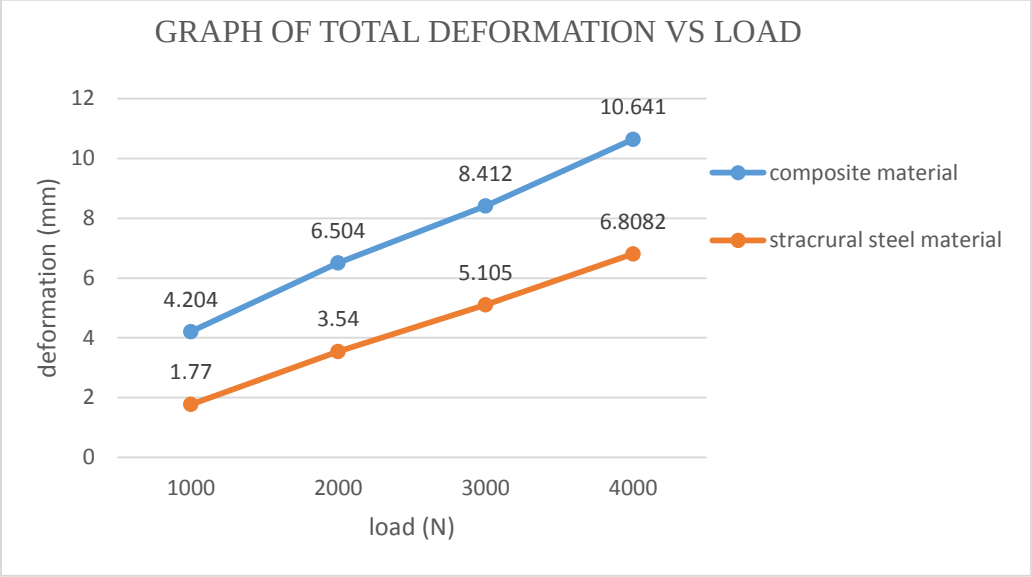


Figure 4.6. Comparison of total deformation of Kevlar/E-glass hybrid composite and conventional steel lower control arm.

Figure 4.7 below shows that the comparison of weight between the current conventional steel lower control arm of LIFAN 530 VIP automobile and the newly designed laminated Kevlar/E-glass hybrid composite lower control arm.

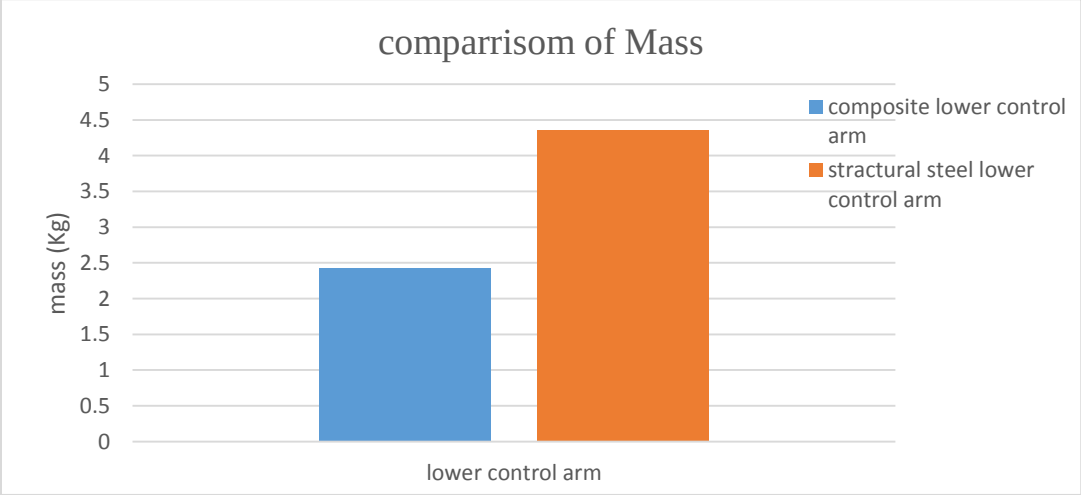


Figure 4.7. Comparison of weight of Kevlar/E-glass hybrid composite and conventional steel lower control arm.

Designed laminated Kevlar/E-glass hybrid composite lower control arm is lightweight than that of the current conventional steel lower control arm of LIFAN 530 VIP automobile and achieve about 44.5% weight reduction in the suspension system.

# CHAPTER FIVE

# Conclusion and Recommendation

## 5.1. Conclusion

This thesis work involves, the comparison of LIFAN 530 VIP automotive laminated Kevlar/E-glass hybrid composite lower control arm with current conventional steel lower control arm under a static loading condition. In this paper, Kevlar/E-glass hybrid composite material was manufactured different composition ratio of 60%/40%, 55%/45% and 50%/50% of fiber/epoxy and its mechanical performance such as the tensile, compression and flexural properties was determined using laboratory experiments. Based on the experimental test results, the composition ratio of 60%/40% fiber/epoxy have higher tensile, compressive and flexural strength as compared to others composition ratio so, it is suitable for lower control arm.

To conclude this work as explained the stress, deformation and weight in laminated Kevlar/E-glass hybrid composite lower control arm with current conventional steel lower control arm of LIFAN 530 VIP automobile suspension system. The stress is maximum in the existing design with structural steel lower control arm of 668.56 MPa and the deformation is maximum in the new design laminated Kevlar/E-glass hybrid composite lower control arm of 10.641 mm. finally, the new design has been developed to reduce stresses and weight existing in the current design with structural steel lower control arm. The stresses are almost reduced to 668.56MPa to 243.25MPa. The redesigned suspension arms achieve an average weight saving of 44.5% with respect to the stractural steel arms.

## 5.2. Recommendations

The properties of composite materials, like high strength to weight ratio and high specific stiffness are attractive for the construction of lightweight, fuel efficient and environmental friendly vehicle components. The fuel efficiency of the vehicle directly depends on the total dead weight of the vehicle. Then in order to maintain light weight, fuel efficient and high speed vehicle design, selecting composite materials is the only best decision. Moreover, laminated Kevlar/E-glass hybrid composite material have 1.695 $\frac{g}{cm^3}$ 419.2 MPa, 372.69 MPa and 375.3MPa density, tensile, compressive and flexural strength respectively. Laminated Kevlar/E-glass hybrid composite material gives good tensile strength, flexural strength and compressive strength So, it is recommended that check aircraft and automotive components that reduces weight and gives more strength.

## 5.3. Future work

Standing from different aspects, working with composite materials has several advantages. From this point of view, regarding laminated Kevlar/E-glass hybrid composite lower control arm several things can be done and improved in the future in which this study didn't address. Therefore; the following research areas are recommended for future studies:

- The design and dynamic analysis of laminated Kevlar/E-glass hybrid composite lower control arm.
- Determine maximum braking impact condition and turning force acting on lower control arm suspension system.
- The designing the lower control arm by changing the orientation of the fiber and ply.
- The manufacturing of laminated Kevlar/E-glass hybrid composite lower control arm.
- Currently the analysis is done on the changing the material, but this will only reduce the weight and stress of the component still there is chance of getting high deformation. So in order to avoid this high deformation we can do it in a shape optimization and made other hybrid composite materials.

# Reference


1. Dr. R.G. TODKAR, MR. BALASAHEB GADADE and "Design, analysis of A-type front lower suspension arm in Commercial vehicle." IRJET, Volume: 02 Issue: 07 | Oct-2015.
2. HARDIAL SINGH, GIAN BHUSHAN "Finite Element Analysis of a Front Lower Control Arm of LCV Using Radios Linear"
3. DATTATRAY KOTHAWALE and DR. Y. R. KHARDE "Analysis of Lower Control Arm in Front Suspension System Using F.E.A. Approach" International Journal of Engineering Research and Development, Volume 5, Issue 12 (February 2013), PP. 18-23
4. KHARADE, MISS. P. B. PATIL and PROF. M. V. "Finite Element Analysis and Experimental Validation of Lower Control Arm." IJEDR | 2016, Volume 4, Issue 2 | ISSN: 2321-9939.
5. SAHA, JAGWINDER SINGH and SIDDHARTHA. "Static Structural Analysis of Suspension Arm Using Finite Element Method." Volume: 04 Issue: 07 | July-2015., IJRET.
6. PROF. A. M. PATIL, PROF. A.S. TODKAR, PROF. R. S. MITHARI and PROF. V. V. PATIL. "Experimental & Finite Element Analysis of Left Side Lower Wishbone Arm of Independent Suspension System." IOSR Journal of Mechanical and Civil Engineering (IOSR-JMCE), Volume 7, Issue 2 (May. - Jun. 2013), PP 43-48.
7. SANJAY K. MAZUMDAR, PH.D. "COMPOSITES MANUFACTURING Materials, Product, and Process engineering" text book, 2002 by CRC Press LLC
8. AUTAR K. KAW. "Mechanics of Composite Materials" second edition, 2006 by Taylor & Francis Group, LLC
9. DANIEL GAY, SUONG V. HOA and STEPHEN W. TSAI "COMPOSITE MATERIALS design and application" Boca Raton London New York Washington, D.C. 2003 by CRC Press LLC.
10. CARL ZWEBEN, "Composite Materials." Mechanical Engineers' Handbook Materials and Mechanical Design, Volume1, Third Edition.
11. RAMESH UDHAYAKUMAR A, SIDDHARTHA D, SETHU RAMAN A, RAMANAN N and KARTHI V. "Modeling and Analysis of Lower Wishbone for Independent Suspension System for Commercial Vehicles." JCHPS Special Issue 2: February 2017.
12. WŁADYSŁAW PAPACZ, PIOTR KURYŁO, EDWARD TERTEL. "The Composite Control Arm – Analysis of the Applicability in Conventional Suspension" American Journal of Mechanical Engineering, 2013, Vol. 1, No. 7, 161-164

13. PAOLO FERABOLI1, FEDERICO GASCO, BONNIE WADE "Lamborghini Forged Composite Technology for the Suspension Arms of the Sesto Element to" Journal of Composite Materials, 43/19, 2010, pp. 1947-1965.
14. ZENGFENG SONG, XIAOYU ZHAO "Research on Lightweight Design of Automobile Lower Arm Based on Carbon Fiber Materials" World Journal of Engineering and Technology, 2017, 5, 730-742
15. CHRISTIAN JANSEN, CTO AND ANTHONY WEI, CEO "Design of a carbon fiber isogrid-stiffened automo1ve suspension arm" JEC Composite 2013, June 25, 26
16. SANGHYUK YOO, JAEHYEOK DOH, JUHEE LIM, OHSUNG KANG, JONGSOO LEE and KEONWOOK KANG "TOPOLOGICALLY OPTIMIZED SHAPE OF CFRP FRONT LOWER CONTROL ARM" International Journal of Automotive Technology, Vol. 18, No. 4, pp. 625−630 (2017)
17. M.SRIDHARAN AND DR.S. BALAMURUGAN "Design and Analysis of Lower Control ARM" International Journal of Innovative Research in Science, Engineering and Technology, Vol. 5, Issue 4, April 2016.
18. SWAPNIL S. KHODE, PROF. AMOL N. PATIL, and PROF. AMOL B. GAIKWAD "Design Optimization of a Lower Control Arm of Suspension System in a LCV by using Topological Approach" International Journal of Innovative Research in Science, Engineering and Technology, Vol. 6, Issue 6, April 2017.
19. VINAYAK KULKARNI, ANIL JADHAV and P. BASKER. "Finite Element Analysis and Topology Optimization of Lower Arm of Double Wishbone Suspension using RADIOSS and Opti-struct." Volume 3 Issue 5, May 2014, International Journal of Science and Research (IJSR).
20. TILOTTAMA A. CHAUDHARI, ER NAVNEET K. PATIL and JAGRUTI R SURANGE. "Review: Design and Failure analysis of Front Lower Suspension Arm of Car." IJIRSET Volume 6, Special Issue 1, January 2017.
21. R. PRASHANTHASAMY R.M.T, DR. SATHISHA, MR. IMRAN ALI M.R and MR. JNANESH. K. "Design and Model Analysis of Lower Wishbone Suspension Arm Using F.E. Approach" Imperial Journal of Interdisciplinary Research (IJIR) Vol-2, Issue-9, 2016.
22. MUHAMAD FAHRURRAZI and BIN JUBRI "Design and Development of Car Suspension Lower Arm" 30 November 2015.

23. A. KALAIYARASAN, S. PALANISAMY, R. RAMESH and DR. S. SUNDARAM "Re-engineering of Suspension Control Arm using Aluminum Alloy (al6065) and Validation using FEA/FEM" International Journal of Mechanical Engineering Research. ISSN 2249-0019 Volume 7, Number 1 (2017), pp. 21-33.
24. DO-HYOUNG KIM, DONG-HOON CHOI and HAK-SUNG KIM "Design optimization of a carbon fiber reinforced composite automotive lower arm" 2013 Elsevier Ltd. All rights reserved, Composites: Part B 58 (2013) 400–407.
25. ALFREDO LAMBERTI, GABRIELE CHIESURA, GEERT LUYCKX, JORIS DEGRIECK, MARKUS KAUFMANN and STEVE VANLANDUIT "Dynamic Strain Measurements on Automotive and Aeronautic Composite Components by Means of Embedded Fiber Bragg Grating Sensors" Sensors 2015, 15, 27174-27200;
26. GURURAJE GHANU and PROF. R.S. KATTIMANI "Comparison Study of Lower Control Arm with Different Material" International Research Journal of Engineering and Technology (IRJET) e-ISSN: 2395 -0056 Volume: 03 Issue: 10 | Oct -2016.
27. G. ABUMERI, B. K. KNOUFF, D. LAMB, D. HUDAK, and R. GRAYBILL "Benefits of High Performance Computing in the Design of Lightweight Army Vehicle Components" USC Information Sciences Institute, Arlington, 13 SEP 2010
28. HEMIN M. MOHYALDEEN'S "Analysis of an automobile suspension arm using the robust design method" 2011.
29. PATIK S. AWATI PROF. L. M. JUDULKAR "Model and Analysis of Lower Wishbone Arm Along with Topology" International Journal of Application or Innovation in Engineering & Management (IJAIEM) Volume 3, Issue 5, May 2014 ISSN 2319 – 4847.
30. K.K. HERBERT YEUNG AND K.P. RAO "Mechanical Properties of Kevlar-49 Fiber Reinforced Thermoplastic Composites" Received: 29 January 2010, Accepted: 3 October 2011.
31. HIND W. ABDULLAH, DR. HARATH I. JAFFA and DR. KHALID R. AL-RAWI "Study of Bending Property for Epoxy / Kevlar - Glass Fibers and Hybrid Composite" IJSRD - International Journal for Scientific Research & Development| Vol. 33, part (B) no, 9, 2015.
32. file:///D|/Web%20Course%20(Ganesh%20Rana)/Dr.%20Mohite/CompositeMaterials/lecture17/17_4.htm[8/18/2014 12:35:24 PM]

33. F.-X. IRISARRI, A. LASSEIGNE, F.-H. LEROY and R. LE RICHE "Optimal design of laminated composite structures with ply drops using stacking sequence tables" Composite Structures 107 (2014) 559–569.
34. SUBHAN ALI JOGI, MUHAMMAD MOAZAM BALOCH, ALI DAD CHANDIO, IFTIKHAR AHMED MEMON and GHULAM SARWAR CHANDIO. "Evaluation of Impact Strength of Epoxy Based Hybrid Composites Reinforced with E-Glass/Kevlar 49" Mehran University Research Journal of Engineering & Technology, Volume 36, No. 4, October, 2017 [p-ISSN: 0254-7821, e-ISSN: 2413-7219].
35. SANDESH K.J., UMASHANKAR K.S., MANUJESH B.J., THEJESH C.K., MOHAN KUMAR N.M. "Mechanical Characterization of Kevlar/Glass Hybrid Reinforced Polymer composite laminates" International Advanced Research Journal in Science, Engineering and Technology ISO 3297:2007 Certified Vol. 3, Issue 12, December 2016.
36. YASH M. KANITKAR, ATUL P. KULKARNI, and KIRAN S. WANGIKAR. "Characterization of Glass – Kevlar hybrid composite" International Engineering Research Journal Page No 1626-1632.
37. LEVENT ONAL and SABIT ADANUR "Effect of Stacking Sequence on the Mechanical Properties of Glass–Carbon Hybrid Composites before and After Impact" JOURNAL OF INDUSTRIAL TEXTILES, Vol. 31, No. 4—April 2002.
38. POP P. ADRIAN and BEJINARU MIHOC GHEORGHE. "Manufacturing Process and Applications of Composite Materials" Annals of the Oradea University. Fascicle of Management and Technological Engineering, Volume IX (XIX), 2010, NR2.
39. "Composite Materials & Manufacturing" Fundamental Manufacturing Processes Study Guide, DV02PUB2.
40. PROF. R. VELMURUGAN. "Composite Materials" Dept. of Aerospace Eng., Indian Institute of Technology, Madras.
41. GURU RAJA M. N & A. N. HARI RAO "Effect of an Angle-Ply Orientation on Tensile Properties of Kevlar/glass Hybrid Composites" International Journal on Theoretical and Applied Research in Mechanical Engineering (IJTARME), ISSN: 2319 – 3182, Volume-2, Issue-3, 2013.
42. S. BANERJEE and B. SANKAR. "mechanical properties of hybrid composites using finite element method based micromechanics" Department of Mechanical and Aerospace Engineering, PO Box 116250, University of Florida, Gainesville, FL 32611, USA.

43. CHAMIS, C. C., LARK, R. F., "Hybrid composites – State-of-the-art review: Analysis, Design, Application and Fabrication", NASA Technical Memorandum, NASA, TM X-73545.
44. ASTM D3039. 1995. "Standard Test Method for Tensile Properties of Polymer Matrix Composite Materials". Annual Book of ASTM Standards, American Society for Testing and Materials, Philadelphia.14 (2): 99-109.
45. Zhao, M.G. Wang Chengming. Application and Development Trend of Automobile Lightweight Technology. Henan Electric Engineering Society of the Seventh Scientific Research Symposium Proceedings (2010).
46. ASTM D7264. 1995. "ASTM D7264 Flexural Properties of Polymer Matrix Composite Materials". Annual Book of ASTM Standards, American Society for Testing and Materials, Philadelphia.14 (2): 99-109.
47. FAVILLA, S. "Tensile Testing Laboratory date of lab exercise": January 28th 2010.
48. Wang, H.Y. and Chen, J.Y. (2009) Car Body Lightweight Structure and Light Material. Peking University Press, Beijing.
49. D 3039/D 3039M – 00***e***1. Standard Test Method for Tensile Properties of Polymer Matrix Composite Materials, revised editorially in December 2002.
50. STRUKTURLABOR, Finite Element Modeling with ANSYS,2010
51. N. Azhaguvel, S. Charles and M. Senthilkumar "Optimization of Mechanical Properties of E-Glass Woven Fabric Composite" PSG College of Technology, Coimbatore, India Accepted May 2017.
52. D 3410/D 3410M – 03 Standard Test Method for Compressive Properties of Polymer Matrix Composite Materials with Unsupported Gage Section by Shear Loading edition approved June 10, 2003.
53. https://addisfortune.net/articles/lifan-motors-has-a-long-road-vision-in-ethiopia/

[14/09/2017, 9:58 PM].

# Appendix A

Stress-strain curve and load Vs displacement for tensile test for different composition ratio of 60%/40%, 55%/45% and 50%/50% of fiber/epoxy is given below.

## 50/50 fiber/epoxy tensile test

### Test one

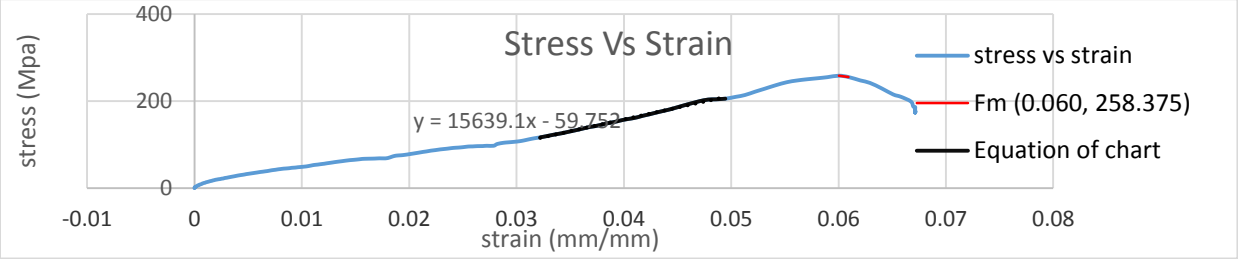


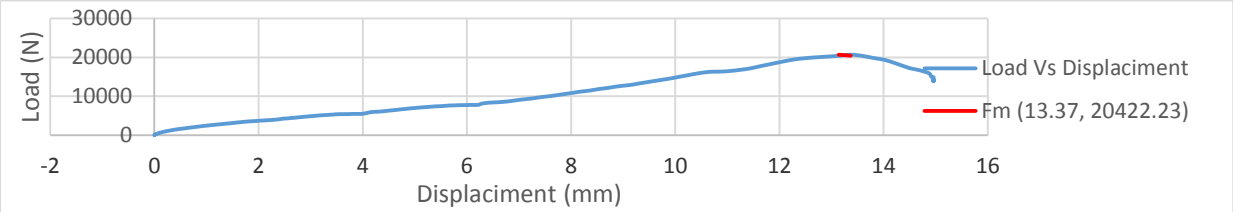


### Test two

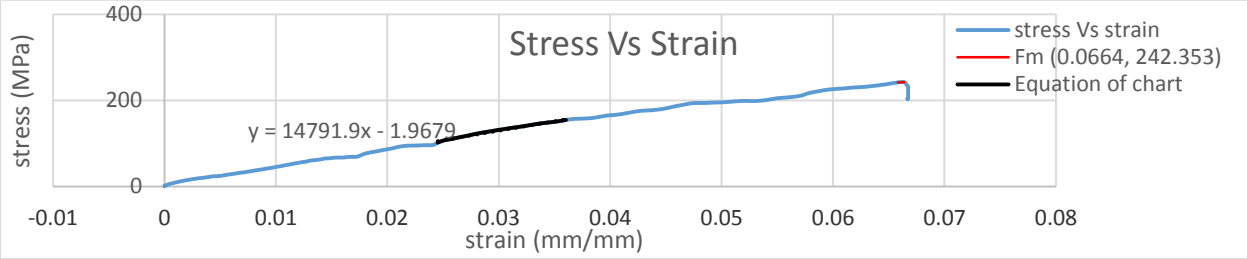


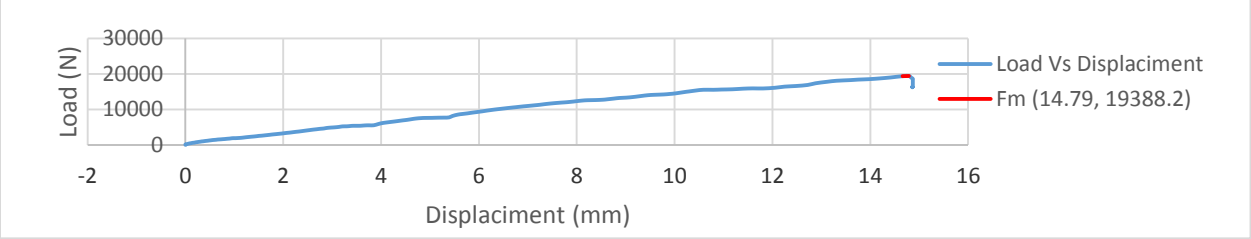


### Test three

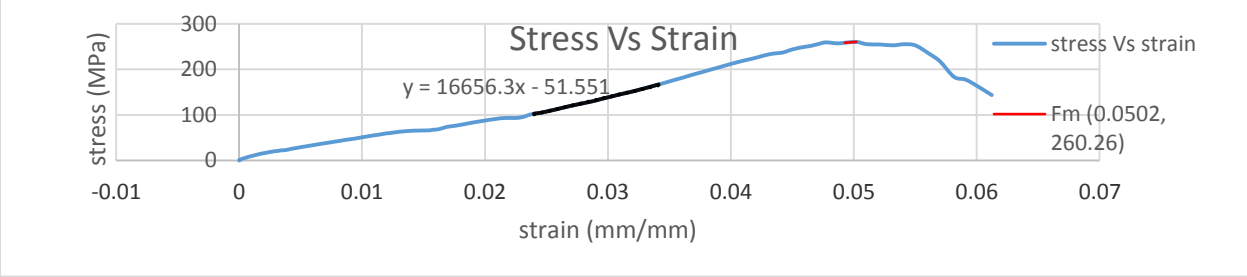

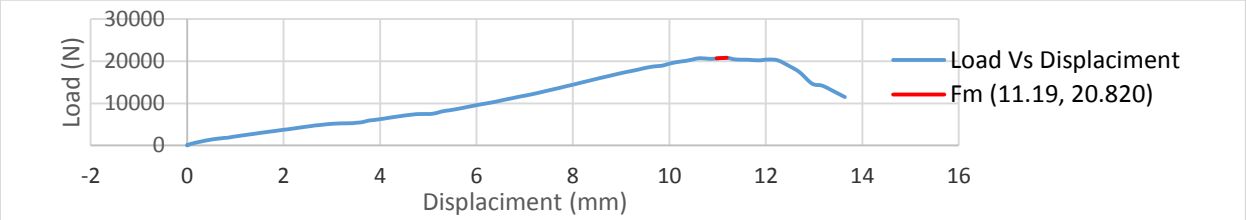


**Test four**

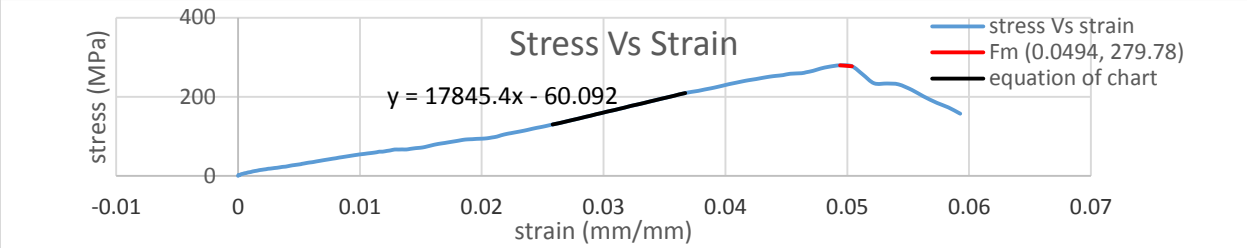


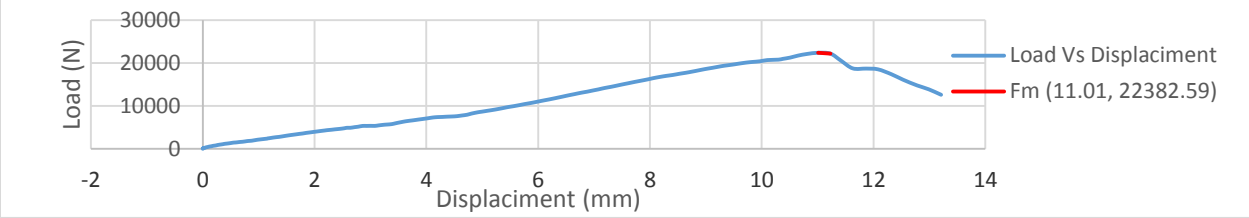


**Test five**

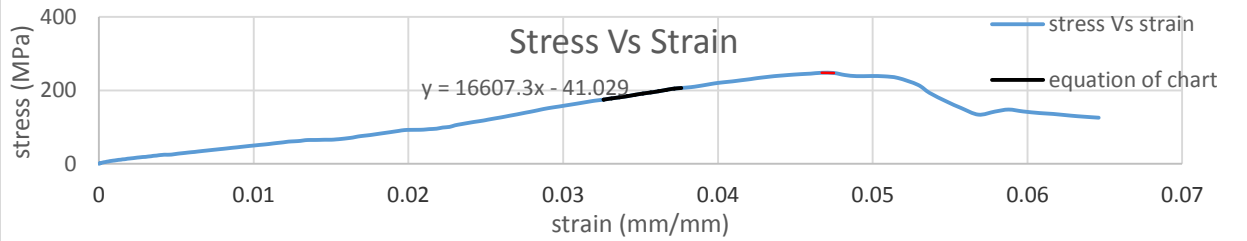


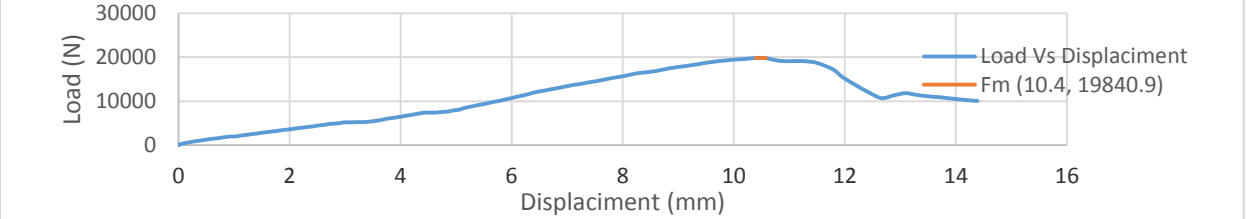


**55/45 fiber/epoxy tensile test**

**Test one**

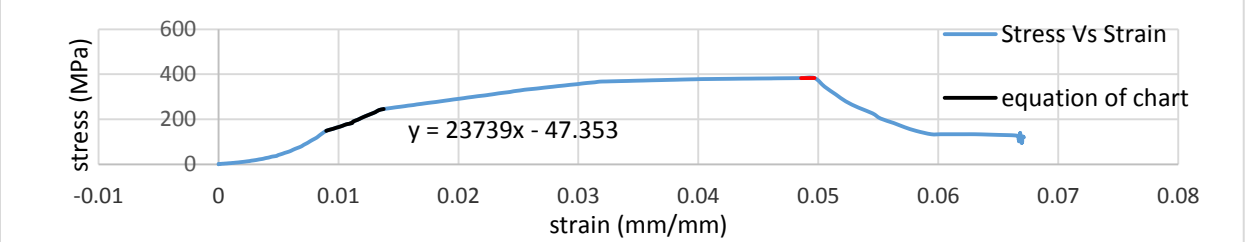

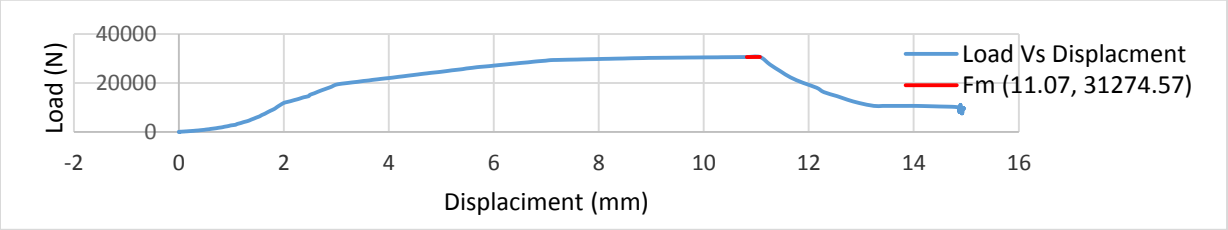


**Test two**

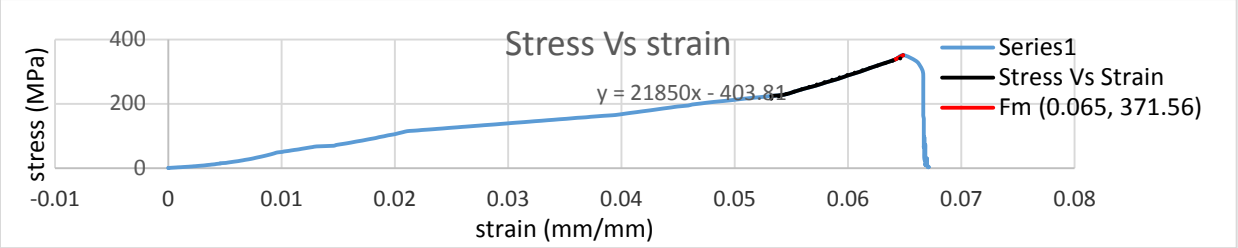


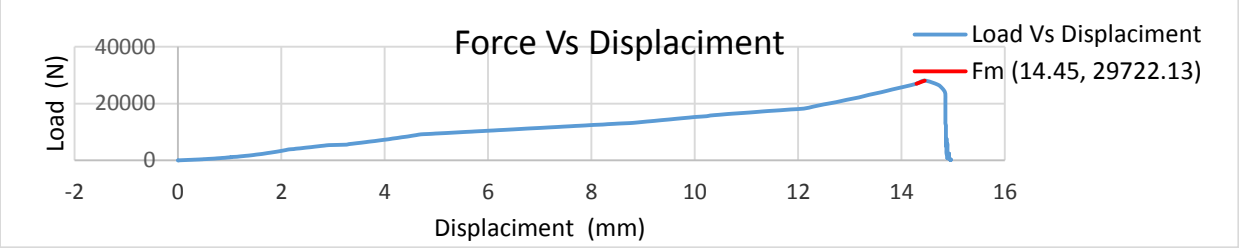


**Test three**

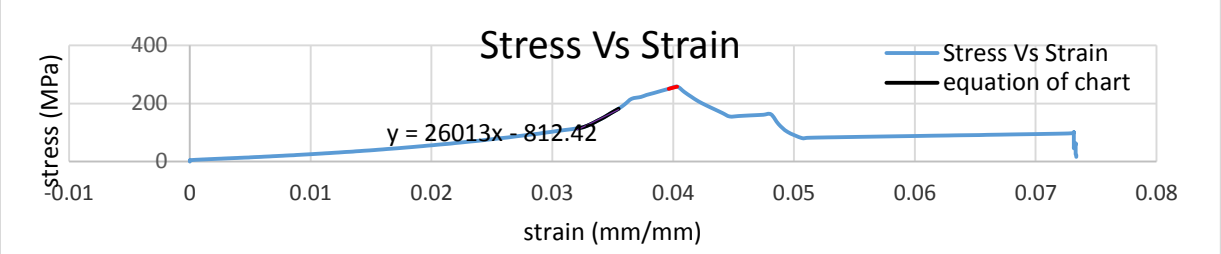


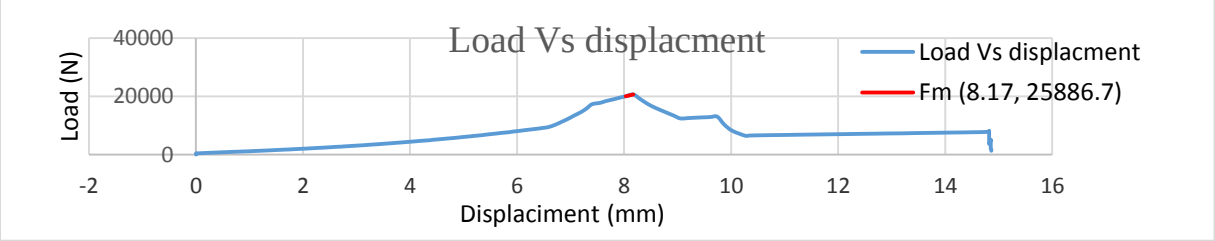


**Test four**

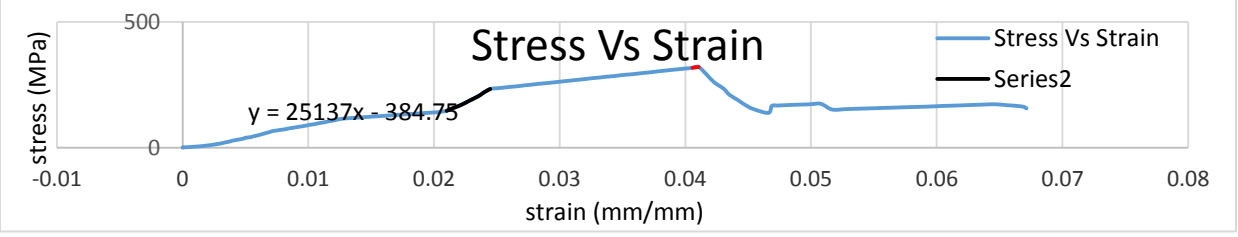

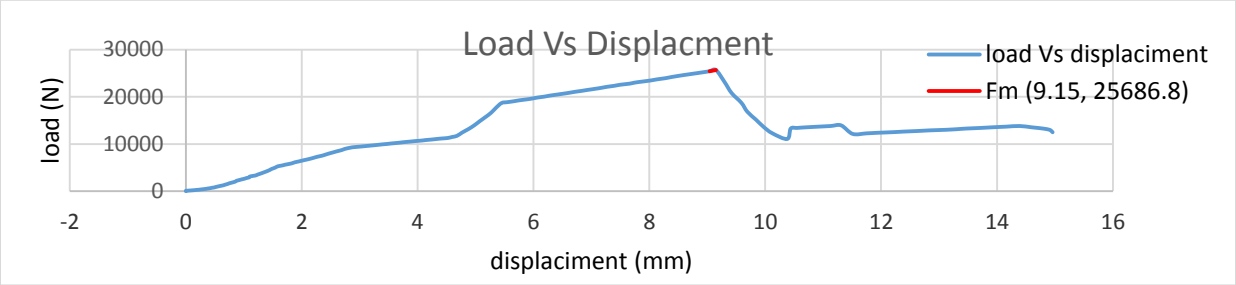


**Test five**

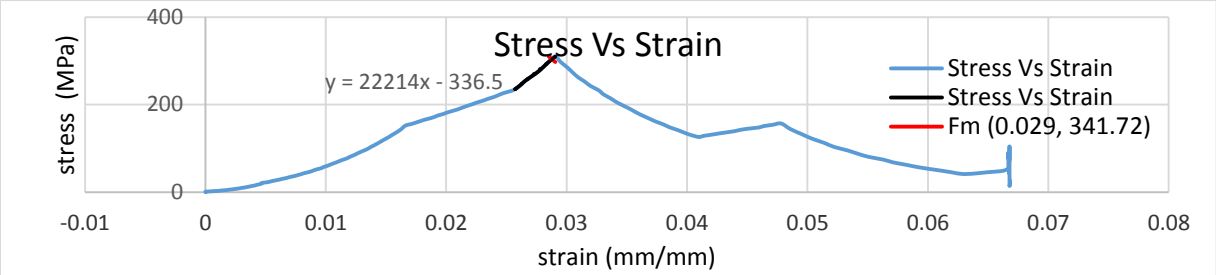


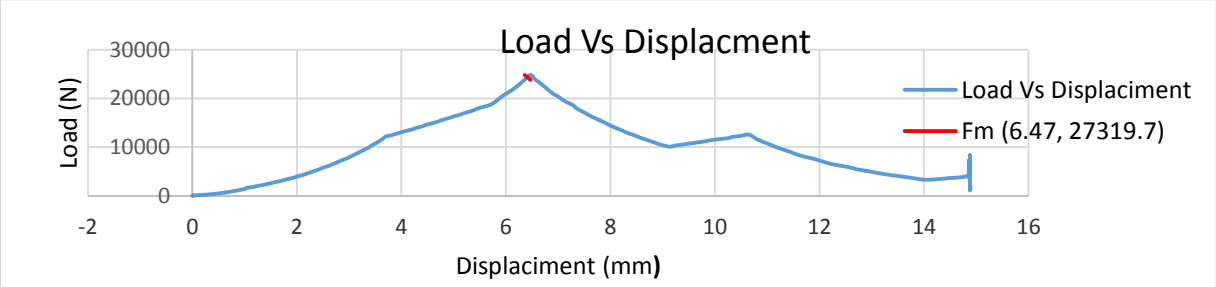


**60/40 fiber/epoxy tensile test**

**Test one**

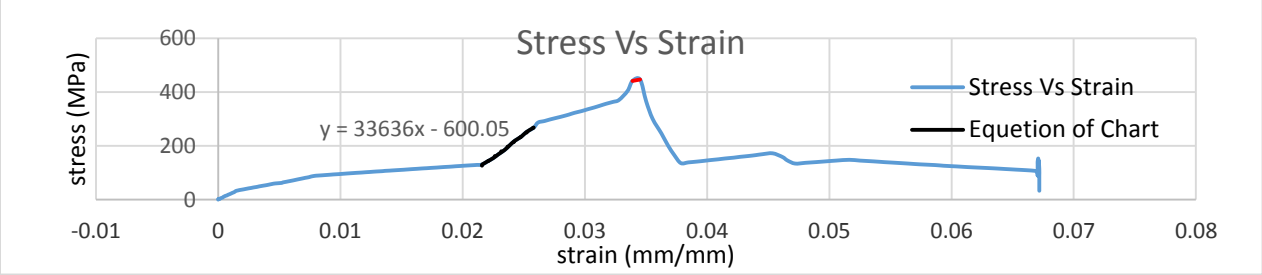


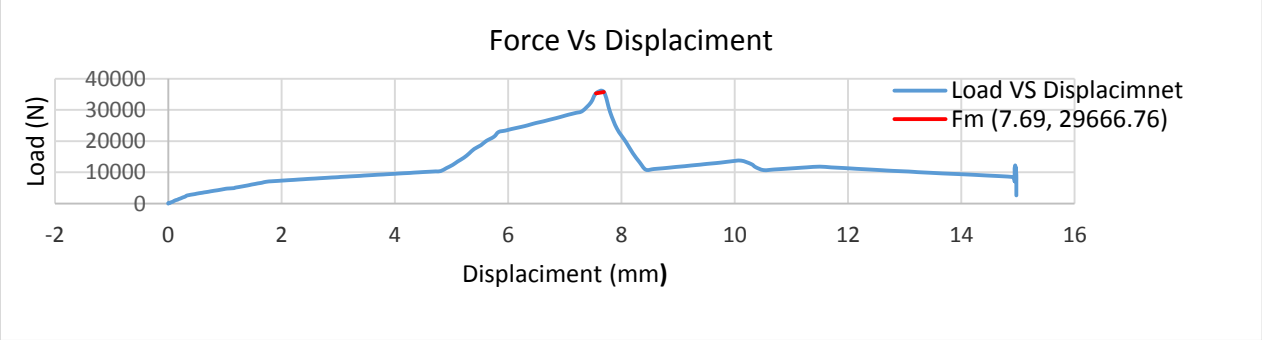

## Test two

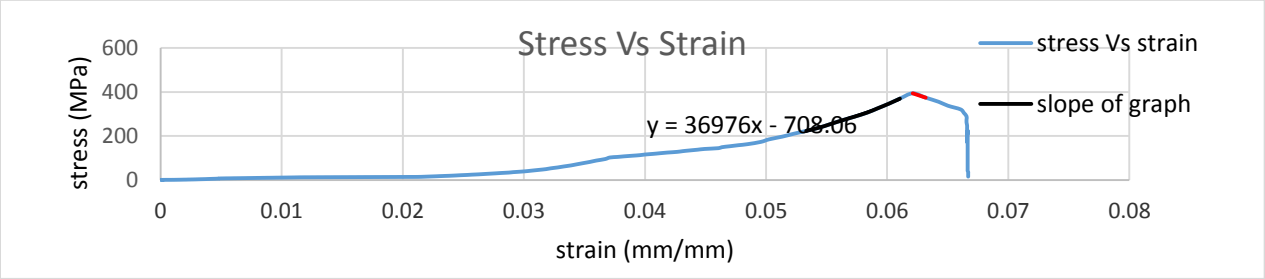


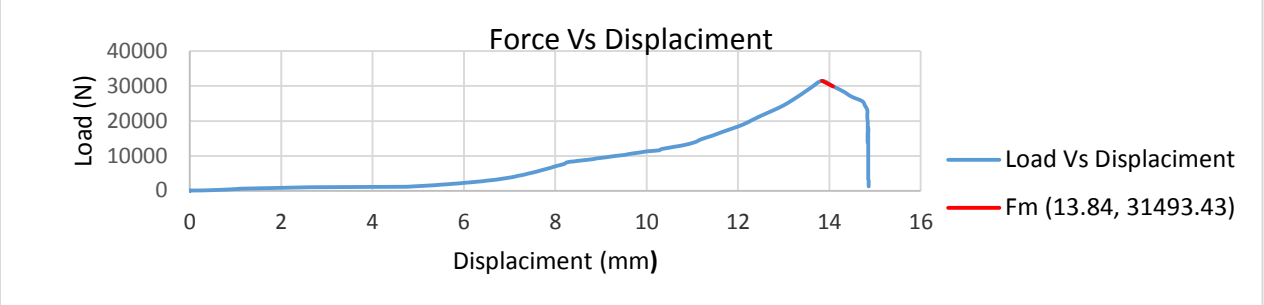


## Test three

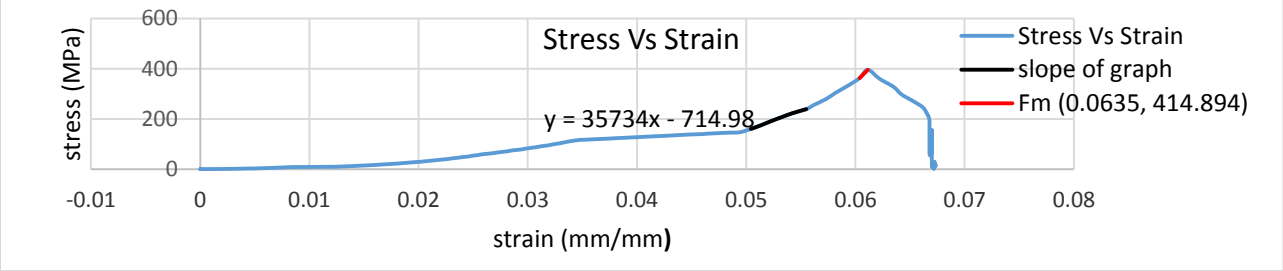


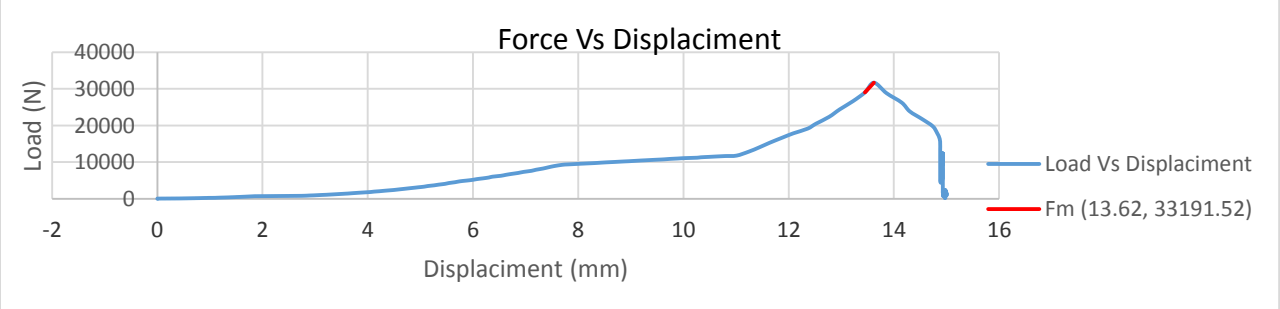


## Test four

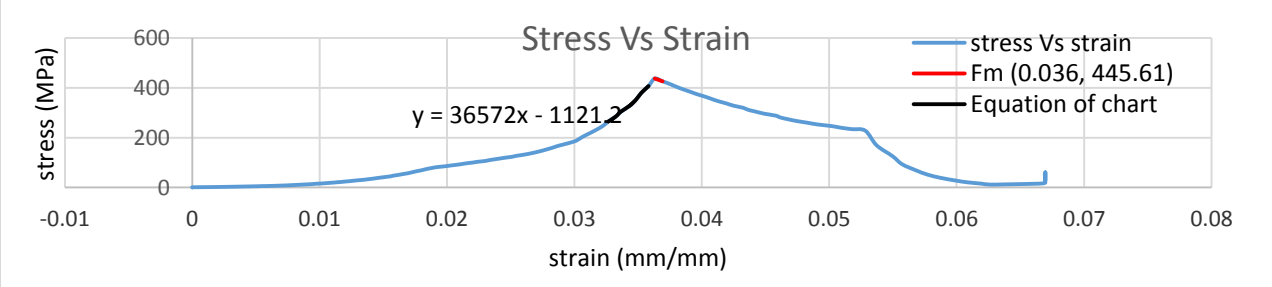

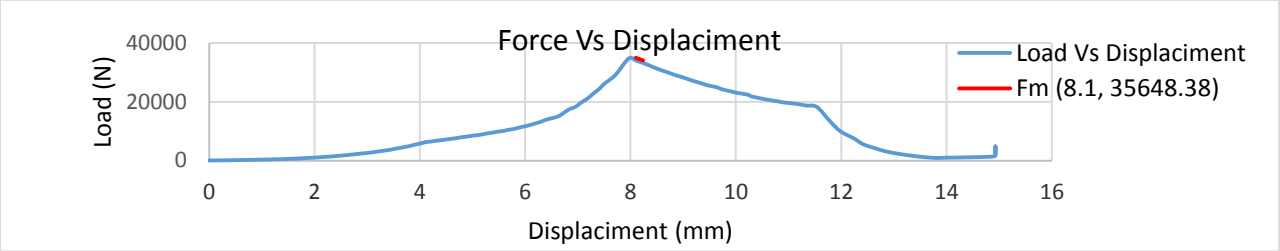


**Test five**

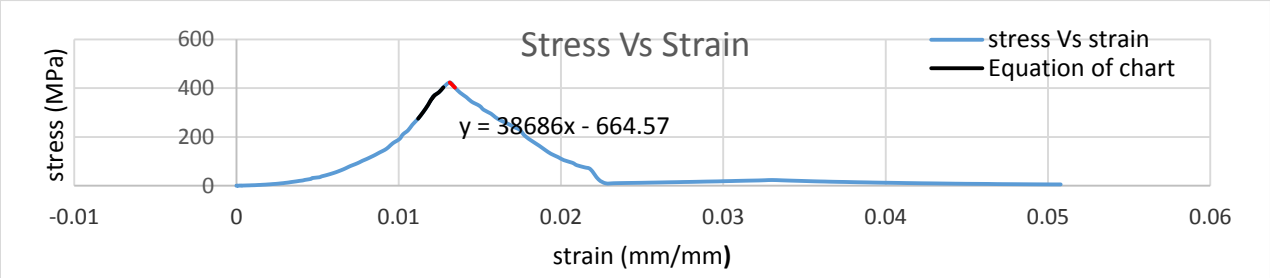


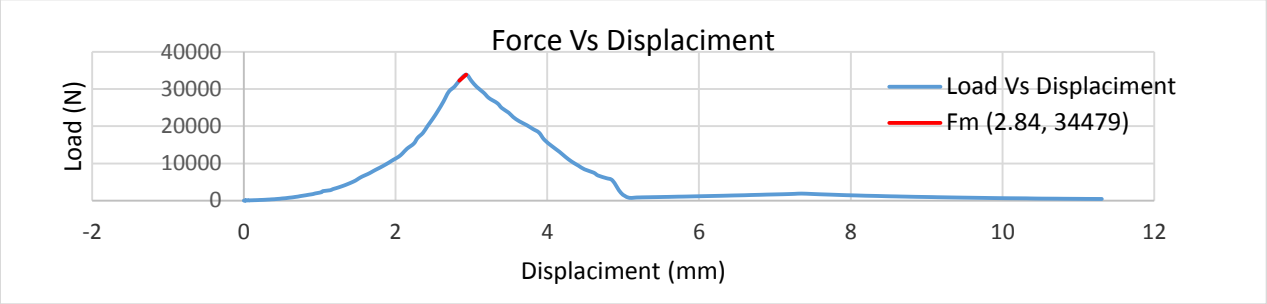


Stress-strain curve and load Vs displacement for flexural test for different composition ratio of 60%/40%, 55%/45% and 50%/50% of fiber/epoxy is given below.

**50/50 fiber/epoxy flexural test**

**Test one**

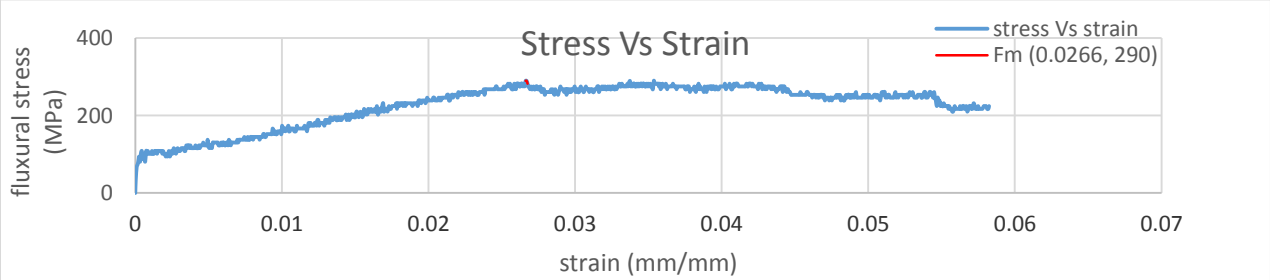


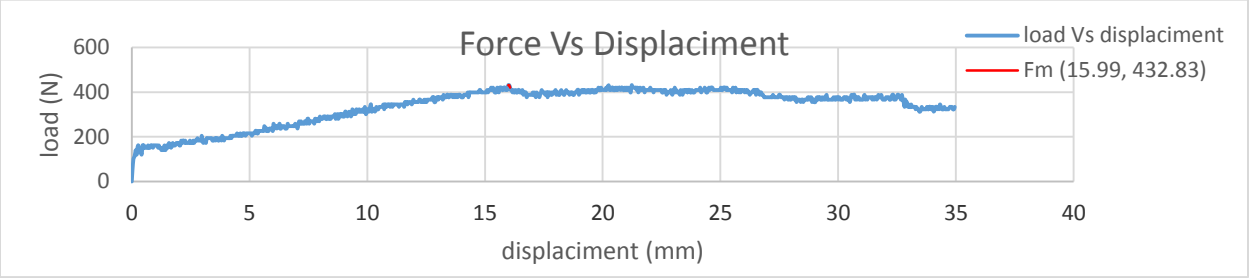

**Test one**

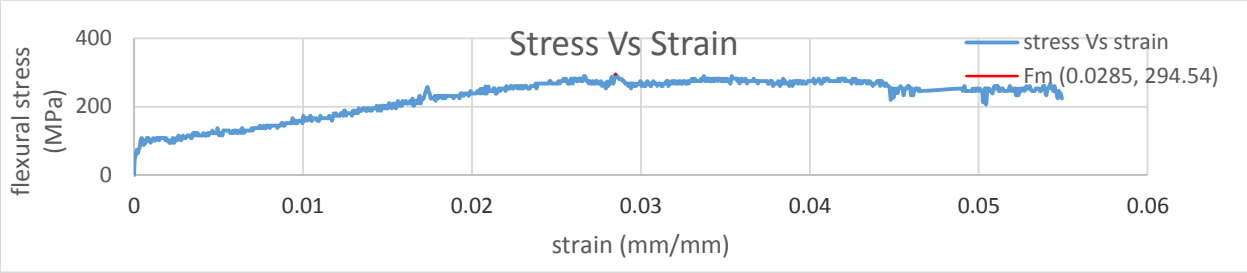


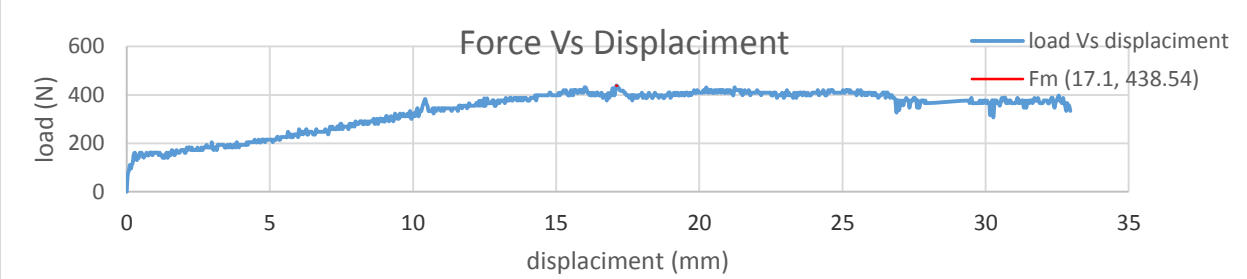


**Test two**

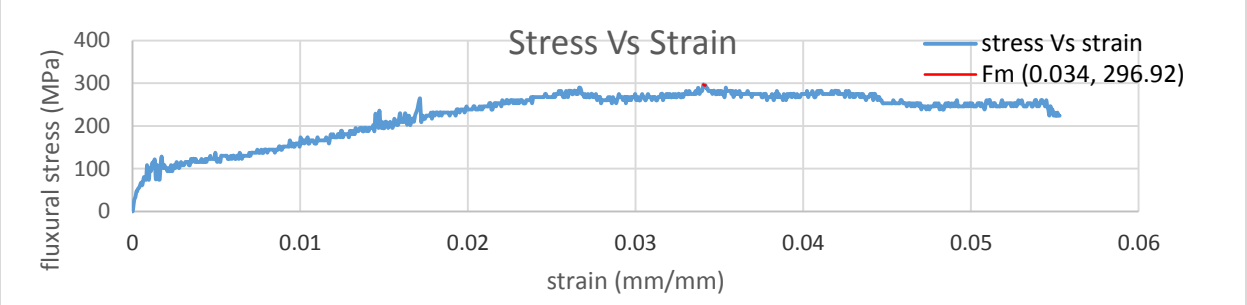


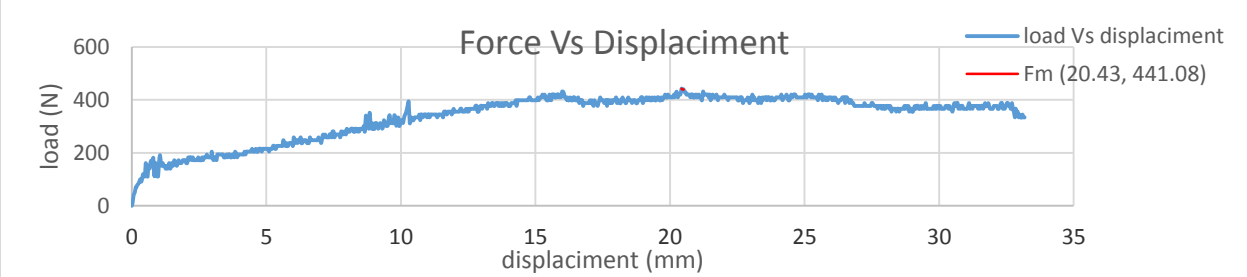


**Test three**

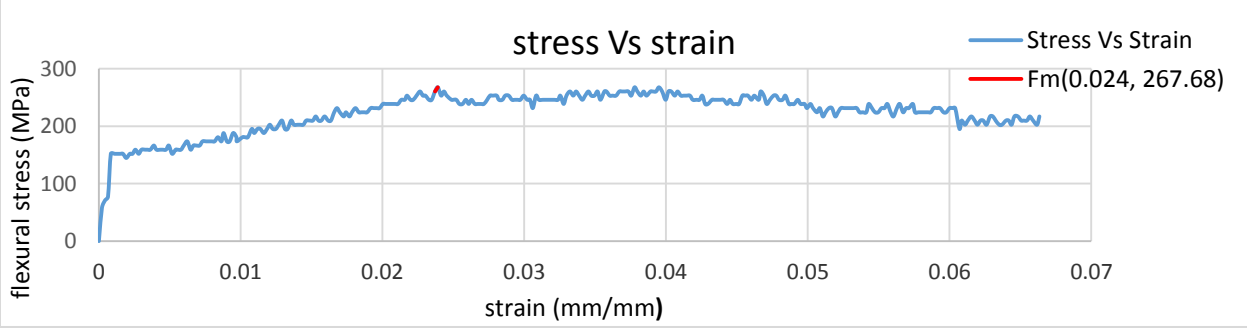

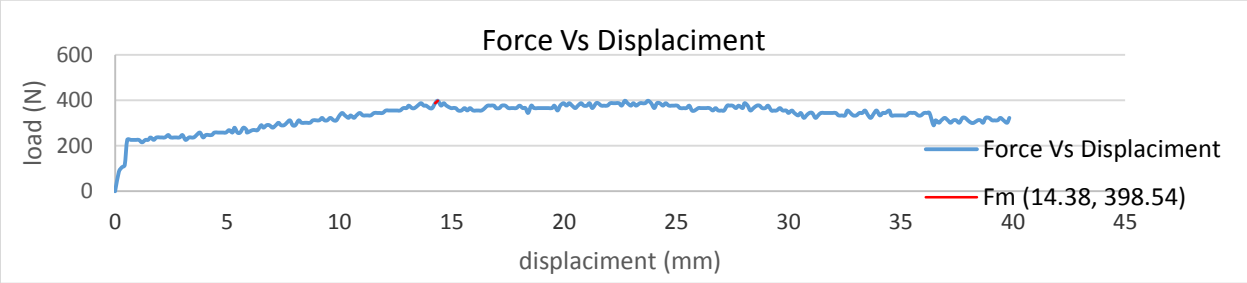


**Test four**

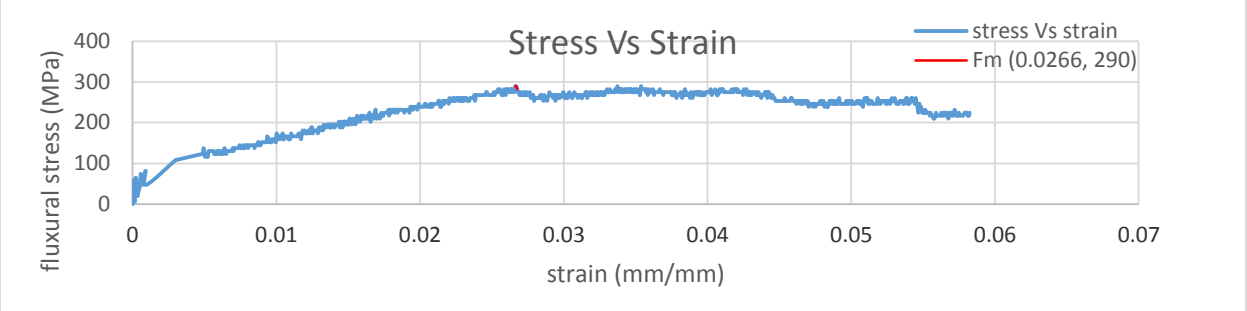


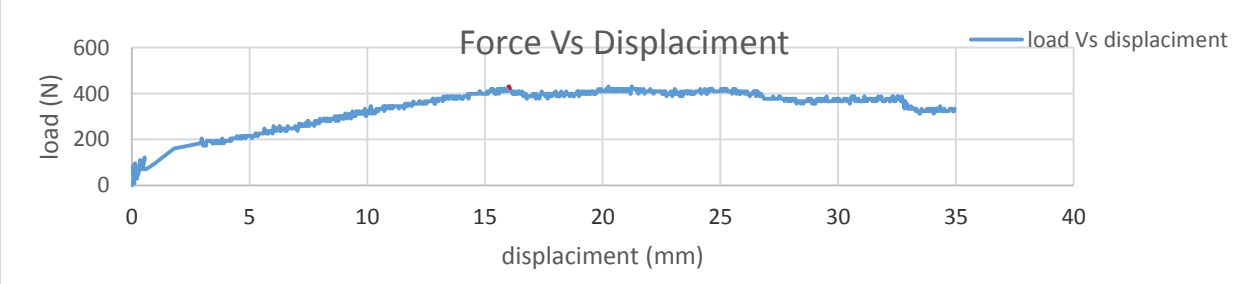


**Test five**

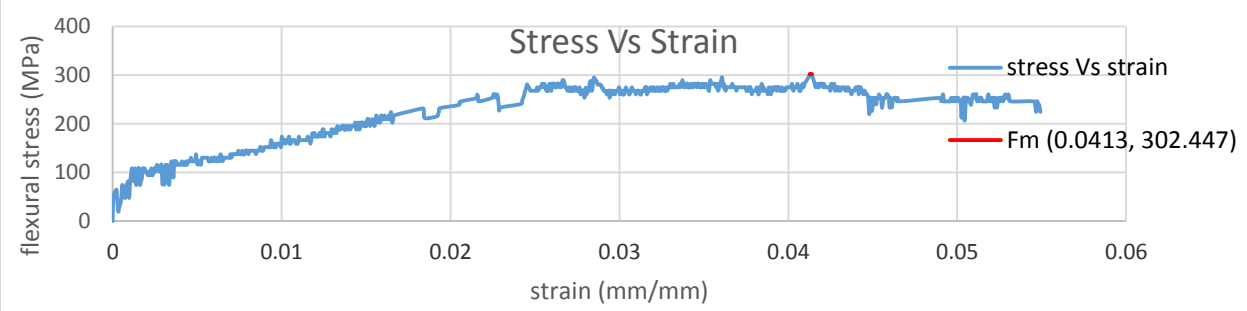


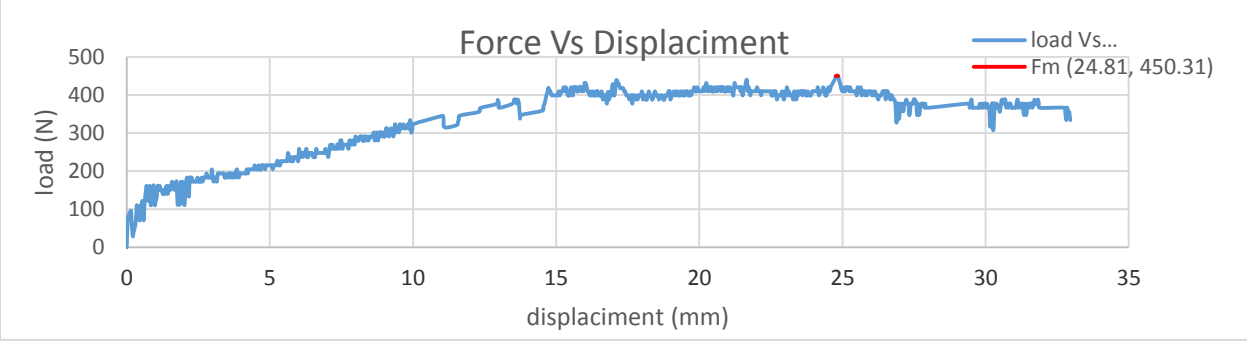

## 55/45 fiber/epoxy flexural test

### Test one

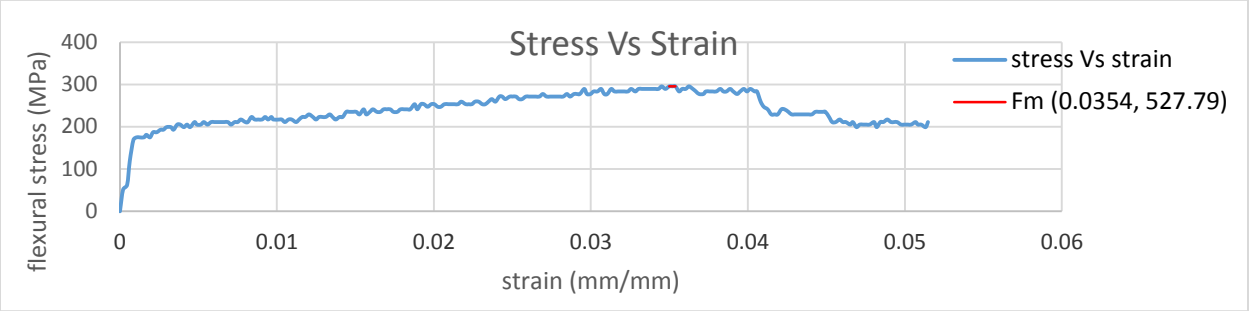


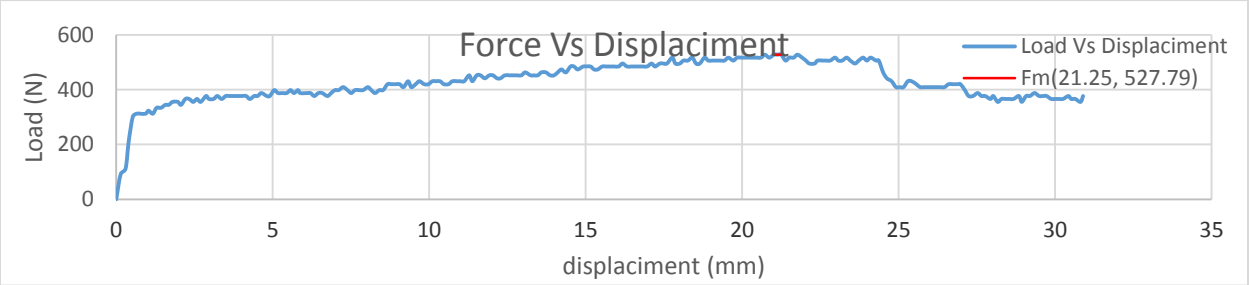


### Test two

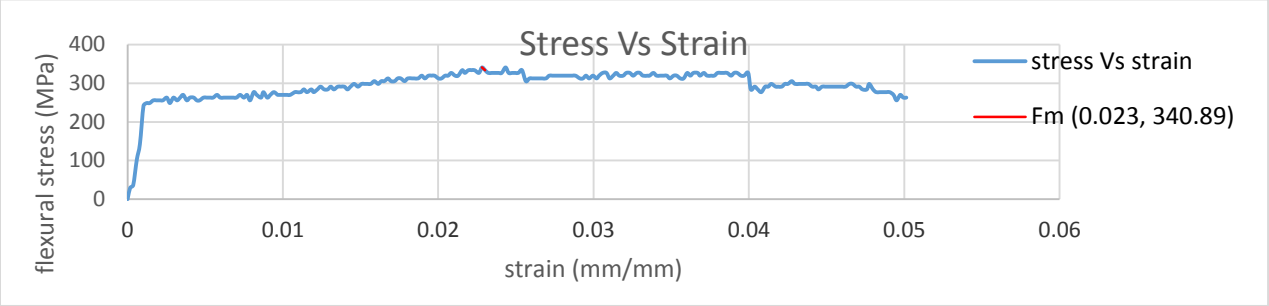


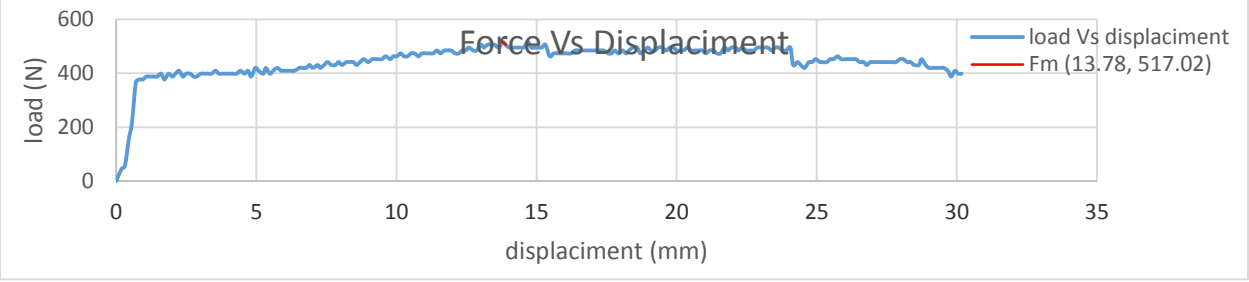


### Test three

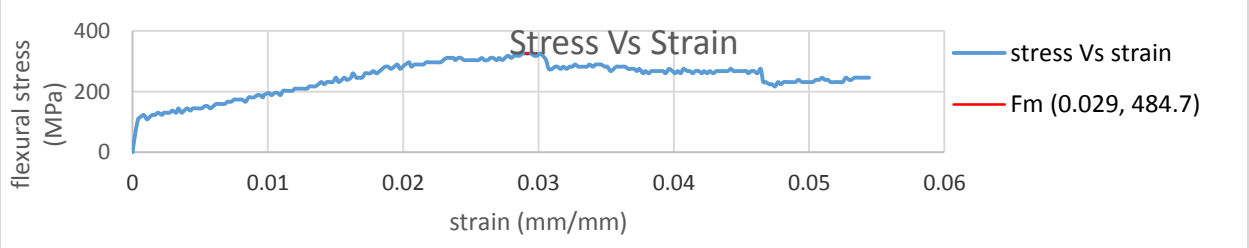

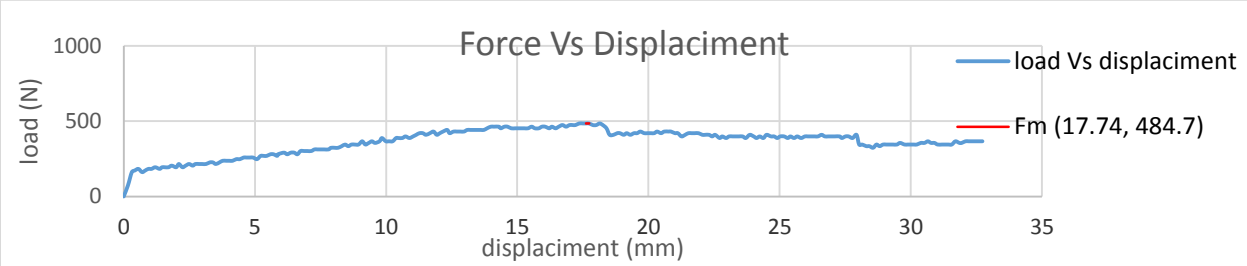


**Test four**

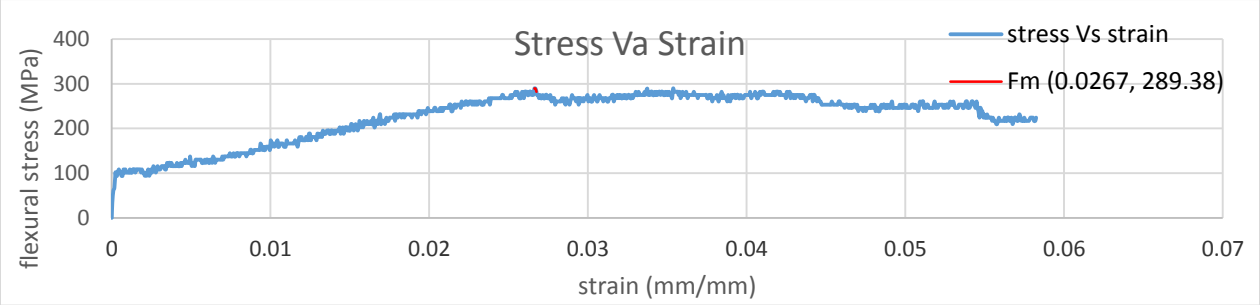


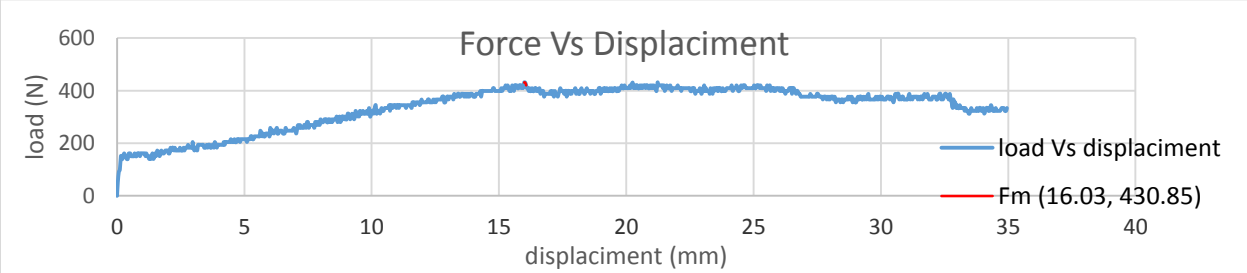


**Test five**

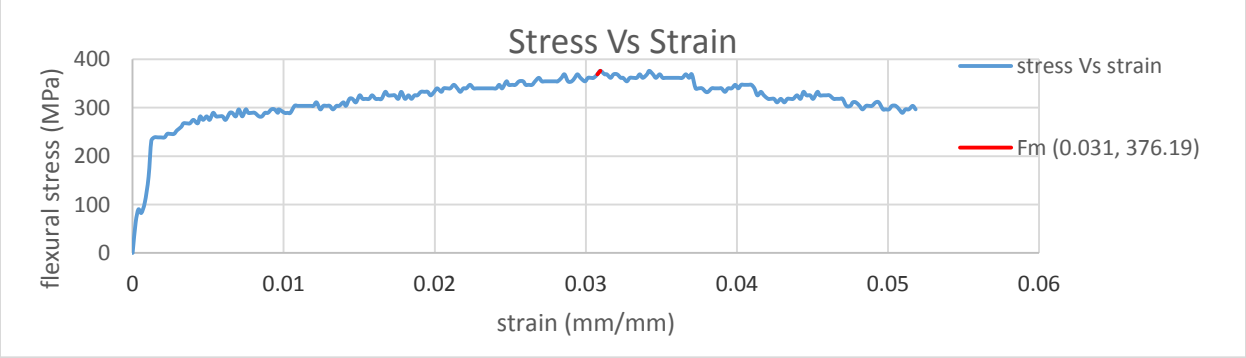


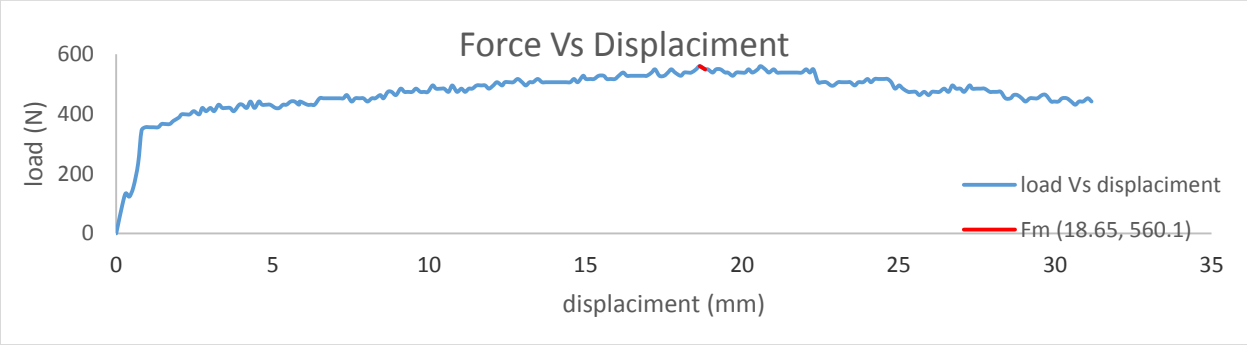

## 60/40 fiber/epoxy flexural test

### Test one

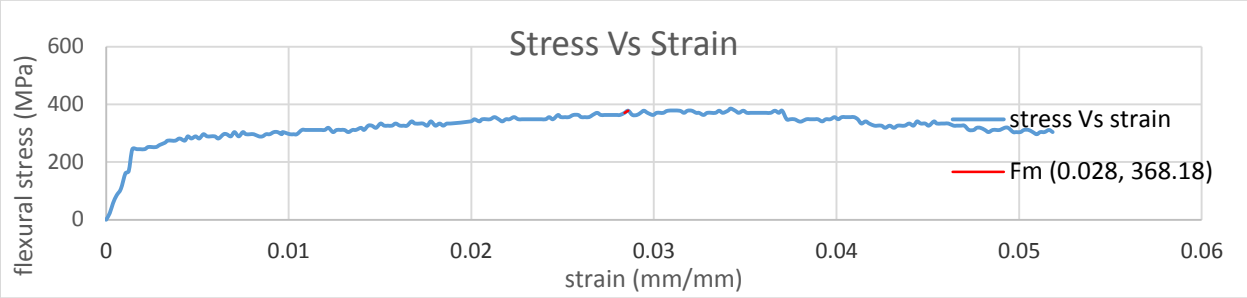


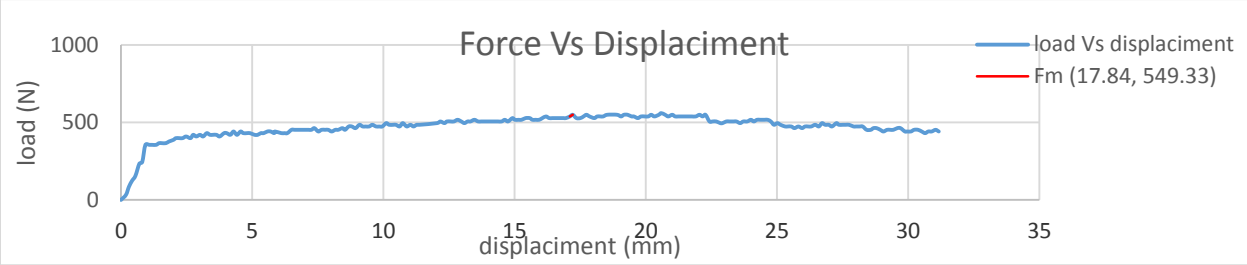


### Test two

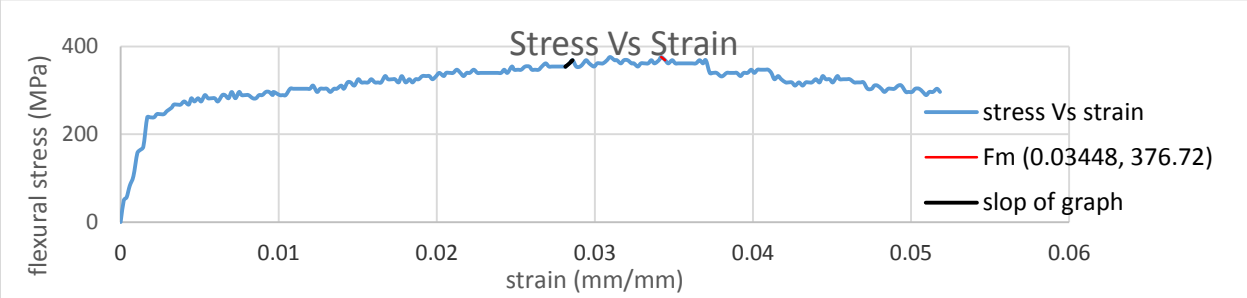


### Test three

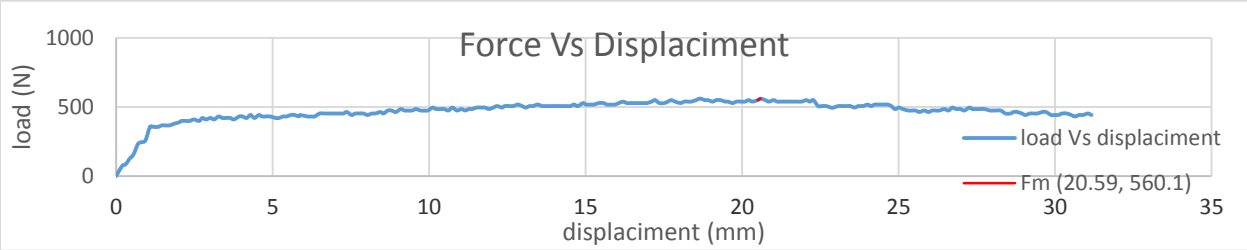


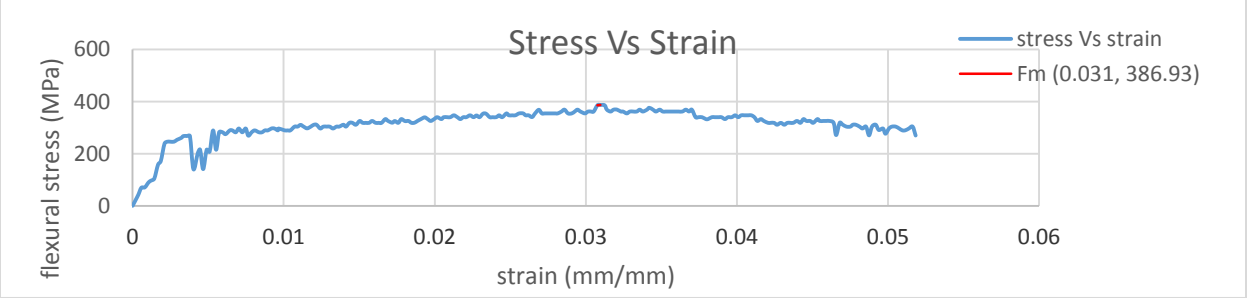

**Test four**

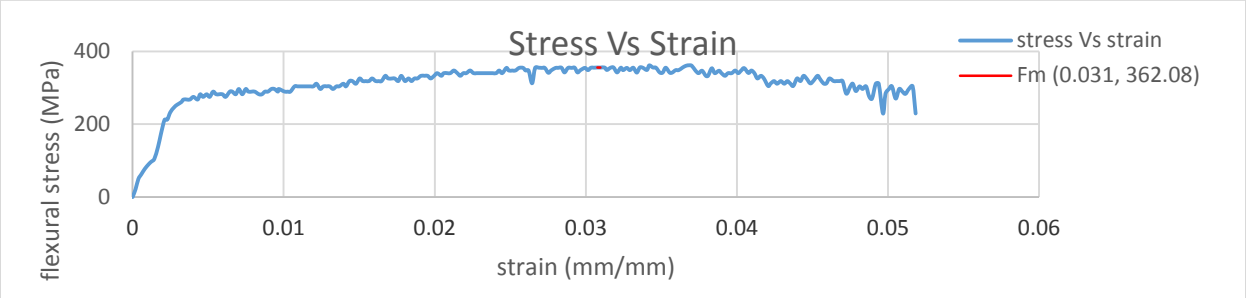


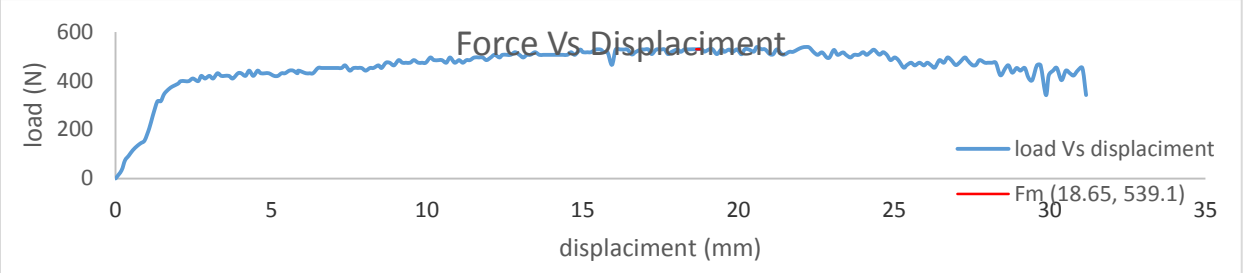


**Test five**

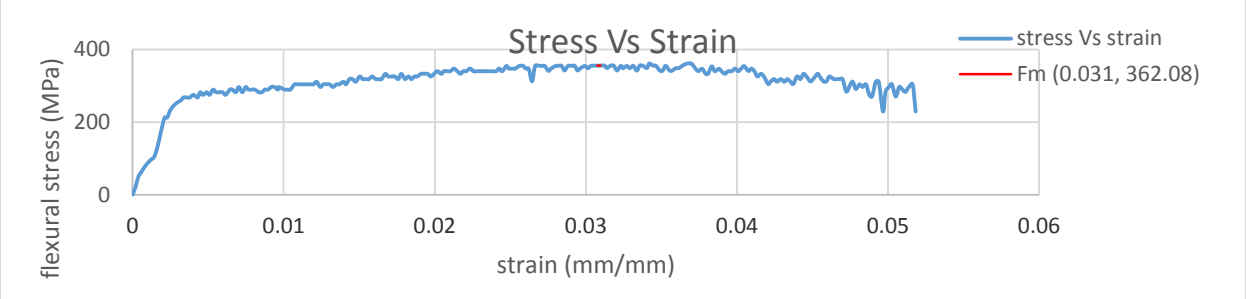


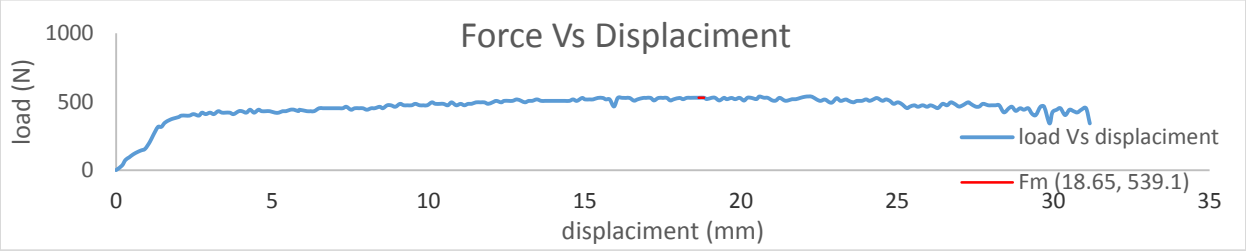


Max compressive force and stress of each test for different composition ratio of 60%/40%, 55%/45% and 50%/50% of fiber/epoxy is given below.

**50/50 fiber/epoxy Compression test**

**Test one**

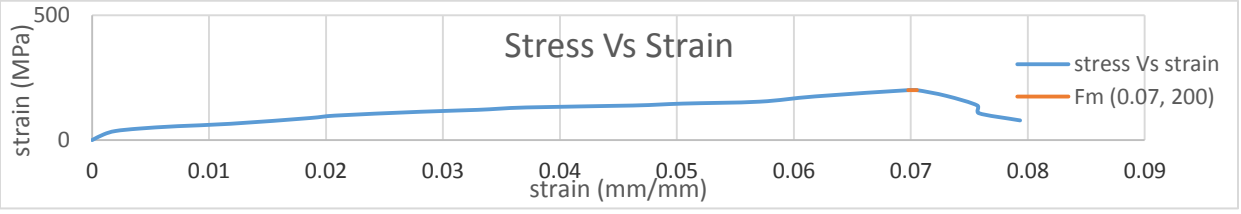

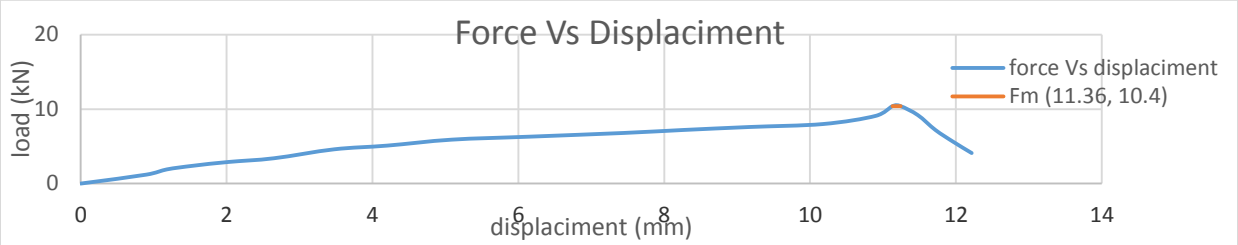


**Test two**

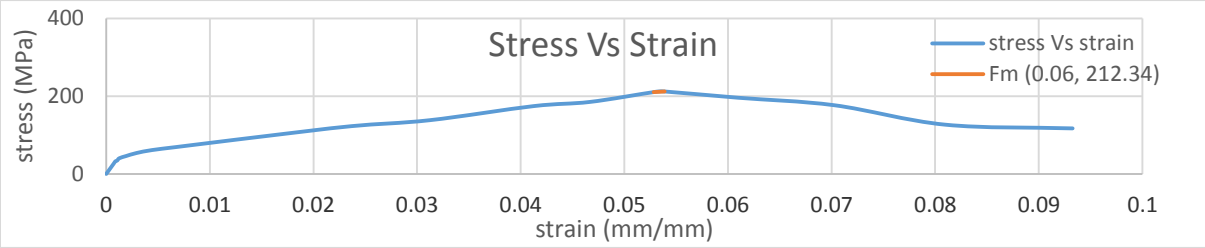


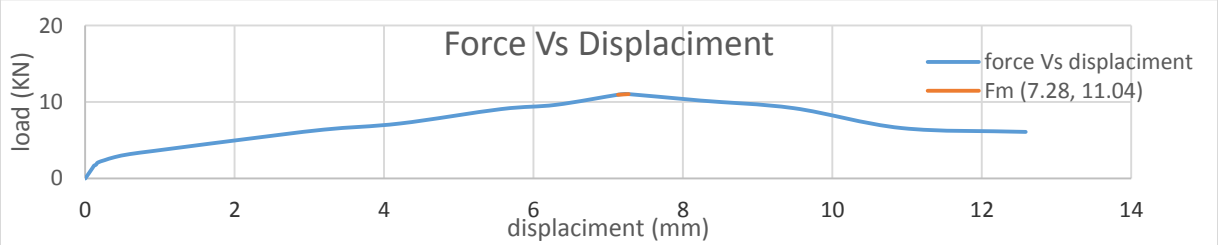


**Test three**

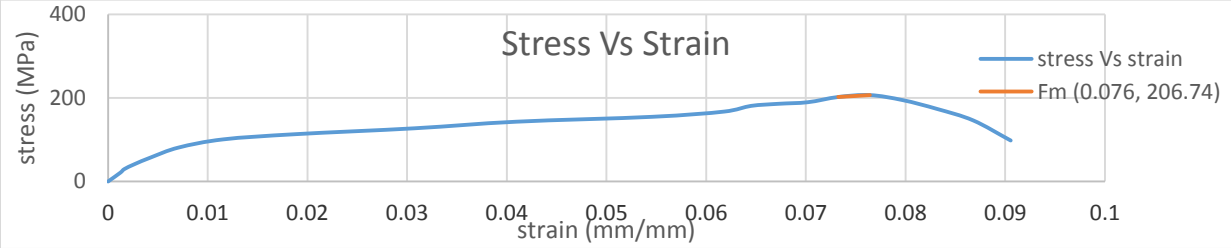


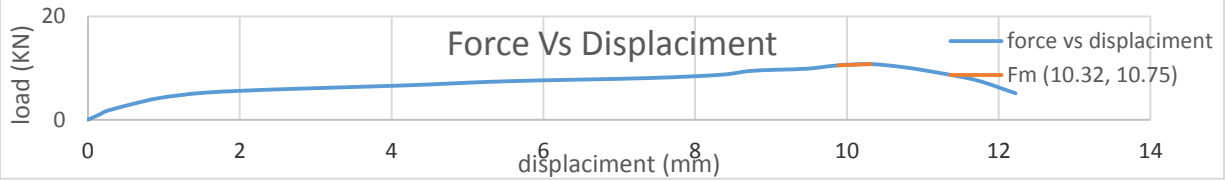


**Test four**

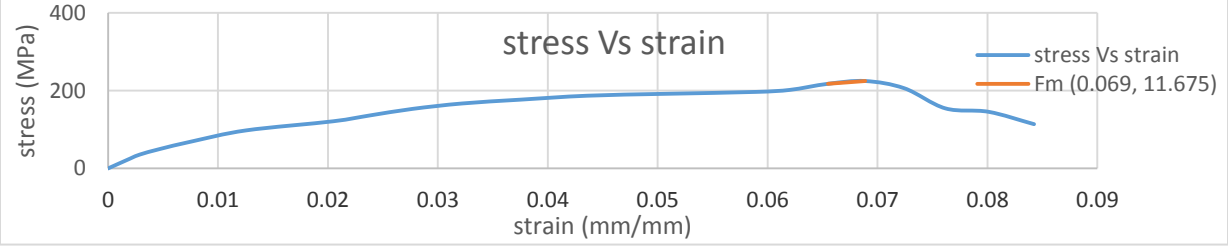

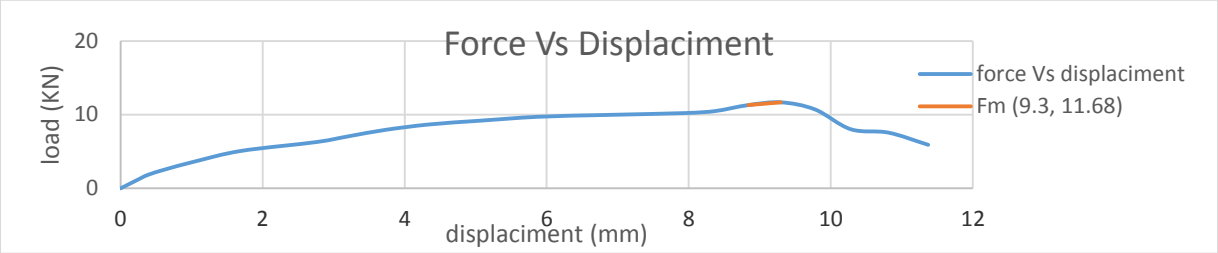


**Test five**

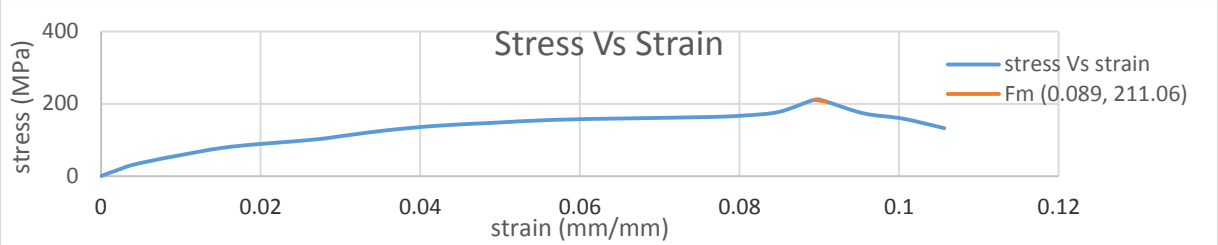


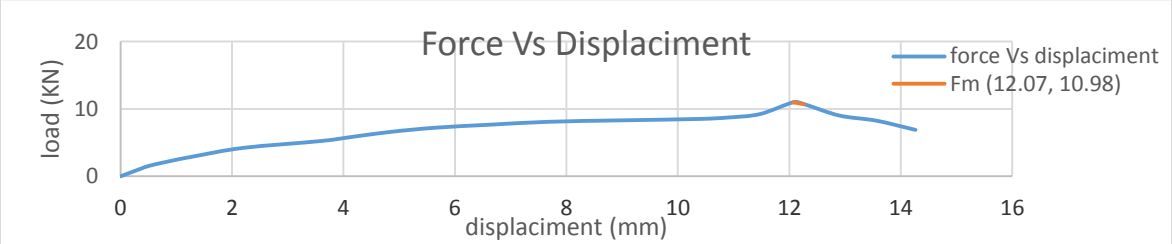


**55/45 fiber/epoxy Compression test**

**Test one**

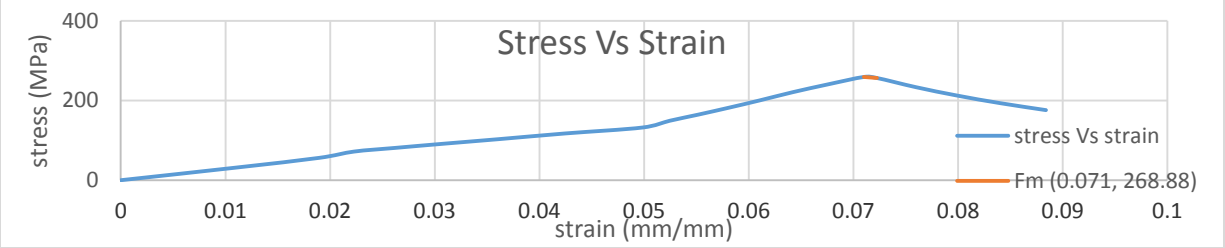


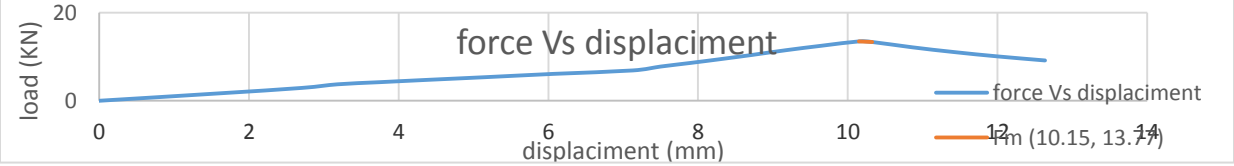


**Test two**

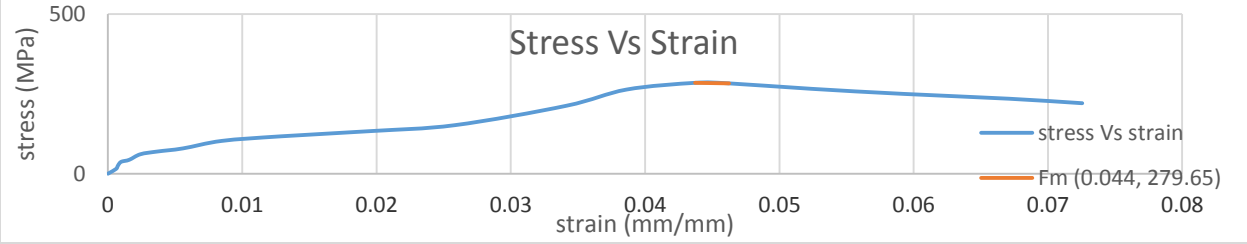

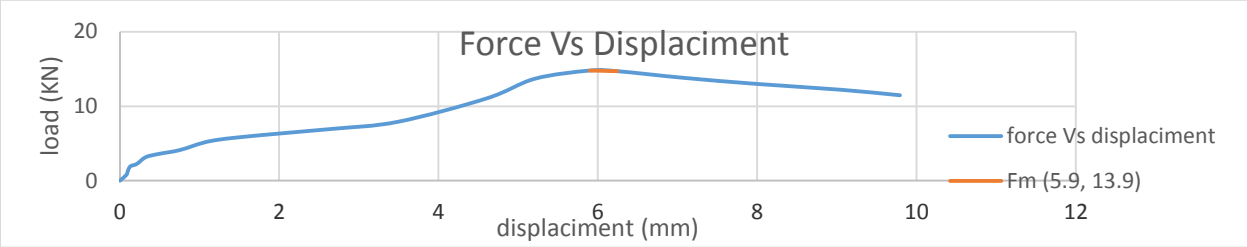


**Test three**

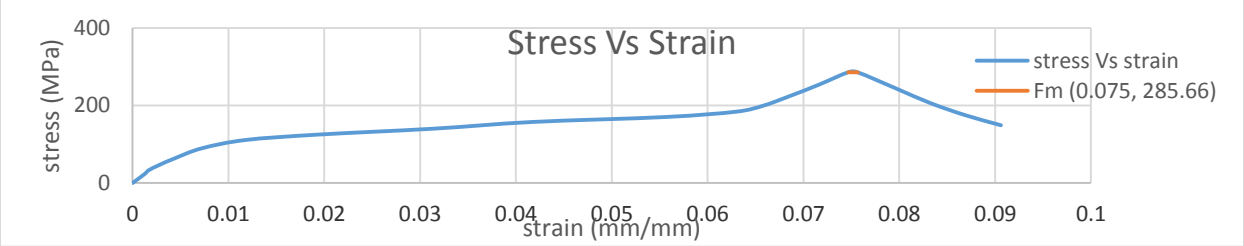


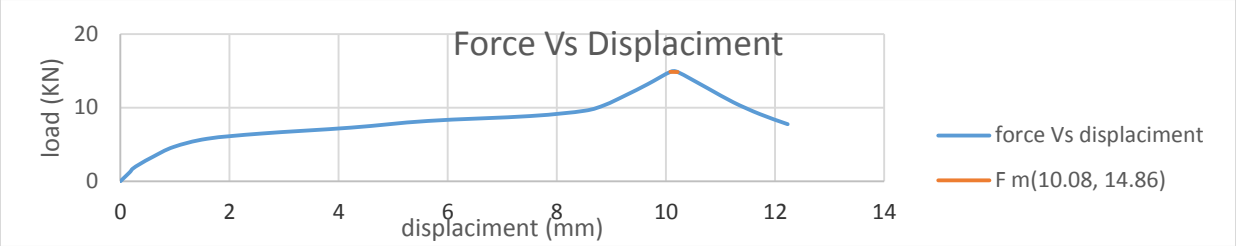


**Test four**

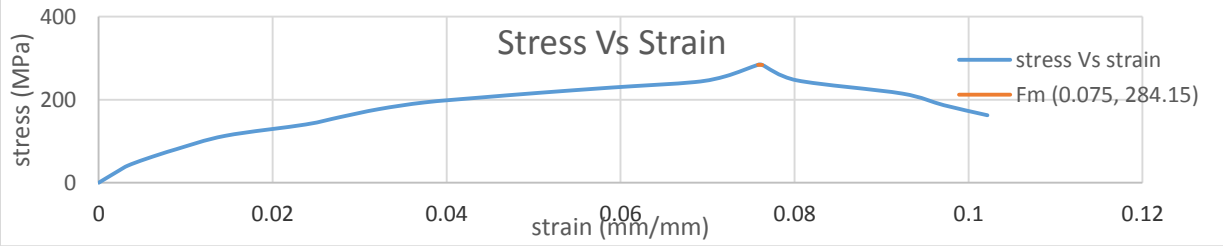


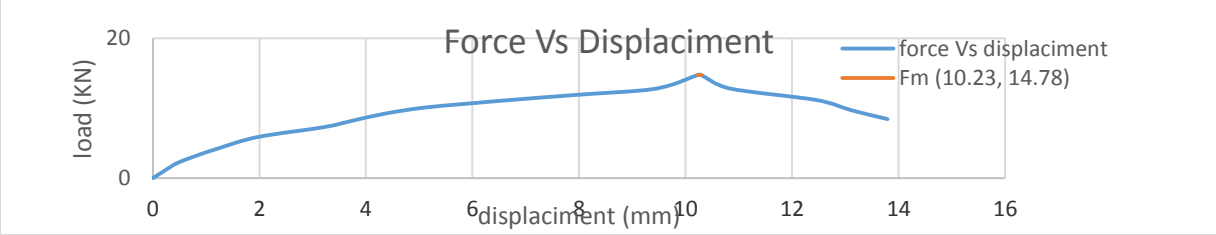


**Test five**

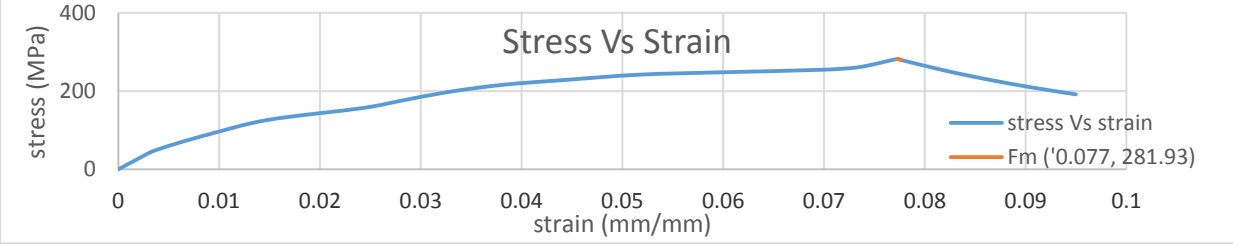

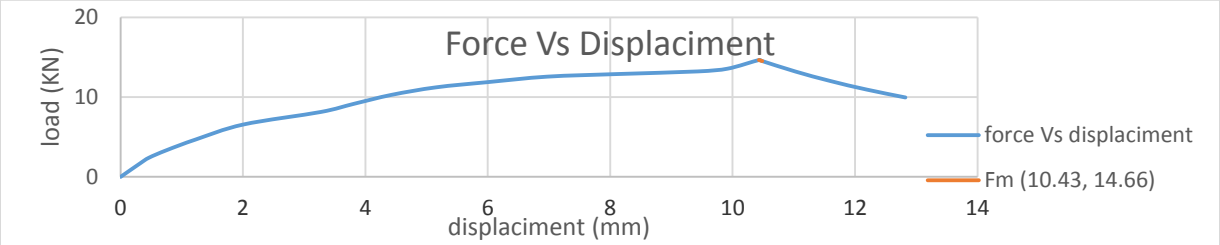


**60/40 fiber/epoxy Compression test**

**Test one**

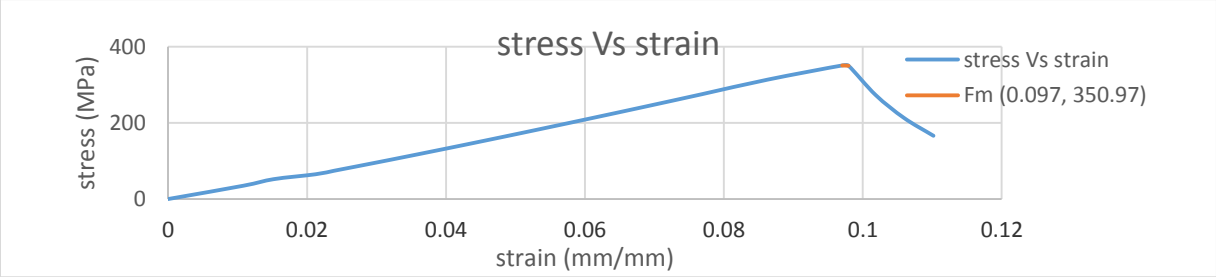


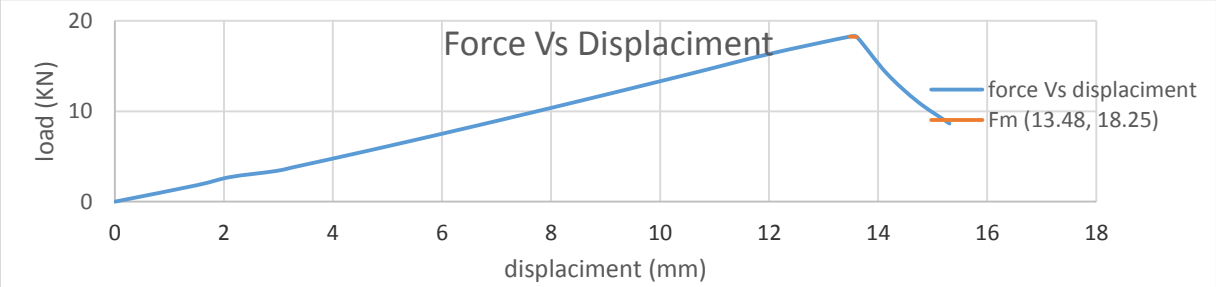


**Test two**

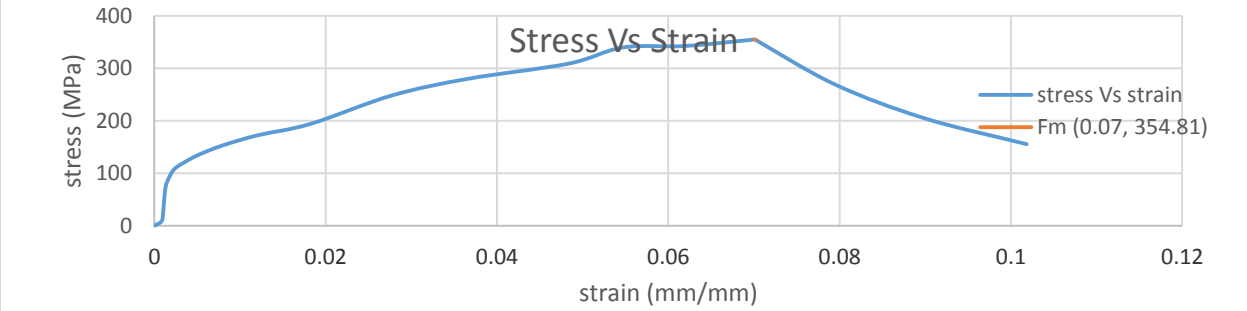


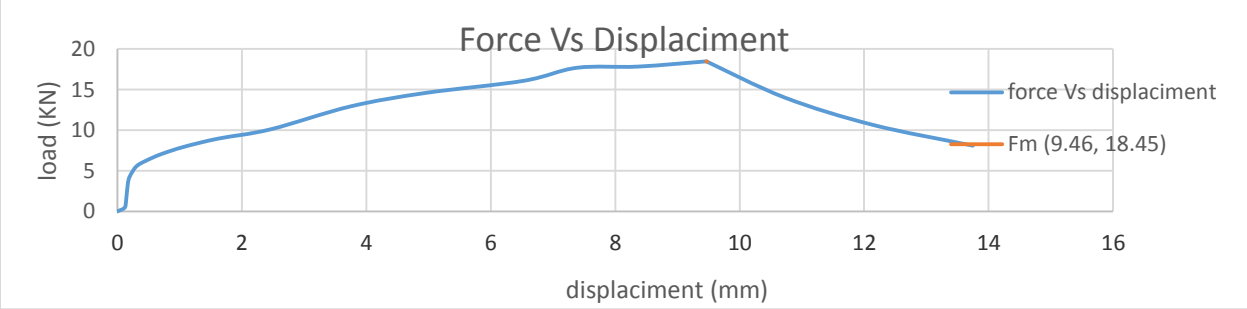

**Test three**

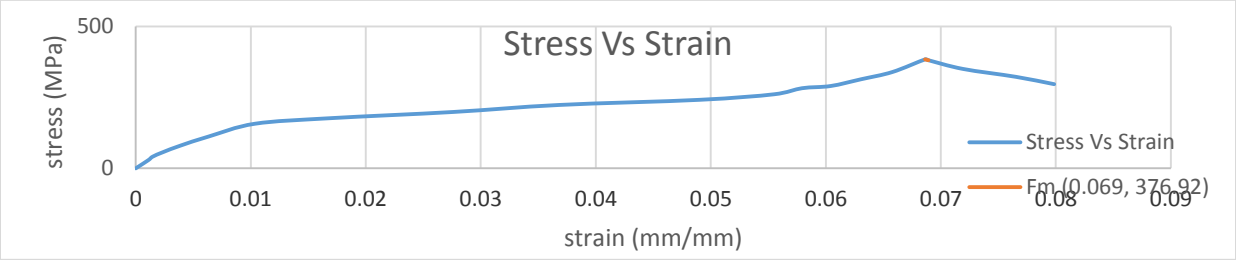


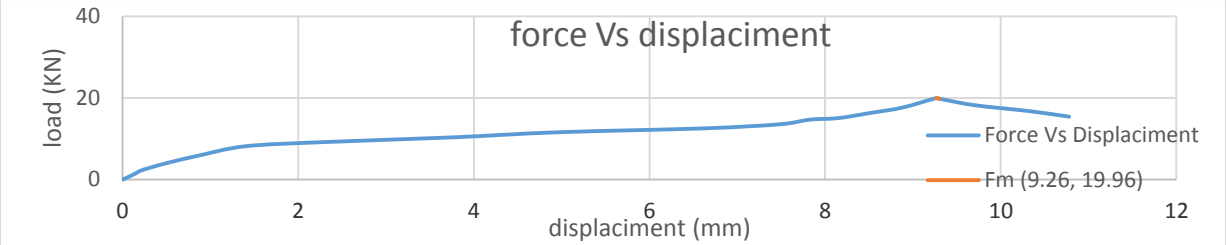


**Test four**

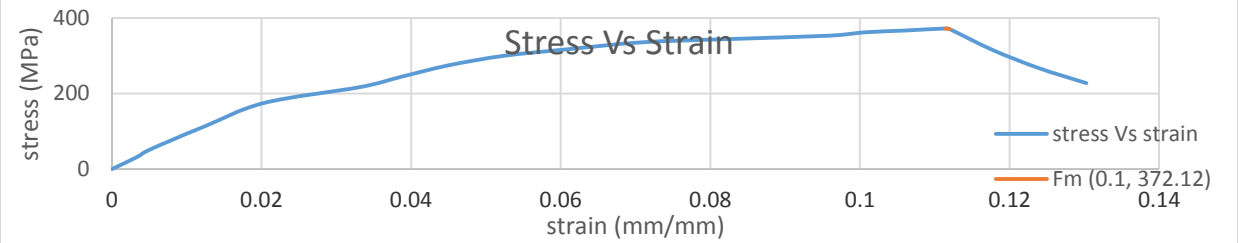


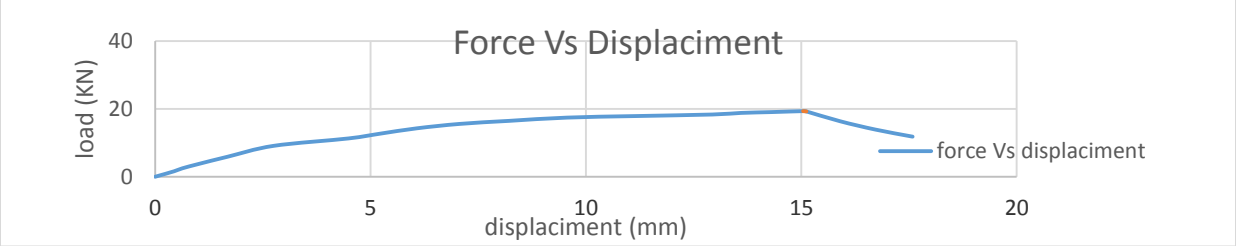


**Test five**

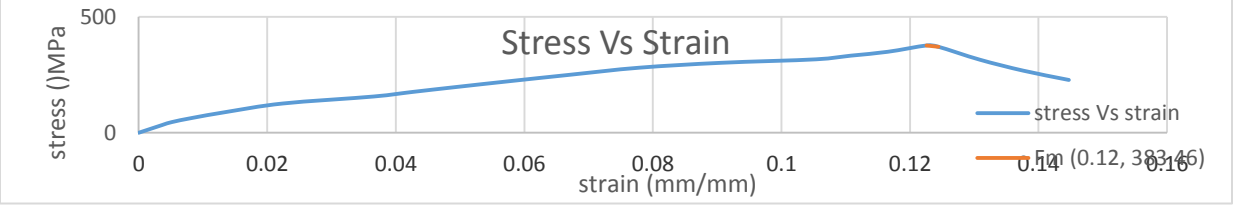


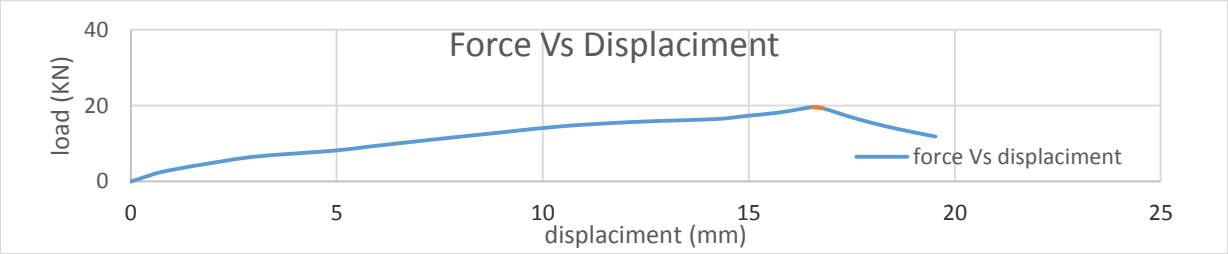

# Appendix B

**Table1. FEA specification result for Kevlar/E-glass hybrid composite**

| Material | |
|---|---|
| Assignment | Kevlar/E-glass hybrid composite material |
| Nonlinear Effects | Yes |
| Thermal Strain Effects | Yes |
| **Bounding Box** | |
| Length X | 357.37 mm |
| Length Y | 42. mm |
| Length Z | 403.33 mm |
| **Properties** | |
| Volume | 1.4306e+006 mm³ |
| Mass | 2.4249 kg |
| Centroid X | 201.17 mm |
| Centroid Y | 14.339 mm |
| Centroid Z | 77.479 mm |
| Moment of Inertia Ip1 | 30433 kg·mm² |
| Moment of Inertia Ip2 | 40340 kg·mm² |
| Moment of Inertia Ip3 | 10249 kg·mm² |
| **Statistics** | |
| Nodes | 64634 |
| Elements | 41666 |
| Mesh Metric | None |

**Table 2. FEA specification result for structural steel**

| Material | |
|---|---|
| Assignment | Structural Steel |
| Nonlinear Effects | Yes |
| Thermal Strain Effects | Yes |
| **Bounding Box** | |
| Length X | 357.37 mm |
| Length Y | 42. mm |
| Length Z | 403.33 mm |
| **Properties** | |
| Volume | 5.5546e+005 mm³ |
| Mass | 4.3603 kg |
| Centroid X | 192.7 mm |
| Centroid Y | 13.206 mm |
| Centroid Z | 58.929 mm |
| Moment of Inertia Ip1 | 26958 kg·mm² |
| Moment of Inertia Ip2 | 83295 kg·mm² |
| Moment of Inertia Ip3 | 57101 kg·mm² |
| **Statistics** | |
| Nodes | 52349 |
| Elements | 26981 |
| Mesh Metric | None |

# Appendix C

**Table 1. Comparison of fiber reinforcement**

| Table 3.1 Comparison of fibres | | | | | |
|---|---|---|---|---|---|
| | Best ⟷ | | | | Worst |
| Cost | E-Glass | S-Glass | Kevlar | Graphite | Ceramic |
| Density | Kevlar | Graphite | S-Glass | E-Glass | Ceramic |
| Stiffness | Graphite | Kevlar | S-Glass | Ceramic | E-Glass |
| Heat | Ceramic | S-Glass | E-Glass | Kevlar | Graphite |
| Toughness | Kevlar | S-Glass | E-Glass | Ceramic | Graphite |
| Impact | Kevlar | S-Glass | E-Glass | Ceramic | Graphite |

**Table2. Properties of Commonly Used Reinforcements**

| Material | Diameter ($\mu m$) | Density (g/cm 3) | Tensile Modulus (E) (GPa) | Tensile Strength (GPa) | Specific Modulus (E/) | Specific Strength | Melting Point (°C) | % Elongation at Break | Relative Cost |
|---|---|---|---|---|---|---|---|---|---|
| E-glass | 7 | 2.54 | 85 | 2.05 | 36 | 1.35 | 1540+ | 4.8 | Low |
| S-glass | 15 | 2.50 | 86 | 4.50 | 34.5 | 1.8 | 1540+ | 5.7 | moderate |
| Graphite, high modulus | 7.5 | 1.9 | 400 | 1.8 | 200 | 0.9 | >3500 | 1.5 | High |
| Graphite, high strength | 7.5 | 1.7 | 240 | 2.6 | 140 | 1.5 | >3500 | 0.8 | High |
| Boron | 130 | 2.6 | 400 | 3.5 | 155 | 1.3 | 2300 | __ | High |
| Kevlar 29 | 12 | 1.45 | 80 | 2.8 | 55.5 | 1.9 | 500(D) | 3.5 | Moderate |
| Kevlar 49 | 12 | 1.45 | 130 | 3.6 | 131 | 1.9 | 500(D) | 2.5 | Moderate |

**Table 3. Properties of Commonly Used Resins**

| Resins | Fiber Dia d($\mu m$) | Density $\rho(kg/m^3)$ | Modulus of Elasticity E(Mpa) | Shear Modulus G(Mpa) | Poisson Ratio Vs Tensile strength $\sigma_{Ult}$(Mpa) | Elongation E(%) | Heat Capacity $c(J/kg°C)$ | Useful Temperature Limit $T_{max}$ (℃) |
|---|---|---|---|---|---|---|---|---|
| Epoxy | 1200 | 4500 | 2260 | 0.4 | 130 | 2(100℃) 6(100℃) | 1000 | 90 to 200 |
| Phenolic | 1300 | 3000 | 1100 | 0.4 | 70 | 2.5 | 1000 | 120 to 200 |
| Polyester | 1200 | 4000 | 1400 | 0.4 | 80 | 2.5 | 1400 | 60 to 200 |
| Vinyl ester | 1150 | 3300 | | | 75 | 4 | | >100 |
| Silicone | 1100 | 2200 | | 0.5 | 35 | | | 100 to 350 |
| Urethane | 1100 | 700 to 7000 | | | 30 | 100 | | 100 |
| Polyimide | 1400 | 4000 | 1100 | 0.35 | 70 | 1 | 1000 | 250 to 300 |
| Polypropylene | 900 | 1200 | | 0.4 | 30 | 20 to 400 | 330 | 70 to 140 |
| Polyphenylene sulfone | 1300 | 4000 | | 65 | 100 | | | 130 to 250 |
| Polyamide | 1100 | 2000 | | 0.35 | 70 | 200 | 1200 | 170 |
| Polyether sulfone | 1350 | 3000 | | | 85 | 60 | | 180 |
| Poly etherified | 1250 | 3500 | | | 105 | 60 | | 200 |